The response of fibrocytes to targeted thoracic and forelimb bone marrow radiation exposure

by

Ana Patricia Marquez

Thesis submitted to the Faculty of the
Molecular and Cell Biology Graduate Program
Uniformed Services University of the Health Sciences
In partial fulfillment of the requirements for the degree of
Masters of Science 2017

UNIFORMED SERVICES UNIVERSITY, SCHOOL OF MEDICINE GRADUATE PROGRAMS
Graduate Education Office (A 1045), 4301 Jones Bridge Road, Bethesda, MD 20814

APPROVAL SHEET

Title of Dissertation: "The response of fibrocytes to targeted thoracic and forelimb bone marrow radiation exposure"

Name of Candidate: **Ana P. Marquez**, Master of Science in **Molecular and Cellular Biology**

October 30, 2017

THESIS AND ABSTRACT APPROVED:

DATE:

DS Merrell 11/9/17

D. Scott Merrell, PhD
DEPARTMENT OF MICROBIOLOGY AND IMMUNOLOGY
Committee Chairperson

11/1/2017

Regina Day, PhD
DEPARTMENT OF PHARMACOLOGY
Thesis Advisor

11/1/17

Andrew Snow, PhD
DEPARTMENT OF PHARMACOLOGY
Committee Member

ACKNOWLEDGMENTS

I'd like to thank Leti and Jessie for all the help they have provided me with and who have made many a milkshake run at my behest. Javi and Katie, thanks for listening to me complain all the time. Los, I can't believe you haven't given up hope of dragging me down to ATX yet. It is very hard to figure out who to thank since all the people I'm surround by are all around amazing and have helped me in one way or another. Between hearing all my woes, many a happy hour and hanging out in emergency rooms (!) I couldn't ask for much more.

On a more scientific note, I'd especially like to thank Mark Smith Ph. D, DMV for the detailed histology reports.

I'd also like to thank my program director Dr. Cutler. Dr. Cutler somehow manages to deal with all the issues from every student in the MCB program, even mine, which I will always appreciate. I'd also like to thank the chair of my committee Dr. Merrell for always providing a balanced view in all my committee meetings.

DEDICATION

To my sister Leticia, her wife Jessie and their newly adopted daughter.

To my mom and to my dad.

COPYRIGHT STATEMENT

The author hereby certifies that the use of any copyrighted material in the thesis manuscript entitled:

The response of fibrocytes to targeted thoracic and forelimb bone marrow radiation exposure

is appropriately acknowledged and, beyond brief excerpts, is with the permission of the copyright owner.

Ana Marquez Digitally signed by Ana Marquez Date: 2017.11.09 16:40:50 -05'00'

Ana P. Marquez

November 2nd, 2017

DISCLAIMER

The views presented here are those of the author and are not to be construed as official or reflecting the views of the Uniformed Services University of the Health Sciences, the Department of Defense or the U.S. Government.

Distribution Statement

Distribution A: Public Release.

The views presented here are those of the author and are not to be construed as official or reflecting the views of the Uniformed Services University of the Health Sciences, the Department of Defense or the U.S. Government.

COPYRIGHT STATEMENT

The author hereby certifies that the use of any copyrighted material in the thesis manuscript entitled:

The response of fibrocytes to targeted thoracic and forelimb bone marrow radiation exposure

is appropriately acknowledged and, beyond brief excerpts, is with the permission of the copyright owner.

_____

Ana P. Marquez

November 2nd, 2017

DISCLAIMER

The views presented here are those of the author and are not to be construed as official or reflecting the views of the Uniformed Services University of the Health Sciences, the Department of Defense or the U.S. Government.

ABSTRACT

The response of fibrocytes to targeted thoracic and forelimb bone marrow radiation exposure

Ana P. Marquez, M.S., 2017

Thesis directed by: Regina Day PhD, Professor, Department of Pharmacology

Fibrocytes have recently stepped out from underneath the shadow of fibrotic diseases. The unique cells that are characterized by their expression of both hematopoietic and mesenchymal cell markers are becoming increasingly recognized in the context of non-fibrotic diseases. Fibrocytes have been shown to aid and abet metastatic tumors evade the host immune system as well as participate in the development of Graves' disease. However, there is still a long list of maladies that have yet to be examined under the lens of fibrocytes, including radiation-induced bone marrow injury. We developed a model of thoracic and partial bone marrow irradiation by selectively exposing the thoracic cavity and humeri of mice to various doses of radiation. 14Gy irradiation effectively depleted exposed bone marrow at 60 days post irradiation. We used this model to study the response of fibrocytes to partial bone marrow irradiation-induced injury. We quantified the number and relative collagen expression of fibrocytes and $CD45^{+}ColI^{+}$ cells isolated from peripheral blood mononuclear cells (PBMC), the spleen, and shielded bone marrow using flow cytometry. Circulating PBMC

and splenic fibrocyte levels peaked 30 days post irradiation. The number of fibrocytes in the spleen drastically decreased soon after irradiation. Additionally, in all tissues the relative collagen expression of fibrocytes was highest at the earlier time points post irradiation. These data demonstrate that fibrocytes respond to thoracic and partial bone marrow irradiation, and that this response is temporally mediated and tissue specific.

TABLE OF CONTENTS

LIST OF TABLES

LIST OF FIGURES

CHAPTER 1: Introduction

FIBROCYTES

Fibrocytes – A cell with many faces

Fibrocytes were first observed in cell aspirates isolated from implanted dermal wound chambers (36). Adherent spindle-shaped cells, similar to fibroblasts were identified and further characterized. These peripheral blood mononuclear cells (PBMCs) were identified as a leukocyte subpopulation of cells expressing both hematopoietic and mesenchymal markers (36). Fibrocytes account for approximately 0.1 – 0.5% of the circulating PBMCs in humans (50). Cultured PBMC fibrocytes were shown to express $CD45^+$ $CD34^+$ $CD11b^+$ $CD18^+$ $CD14^-$ collagen I $(ColI)^+$ $vimentin^+$ $fibronectin^+$ (36). In addition to these markers, fibrocytes are easily identified in PBMC cultures by their unique morphology: a spindle cell body, minimal cytoplasm and large oval nucleus that occupies the bulk of the cell (Figure 1). Subsequent studies have provided additional surface markers for identification, as well as markers to discriminate fibrocytes from fibroblasts, monocytes, and macrophages (174; 207) (Table 1). Fibrocytes also express a wide range of chemokines, chemokine receptors, growth factors, and extracellular matrix proteins (36; 241). Dual labeling with CD45 and ColI is generally accepted as the two necessary markers needed to distinguish fibrocytes from other cell types.

After their discovery, studies probed the role that fibrocytes played in the process of wound repair following injury. Their ability to traffic to wound sites was shown by injecting

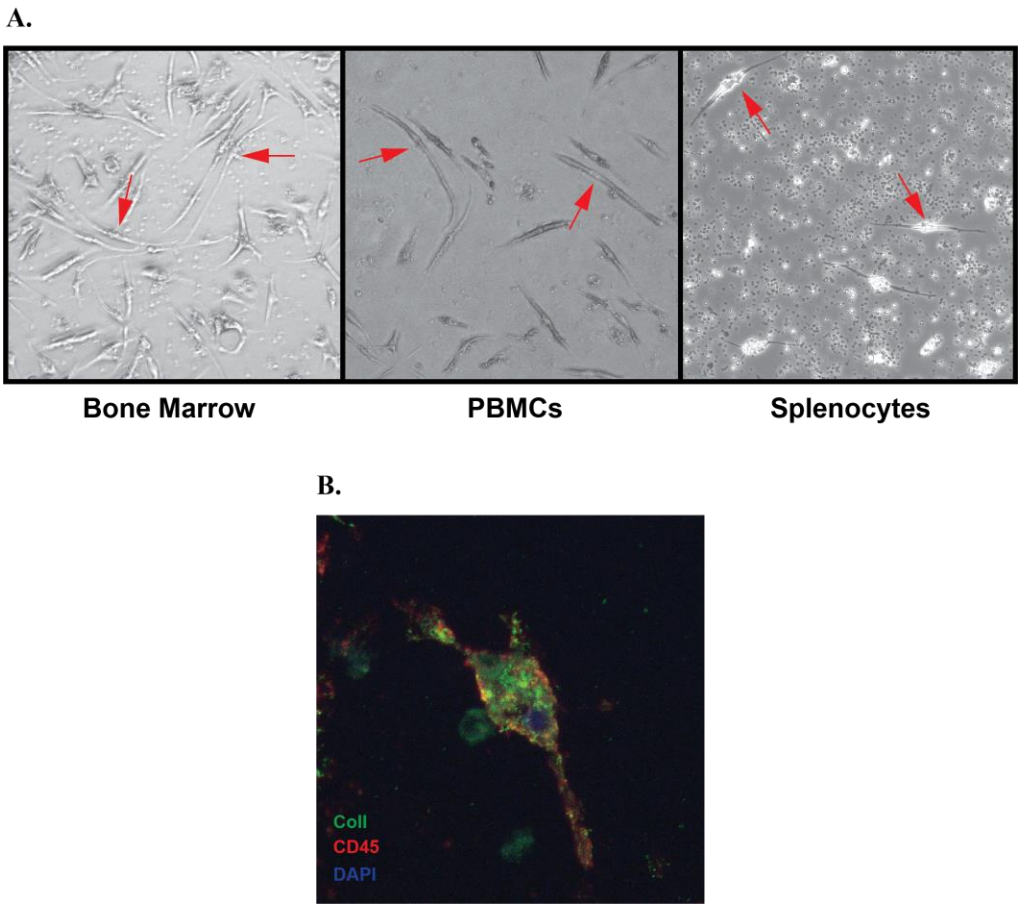

Figure 1. Fibrocytes in culture.

A. Fibrocyte cultures from different tissue sources. B. Bone marrow derived fibrocytes express both CD45 and Collagen I.

Table 1. Markers expressed by human PBMC cultures of monocytes, macrophages, and fibrocytes.

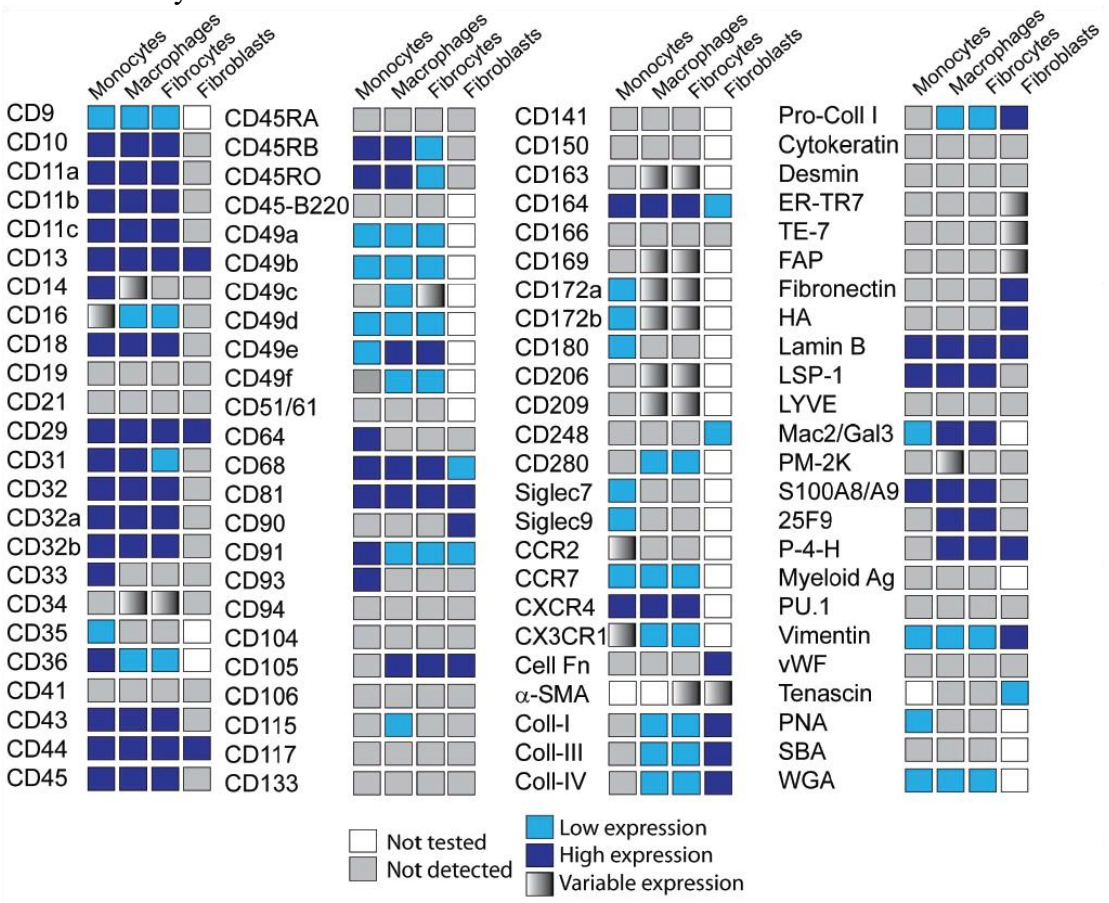

Reproduced with permission from Pilling D, Fan T, Huang D, Kaul B, Gomer RH. Identification of markers that distinguish monocyte-derived fibrocytes from monocytes, macrophages, and fibroblasts. PLoS One. 2009;4(10):e7475., ⓒⓘ Creative Commons – Attribution 2009.

cultured fibrocytes in wounded mice (2). Fibrocytes were shown to transdifferentiate into α-smooth muscle actin (α-SMA) expressing myofibroblasts after recruitment to sites of injury (185). Their increased production of type I collagen in response to transforming growth factor beta (TGF-β) a growth factor demonstrated to induce collagen synthesis in culture, was also demonstrated (50). These findings pointed to the potential role of fibrocytes in fibrosis. Definitive evidence for this role was provided in a seminal study by Phillips et al., in 2004, investigating the role of fibrocytes in a murine model of lung fibrosis. They showed that inhibiting the migration of fibrocytes to the injured lungs of bleomycin exposed mice, through the inhibition of stromal-derived factor (SDF-1, CXCL12)/CXCR4 chemokine trafficking, diminished the degree of lung fibrosis, in injured mice (206).

It should be noted that in the literature, the terms fibrocytes, fibrocyte-like cells, and bone marrow-derived fibroblast precursors are used interchangeably, and all are defined as $CD45^+$ $ColI^+$ cells, or $ColI^+$ transplanted bone marrow cells.

Origin of Fibrocytes: The Bone Marrow

Bucala et al., 1994, postulated that fibrocytes were of bone marrow origin, given their expression of the hematopoietic stem cell marker CD34 (36). To test his hypothesis, he utilized sex-mismatched bone marrow chimeric mice to try and detect cells originating from donor (male) bone marrow cells, in recipient mice (female). He was not able to detect circulating fibrocytes derived from donor bone marrow cells. He suggested that, either circulating fibrocytes originated from radio resistant bone marrow progenitor cells, or that they originated from another tissue.

For the next 10 years fibrocytes were simply classified as, “blood-borne cells”. The preliminary evidence that linked bone marrow cells to fibrocytes, was the demonstration that, a bone marrow $CD45^+$ $ColI^+$ $CXCR4^+$ cell population increased concomitant to the increase of lung fibrocytes during fibrosis. While not definitive proof of the bone marrow origin of fibrocytes, the study did lend credence to this long-held hypothesis (206). Subsequent research using GFP^+-bone marrow cell transplantation, showed GFP^+ cells in the fibrotic lungs of recipient mice. However, isolated fibrocytes from fibrotic lungs, were unable to differentiate into myofibroblast when treated with TGF-β, a growth factor demonstrated to transdifferentiate fibrocytes in to myofibroblast in culture (2; 241). The inability of these cells to differentiate into myofibroblast called into question if the isolated cells were indeed fibrocytes (2).

Undisputable proof of the bone marrow as an origin of fibrocytes was provided by Mori et al., 2005, who employed the use of sex-mismatched bone marrow, the same approach used by Bucala 10 years prior (36). These mouse chimeras contained $ColI^+$ $CD34^+$ $CD45^+$ cells of donor origin, in the dermal wound sites. These $ColI^+$ $CD34^+$ $CD45^+$ cells, i.e. fibrocytes, found in the wound sites, differentiated into α-SMA+ myofibroblast (2; 185).

Interestingly, there have been at least two studies that identified bone marrow-derived myofibroblasts involved in human fibrotic disease (82; 208). Liver biopsies from a female patient, who had received a bone marrow transplant with male donor cells and developed liver cirrhosis shortly after, had a significant population of bone marrow-derived $\alpha\text{-}SMA^+$ myofibroblasts. The majority of the bone marrow-derived $\alpha\text{-}SMA^+$

myofibroblasts were CD45-, however a small number of these bone marrow-derived α-SMA$^+$ myofibroblasts were also CD45$^+$, bonafide fibrocytes (82).

Origin of Fibrocytes: The Spleen

The spleen has also been shown to be a source of fibrocytes. Fibrocytes can be readily cultured from a CD11b$^+$ CD115$^+$ Gr1$^+$ population of splenic monocytes (194). Kidney fibrocytes contributing to fibrosis were demonstrated to originate from the spleen in mice with kidney fibrosis (215).

Chemokine-mediated Fibrocyte Trafficking

Chemokine/chemokine receptor trafficking is the essential mediator of leukocyte trafficking to sites of injury, a process known as 'haptotaxis' (265). The majority of research of chemokine-mediated trafficking has revolved around its function in immune processes (237). Chemokines can be separated into 3 different subgroups: inflammatory, hemostatic, and dual functioning (237). The function of chemokines is not limited to simple trafficking of cells, they activate numerous signaling pathways vital to the regulation of the immune system (33; 187; 193). After cells migrate to the site of injury, chemokines bind to the partner G protein-coupled receptors on their cell surface, triggering signaling pathways (271). Additionally, the variable expression of chemokines by immune cells has allowed researchers to mark specialized subsets of immune cells based on their unique expression of chemokine receptors (210; 237).

A few years after their discovery, fibrocytes were found to express the inflammatory chemokine receptors CCR2, CCR3, CCR5, and the homeostatic chemokine

receptors CCR7, and CXCR4. Chemotaxis assays with several chemokines demonstrated that chemokine receptors on fibrocytes were functional to induce motility (Table 2) (2; 85; 118; 184; 229).

The expression of chemokine receptors can dictate which tissue fibrocytes are likely to migrate to. Fibrocytes expressing CCR2 are likely to traffic to injured kidneys, as do fibrocytes expressing CXCR6 (48; 297; 301). Fibrocyte trafficking to the lungs has been demonstrated to occur through numerous chemokine receptors including CXCR4 and CCR2 (74; 104).

Chemokine mediated migration of fibrocytes to injury sites is essential to the development of fibrosis in numerous murine models of fibrosis. Studies have shown that the abrogation of fibrocyte trafficking to tissues is accompanied by decreased numbers of infiltrating fibrocytes, decreased collagen deposition, and decreased expression of ECM proteins, preventing the development of fibrosis (170; 196; 257). Inhibition of fibrocyte trafficking can also decrease the level of circulating PBMC fibrocytes, as well as cause a decrease in fibrocyte differentiation to α-SMA myofibroblasts (136; 143).

The participation of fibrocytes in disease of mice and men

Since their discovery over 30 years ago, fibrocytes have primarily been implicated in fibrotic diseases. In murine models of lung, kidney, and cardiac fibrosis, the severity of fibrosis, is almost completely dependent on the level of infiltrating fibrocytes in the target organ. There was also shown to be a correlation between fibrocyte levels and disease severity in murine models and human fibrotic disease. However, fibrocytes also participate in non-fibrotic disease, including asthma airway remodeling, mitral valve degeneration, Graves' diseases, and septic peritonitis (21; 22; 68; 192; 211; 315).

Table 2. Chemokine receptors expressed by human and murine fibrocytes

Chemokine Receptor	Expression	
	Human	Mouse
CCR1	−	+
CCR2	−	+
CCR3	+	+
CCR4	+	?
CCR5	+	+
CCR6	−	?
CCR7	+	+
CCR9	+	?
CXCR1	+	?
CXCR2	−	?
CXCR3	+	?
CXCR4	+	+
CXCR5	−	?
CXCR6	−	+

Symbols represent positive expression (+), no expression (-), expression yet to be examined (?).

It has recently been demonstrated that fibrocytes are a unique subset of circulating myeloid derived suppressor cells (MDSC) (244; 315). MDSC aid in the survival of tumor cells in humans and mice via secretion of angiogenic factors, growth factors, and suppression of the host immune system (239; 315; 319). Isolated MDSC fibrocytes from patients with metastatic cancer increased angiogenesis and inhibited T-cell proliferation *in vitro* (315). In a murine model of tumor pulmonary metastasis, inhibiting the differentiation of MDSC to fibrocytes effectively decreased lung metastasis (244). A very recent study identified circulating MDSC-fibrocytes in patients with COPD. Patients with higher levels of circulating MDSC-fibrocytes had greater preserved lung function (294). The researchers postulated that MDSC-fibrocytes slowed the progression of disease by suppressing the T-cell mediated inflammation in the small airways of patients with COPD.

Heart disease

Cardiovascular disease is the leading cause of death around the world and accounts for one third of all deaths in the United States (30). It has been estimated that ~44% of Americans will have some form of coronary vascular disease by 2030 (186). Fibrotic remodeling of the heart interferes with blood circulation, primarily in the left ventricle, often leading to cardiac failure (37; 153). Numerous animal models of cardiovascular disease have demonstrated that fibrocytes are involved in the fibrotic remodeling of the heart after injury.

The renin-angiotensin system (RAS) is the foremost endocrine mechanism for regulation of the cardiovascular system. The regulatory activity of RAS centers around

the production and processing of angiotensin II (Ang II), a peptide hormone generated from the cleavage of angiotensin I (Ang I) by the angiotensin converting enzyme (ACE) (170). Ang II functions through the angiotensin type 1 receptor (AT_1R) and the angiotensin type 2 receptor (AT_2R) (170).

The Ang II-induced cardiac fibrosis murine model is commonly used to study the pathogenesis of cardiac fibrosis. This model highlights the substantial role of fibrocytes in the development of fibrosis, as well as the relationship between fibrocytes and Ang II that mediates cardiac fibrosis. Administration of Ang II increases fibrocyte recruitment to the heart, and expression of TGF-β1, and collagens I and III (103). These fibrocytes account for up to 68% of the population of collagen producing cells in the heart (272; 295). Histone deacetylase (HDAC) inhibitors were shown to block Ang II-induced fibrosis. Investigation of the mechanism by which HDAC inhibitors prevent cardiac fibrosis revealed that HDAC inhibitors function by blocking fibrocyte differentiation to myofibroblasts in the heart (288).

Ischemic cardiomyopathy, the inadequate ability of the heart to pump blood, arises from the narrowing of the blood vessels responsible for supplying the heart with blood and oxygen. Fibrotic cardiomyopathy (I/RC) is recapitulated in mice by narrowing the left anterior descending artery (65; 104). Fibrocytes are increased in the hearts of mice subject to I/RC, making up 3% of the population of non-cardiac muscle cells. Treatment with serum amyloid P (SAP) decreases the number of fibrocytes in the heart, inhibiting the development of cardiac fibrosis and ventricular dysfunction (104).

Myocardial infarction (MI), or myocardial cell death, is caused by a prolonged period of oxygen deprivation of the heart. MI modeled in mice is performed by

permanent ligation of the coronary arteries (136). The role of fibrocytes in MI is a beneficial one. After MI the formation of a robust collagen scar is vital to maintaining the structural integrity of the heart necessary to properly pump blood throughout the body (55; 249). Fibrocytes have been demonstrated to actively participate in the formation of scar tissue, by producing and depositing collagen in the infarct area neoangiogensis (180; 272). In MI the recruitment of fibrocytes augments cardiac remodeling (87).

Fibrocytes in human cardiac disease

Increased numbers of fibrocytes are found in cardiac tissue from patients with coronary heart disease (CHD). Additionally, the number of these fibrocytes are directly correlated with disease severity (152). Circulating fibrocytes are increased in patients suffering from hypertrophic cardiomyopathy (HCM) with reactive fibrosis. However, this increase was not found in HCM patients without reactive fibrosis (75). Fibrocytes make up a large portion of mitral valve stromal cells and their dysregulation has been postulated to mediate myxomatosis mitral valve degeneration (21).

Patients with hypertensive heart disease have higher numbers of circulating fibrocytes compared to healthy individuals. Additionally, the level of these circulating fibrocytes positively correlated with disease severity (129). Patients with previous MI have decreased levels of circulating fibrocytes compared to healthy individuals and patients with stable angina (76). This finding falls in line with the beneficial role of fibrocytes in murine models of MI.

Kidney Fibrosis

The penultimate stage of all kidney maladies, no matter the underlying etiology, is chronic kidney disease (CKD) (71). In 2013 alone, almost one million deaths were reported to be caused by CKD, the NIH estimates that over 10% of the Medicare budget goes to treating this disease (124; 176). CKD is marked by the loss of function, sustained inflammation, and tubulointerstitial fibrosis of the kidney (263). The severity of fibrosis is the metric used to determine the progression of CKD.

Since CKD has many etiologies, there are a vast array of animal models used to study the specific features of CKD (307). These models recapitulate specific etiologies of CKD as well as symptoms of CKD (24). The murine model of ureteral obstruction (UUO)-induced progressive interstitial kidney fibrosis is commonly used to study the molecular mechanisms governing tubulointerstitial fibrosis (51). This model involves the surgical ligation of the ureter in mice. After surgery, fibrosis develops in 1-2 weeks and increases in severity over time.

A highly debated topic in the kidney research community is the origin of kidney myofibroblasts, the producers of the abundant ECM proteins found in kidney fibrosis (140; 191). Several cell types have been suggested as the source of myofibroblasts, including fibrocytes and pericytes (140; 251).

There is robust evidence showing that fibrocytes are a major source of myofibroblasts in the fibrotic kidney. Perhaps more importantly, even studies that did not directly investigate the contribution of fibrocytes to the myofibroblast population in the kidney have demonstrated the paramount role of fibrocytes in the development of fibrosis (157; 228; 306).

Research focused on the signaling mechanisms governing fibrocytes has shown that RAS signaling regulates fibrocytes during kidney fibrosis. In vitro, inhibition of AT_2R signaling increased the expression of collagen I after treatment with Ang II. Conversely, inhibition of AT_1R signaling decreased the expression of collagen after Ang II treatment. In vivo, $AT_2R^{-/-}$ mice have increased collagen expression and fibrocyte infiltration in the kidney compared to wild type mice in a model of TGF-β-induced renal fibrosis. Inhibition of AT_1R with valsartan decreased collagen expression and fibrocytes infiltration (228). These findings fall into line with what is well known about the relationship between the AT_2R and AT_1R receptors. Ang II signaling through the AT_1R activates profibrotic signaling pathways (59; 90; 128; 170). AT_2R is an antagonist of the AT_1R and has been shown to regulate the pro-fibrotic and inflammatory actions of AT_1R (1; 189; 197).

The CXCL16/CXCR6 signaling axis has emerged as a significant mediator of fibrocyte trafficking in kidney fibrosis. After fibrotic inducing injury, the levels of CXCL16 expression in kidney epithelial cells significantly increases. This observation was made in three different models of kidney fibrosis, suggesting that CXCL16 upregulation may be a universal early mediator of renal fibrosis (48; 150; 157). In all three models, $CXCL16^{-/-}$ mice had lower levels of collagen deposition and lower numbers of myofibroblasts in their kidney, which was accompanied by a decrease in infiltrating fibrocytes (48; 150; 157). These data demonstrate that fibrocytes are a significant source of collagen in kidney fibrosis.

Kidney disease in humans

Fibrocytes have also been identified in human CKD. Fibrocytes were identified in kidney biopsy samples from patients with CKD. Additionally, there was a positive correlation between the number of fibrocytes present in the kidney, and severity of kidney disease. Researchers also found that the number of fibrocytes in the kidney also correlated with urine CCL2 levels in patients suffering from CKD (227).

Fibrotic Lung disease

Lung diseases involving tissue remodeling, such as chronic pulmonary obstructive disease (COPD), cystic fibrosis, asthma, and idiopathic pulmonary fibrosis (IPF), are together leading causes of death in the United States (255) (19; 156; 160). Asthma, IPF, COPD, cystic fibrosis, and irradiation pneumonitis are sometimes considered to be types of fibrotic lung disease. Patients with lung fibrosis suffer from decreased pulmonary function, and there is only a 20% 5-year survival rate (86; 138; 238). Mortality occurs as a result of respiratory insufficiency (86). Recently, increased levels of fibrocytes have been detected in the blood and bronchoalveolar lavage fluid (BAL) of patients suffering lung fibrosis (44; 169).

Numerous murine models have been developed to recapitulate the features of disease found in human fibrotic lung disease (183). Bleomycin, fluorescein isothiocyanate (FITC), irradiation, and silica- induced pulmonary fibrosis are some of the models used to study the molecular mechanisms governing pulmonary fibrosis (135). These models have demonstrated the role of fibrocytes in the development of fibrotic lung disease (259; 298; 303).

CXCL12/CXCR4 signaling is the primary regulator of lung fibrosis in experimental animal models. Numerous studies have clearly shown that inhibition of the CXCL12-CXCR4 signaling decreases the recruitment of fibrocytes and amount of collagen in the lung. Administration of anti-CXCL12 antibody, or CXCR4 antagonists, significantly reduces the number of fibrocytes in the lung after bleomycin treatment (159; 168; 206; 302). The decreased number of infiltrating fibrocytes is tied to the decrease of collagen and development of fibrosis in the lungs (159; 206; 246). CXCR4 expression in fibrocytes is regulated via the PI3K/mTOR signaling pathways (168).

Fibrocytes have been demonstrated to participate in asthma. In a model of cockroach allergen-induced asthma, fibrocytes increase the production of IL-6 and TNF-α in response to the purified cockroach allergen Bla g2. Bla g2 activation is mediated by the CD206 surface receptor of fibrocytes (269). In a different mouse model of asthma, fibrocytes were identified as a source of bronchial myofibroblasts (233).

Models of pulmonary hypertension have highlighted the relationship between hypoxic conditions and fibrocytes. Hypoxic conditions increase the recruitment of fibrocytes to pulmonary arteries. Treprostinil, a drug approved for the treatment of pulmonary arterial hypertension, was found to reduce the number of infiltrating fibrocytes via inhibition of ERK signaling (195). Additionally, HIF-1α signaling mediates the recruitment of fibrocytes to bleomycin-injured lungs through PI3-kinase and mTOR signaling. In vivo, rapamycin, an inhibitor of mTOR, treatment decreased the level of circulating and lung $CXCR4^{+}$ fibrocytes concomitant with a decrease of collagen in the lung (168).

Fibrocytes in lung disease in humans

Fibrocyte levels in patients with fibrotic lung disease can serve as biomarkers of disease. Patients with asthma have increased levels of circulating fibrocytes (277), additionally fibrocyte levels correlate with the severity of asthma (138). Elevated levels of circulating fibrocytes also correlate with decreased survival in patients with IPF and COPD (277; 313). In patients with COPD, spikes in the levels of circulating fibrocytes were indicative of periods of disease aggravation (69). In patients suffering from IPF, fibrocyte levels correlate with disease severity. Additionally, the highest level of fibrocytes were found in patients with recently aggravated disease (179). Increased fibrocytes are also seen in patients with pulmonary fibrosis, bronchiolitis obliterans, and cystic fibrosis (10; 93).

Fibrocytes in other diseases

The participation of fibrocytes in disease spans well beyond these mentioned maladies. Fibrocytes participate in forming keloid scars, remodeling of skin injury in burn patients, promoting metastatic cancer, and reprogramming splenic megakaryocytes in patients suffering from idiopathic myelofibrosis (116; 308; 315).

Fibrocytes, a fresh perspective on disease

It is clear that fibrocytes cannot be boxed into any one category, capable of being reparative or pathogenic, and anti- or pro-inflammatory (272). Elevated levels of fibrocytes in patients can serve as a marker of increased as well as decreased disease severity (129; 277). Abrogation of fibrocytes can halt the development of disease (246).

Conversely, treatment with fibrocytes can promote injury repair (192). Fibrocytes recruited in the early stages of disease promote injury and disease, whereas fibrocytes recruited in the late stages of disease may promote injury repair (184). Additionally, fibrocytes isolated from patients suffering from disease, are phenotypically distinct than those isolated from healthy patients (118).

Initially associated and studied in fibrotic disease, fibrocytes are increasingly being studied in non-fibrotic diseases. Research centered around fibrocytes has started to fill in gaps of the pathogenic mechanisms governing these diseases. These oddly shaped cells are in a league of their own, managing to take center stage in an ever-growing number of diseases.

RADIATION

Radiation – It is all around us

Every day humans are constantly exposed to varying forms of radiation. It is all around us, in different forms. Some types of radiation, such as radio waves and microwaves, are harmless and do not possess enough energy to alter chemical bonds or atomic structures. Some types of radiation are very harmful and are known as "ionizing radiation", which include x-radiation and gamma radiation. Ultraviolet (UV) radiation is not classified as ionizing, however it still has enough energy to harm living organisms (89). The deleterious effects of ionizing and UV radiation are dependent on the dose of radiation (how much energy) and dose rate (how long you were exposed) (5; 97) as well as specific genetic factors (39; 61; 97; 121; 304). Additionally, the level of damage

sustained at similar doses of exposure differs between organisms and cell types (38). For example, insects exposed to doses of radiation that are lethal to humans survive and thrive (27).

Sources of Radiation Exposure in Humans

Exposure to radiation can be therapeutic, accidental, occupational, or weaponized (Table 3). The variability in the dose and type of radiation that can occur in these different settings makes it difficult to accurately predict the long-term and short-term health effects of radiation exposure (15; 287).

Radiotherapy is an indispensable tool in the treatment of malignant and non-malignant neoplasms (63). Although treating patients with higher doses of radiation increases the elimination of cancerous cells, these higher doses also translate into an increased risk of late radiation-induced injury of these patients (26; 161; 205; 223; 247). Balancing the potential of benefit and harm often place physicians in a quandary (73). However, medical and technological advancements have significantly decreased secondary injury in healthy tissue. Advancements in DNA sequencing have made radiogenomics, determining a patient's radiosensitivity based on single nucleotide polymorphisms (SNPs), a tool to create patient-specific regimes of radiotherapy to further reduce the risk of late term radiation-induced injury (130; 131; 284).

Accidental and weaponized radiation exposures present a different set of challenges for both researchers and physicians. In emergencies, the type of ionizing radiation, total body area, and dose rate and length of exposure time must be assessed as quickly as possible (80). The growing possibility of a large-scale radiation accident has

Table 3. Reported radiation overexposure accidents by sector and type of overexposure worldwide, 1980-2013.

Characteristics of overexposure	Reported Accidents	No. People Overexposed	Deaths
Industrial	**169 (27%)**	**513 (22%)**	**45 (24%)**
Local organ	1	1	0
Local skin	120	158	1
Local skin & Global	34	323	35
Global	14	31	9
Radiation Therapy	**202 (32%)**	**1127 (47%)**	**96 (51%)**
Local Organ	129	407	3
Local skin	61	523	28
Local skin & Local organ	9	182	58
Local skin & Global	2	13	0
Local organ & Global	1	2	7
Fluoroscopy	**194 (31%)**	**400 (17%)**	**0 (0%)**
Local Organ	41	41	0
Local Skin	152	358	0
Local organ & Global	1	1	0
Orphan Source	**32 (5%)**	**225 (9)**	**37 (19)**
Local skin	7	9	0
Local skin & Global	20	171	31
Global	5	45	6
Military	**4 (1%)**	**64 (3%)**	**12 (6%)**
Local skin	1	1	0
Local skin & Global	1	59	10
Global	2	4	2
Other*	**33 (5%)**	**61 (3%)**	**0 (0%)**
Local organ	2	2	0
Local skin	29	57	0
Local skin & Global	1	1	0
Global	1	1	0
Total	**634**	**2390**	**190**

prompted the development of the National Institutes of Health Radiation Countermeasures Program (RCP), which oversees numerous programs that include the development of countermeasures against accidental and weaponized radiation exposure and dosimetry tools (106; 231).

The Basic Mechanisms of Radiation Injury

Ionizing radiation damages biological molecules in living organisms. Ionizing and UV radiation alters the molecular composition of DNA and other biological molecules through hydrolysis, hydroxylation, photoisomerization, and other organic reactions (32; 158; 212; 261). Damage to these macromolecules triggers a complex cascade of repair, inflammatory, and cell death signaling pathways (115; 154).

DNA Damage

Radiation-exposure introduces single and double stranded breaks in the phosphate backbone of DNA. Double stranded DNA breaks (DSB) are responsible for the more deleterious effects of radiation damage: chromosomal mutations (198). Radiation-induced DNA DSBs can be repaired through homologous recombination or through non-homologous DNA end joining (NHEJ) pathways (258; 273). The specific repair method used is governed by multiple factors (245). NHEJ can be error prone and is responsible for introducing chromosomal mutations after radiation-induced DNA damage (46; 151). The mutation of key cell cycle regulatory genes can result in uncontrolled cell replication and the development of cancer (99; 220; 222).

Genetic mutations are not the only biological consequence of DSB. Ionizing radiation-induced DSB recruits the ataxia telangiectasia mutated protein (ATM) (256), which self-activates (219) and in turn phosphorylates p53 (43). The accumulation of phosphorylated p53 initiates cell cycle arrest (43; 127). At this point the cell may successfully repair the DNA damage, undergo apoptosis, or remain in a permanent state of cell-cycle arrest known as senescence (41; 52; 56; 221).

Generation of Reactive Oxygen Species (ROS)

Ionizing radiation cleaves water and creates numerous reactive oxygen species (ROS), hydroxide radicals ($OH^{\cdot}$), hydrogen peroxide (H_2O_2) and superoxide anions ($O2^{\cdot -}$) (91; 100; 178). These ROS self-propagate and damage DNA and other biological molecules (8; 217). The radiolysis of water also generates hydroxyl radicals and aqueous electrons which damage DNA and other biological molecules (20; 92; 100). The consequences of ROS-induced DNA damage are similar to those of radiation-induced DNA damage and utilize the same repair mechanisms (62; 245). ROS are involved in numerous physiological cell processes; however, due to their high reactivity, their levels are normally tightly regulated. Disruption of their homeostatic levels activates numerous injury response mechanisms inside cells (144; 162).

Consequences of radiation injury

Radiation exposure can cause both short- and long-term injuries. Types of early injury after radiation exposure include: the suppression of the hematopoietic system (165), gastrointestinal damage (165), pneumonitis (282), and erythema and desquamation

of the skin (165). The types of late injury that occur after radiation exposure include: lung (126; 240), cardiac (98; 260), bone marrow (12), and dermal fibrosis (250), necrotic wounds (64), cardiac disease (98; 260), and neurological decline (200) (Figure 2). Additionally, over time, there is an increased risk of developing solid tumors (31; 34; 276), leukemia (12; 29), and myeloid neoplasms (12; 223) after radiation exposure.

Immediate Injury

Acute Radiation Syndrome (ARS) occurs in response to high doses of total body radiation exposure (80). ARS is a multi-systemic response to radiation exposure consisting of injuries to the gastric, pulmonary, nervous, and hematopoietic systems (80; 283). In the Chernobyl and Tokai-mura nuclear reactor meltdown catastrophes, many of those exposed to radiation developed ARS, which was lethal in many cases (119; 173). The former Soviet spy Alexander Litvinenko was poisoned with Polonium210 laced tea, and died of severe ARS (167). The use of Polonium210 was ingenious, albeit sadistic, given that it is only lethal if ingested, making it rather easy to transport (145).

Late Injury

Early and late radiation injury were originally described as two temporal and cellular disconnected phases, in which early injury was governed by a population of radiosensitive cells and late injury was mediated by a separate population of radioresistant cells (57). However, we now know that late radiation injury is an insidious process initiated immediately following radiation-exposure.

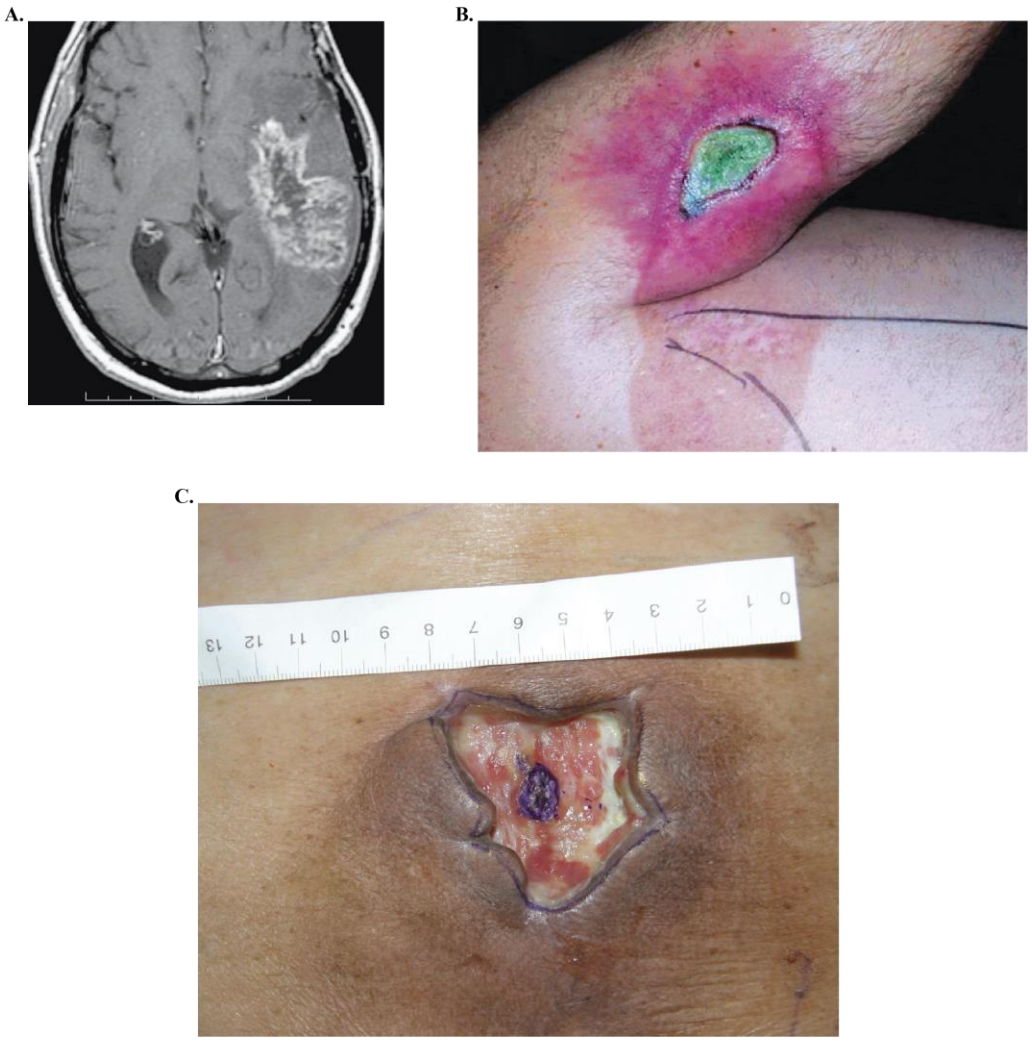

Figure 2. Examples of radiation injury

A. Axial post–Gd-DTPA T1-weighted image of Swiss-cheese appearance of contrast enhancement in a case of surgically proved radiation necrosis. **B**. A 52-year-old man underwent an ablative procedure for supraventricular arrhythmias, and a painful ulceration developed on the posterior surface of his right arm four months later. His arm had accidentally been positioned within the radiation field during the 10-hour procedure. The estimated dose of radiation was in the range of 1500 to 2000 cGy. After plastic surgery, the patient's ulceration healed, and his pain resolved. **C**. 89-year-old woman underwent a uterine cancer surgery followed by 50-Gy fractionate radiation therapy 40 years previously. In 10 × 10 cm area of radiation, 5 × 10 cm area was exposed. Bone, fascia, and muscle as well as skin and fat were affected.

The first evidence connecting early and late radiation damage was provided by Rubin and colleagues by demonstrating that immediately after radiation exposure TGF-β1 is significantly upregulated and remains so concurrent with increases in expression of collagen (77; 226). Since then our knowledge of the mechanisms governing injury response and repair has significantly expanded, allowing us to connect the immediate responses to radiation injury to the development of latent injury, especially fibrosis (309).

Radiation-Induced Fibrosis

Fibrosis is the accumulation of excessive extracellular matrix proteins, especially collagen I, resulting in aberrant tissue remodeling that can occur in virtually every tissue in the body. Fibrosis is the result of dysfunctional wound repair or constant injury that culminates in sustained inflammation. The exacerbated inflammatory response after radiation injury increases a patient's risk of developing fibrosis (248; 296). The underlying theme in radiation-induced fibrotic diseases is the dysregulation of TGF-β, a pleotropic cytokine that serves as a potent regulator of both anti-inflammatory and pro-inflammatory processes (230)(163; 275). Perturbations in the TGF-β immune-regulated inflammatory response can set up a situation of chronic inflammation, creating an environment more susceptible to fibrotic remodeling (267; 291). TGF-β drives pathogenic fibrotic remodeling by stimulation collagen production in myofibroblasts, fibroblasts, and fibrocytes (2; 88; 112; 204; 218; 314). TGF-β also promotes the survival and proliferation of these collagen-producing cells (113; 123; 214; 317).

Radiation-induced pulmonary fibrosis is an important field of research in the radiation community. In patients undergoing radiotherapy have been found to have

increased serum and bronchoalveolar TGF-β levels (23; 279). Increased levels of TGF-β after stem cell transplantation are correlated with greater risk of developing radiation-induced liver and lung fibrosis (13). The correlation between TGF-β and the increased risk of developing radiation-induced fibrosis is common among different types of radiotherapy (94; 126; 148). To examine the relationship between TGF-β and radiation-induced pulmonary fibrosis many animal models that expose mice to thoracic irradiation have been developed (101; 183). Investigations using these animal models have shown that TGF-β levels are upregulated in the lung tissue and the bronchoalveolar lavage (BAL) after exposure to thoracic irradiation (225; 310). These animal models have also provided evidence that abrogation of TGF-b signaling is able to dampen irradiation-induced pulmonary fibrosis (78). The wealth of information gleaned using these murine models suggest that therapies targeting TGF-β may aid in the management of pulmonary fibrosis in patients undergoing radiotherapy (11).

The need for new insights on radiation injury

The overall incidence of cancer has decreased over the last 3 years, owing in part to the increased public awareness of the importance of early screening and new treatments (117; 175; 254). Radiotherapy is still an important modality in the fight against cancer, making it vital to keep advancing our knowledge of the mechanisms of radiation injury. Also, the scenario of large-scale radiation exposure to the public should not be overlooked. Characterizing new mechanisms of radiation injury is important for the successful treatment of patients and for the safety of the public.

THE BONE MARROW ENVIRONMENT

Bone marrow is the site where hematopoiesis occurs and where hematopoietic stem cells (HSCs) are housed and maintained. In mice, 'active' bone marrow, marrow active in hematopoiesis, is present in the cavities of the humeri, femur, sternum, and pelvis. In adult humans, most of the active, red marrow is in the femur and pelvis (181; 268). Primitive HSCs self-renew throughout their lifespan (84). Primitive HSCs, also called long term- (LT-) HSCs, give rise to short term- (ST-) HSCs and lineage committed HSCs, which have limited self-renewal capability. In addition to HSCs, another group of stem cells, mesenchymal stem cells (MSCs), also reside in the bone marrow (252). MSCs differentiate into the stromal cells that support and maintain HSCs (125; 171).

Stromal Cells and HSC Niches

Bone marrow stromal cells consist of osteoblasts, chondrocytes, adipocytes, and fibroblasts (209). Additionally, endothelial cells in the bone marrow are important regulators of hematopoiesis and are often lumped into the category of bone marrow stromal cells (290). Stromal cells provide a physical scaffolding that houses HSCs. However, their role goes beyond mechanistic support. Stromal cells help tightly regulate the proliferation of HSCs through a variety of mechanisms (40; 171; 252).

HSCs reside in specific areas of the bone marrow labeled “niches”, these niches are responsible for regulating HSC proliferation, differentiation, and state of quiescence (97; 141; 292). These niches are composed of numerous cell types including, stromal cells, neuronal cells, specialized macrophages, and megakaryocytes (107; 155; 290; 292;

305) (Figure 4). There is evidence of two distinct HSC niches in the bone marrow the endosteum niche (also known as the osteoblastic niche), and the vascular niche (also known as the reticular niche) (40; 274; 290). The endosteum niche is found along the bone surface of the marrow cavity and the vascular niche is found at the bone marrow sinusoids (40; 274; 290). Immunofluorescent imaging has shown that most HSCs reside in the vascular niche (~70%), while the endosteal niche houses ~20% of the HSCs. The remaining ~10% of the population is randomly distributed in the bone marrow (196). It has also been proposed that quiescent HSC and quiescent nestin^{+} MSC constitute their own exclusive niche (171).

HSC Quiescence

The maintenance of HSCs in a state of quiescence prevents their premature exhaustion by limiting cellular stress from normal metabolic activity (199). At any time in regular conditions, the majority of LT-HSCs (~70%) are quiescent and arrested in G0 (289). Quiescence is thought to render LT-HSCs radioresistant, allowing them to repopulate injured and depleted bone marrow. After restoring proper hematopoiesis, LT-HSCs return to their quiescent state (289).

The regulation of HSC quiescence is a complex process involving numerous cell types (149). Each HSC niche utilizes specific mechanisms to regulate HSC quiescence. In the endosteal niche, megakaryocytes and osteoblastic cells work in concert to activate HSC or to render them quiescent by manipulating myeloproliferative leukemia protein (MPL- the receptor for thrombopoietin) and thrombopoietin (TPO) signaling (312). Megakaryocytes also control quiescence of HSC through TGF-β1 signaling (318).

Osteoblasts also use angiopoietin-1/Tie-2 signaling to regulate HSC quiescence (14). HSCs localized around stromal $HG2^{+}$ perivascular cells are maintained in their quiescent state; however, the exact mechanisms governing this regulation is not yet known (141). Endothelial cells maintain HSCs quiescence via direct cell surface to cell surface contact (201). A shared mechanism regulating HSC quiescence between the two niches is the regulation of CXCL12 (96; 252). CXCL12 is responsible for retaining HSC in the bone marrow cavity, and maintaining HSCs quiescence (270).

HSC Oxidative Stress

In order to maintain their genomic integrity, HSC have many mechanisms to reduce oxidative stress, and limit the number of ROS (188). HSC reside in hypoxic areas of the bone marrow (54; 202). Additionally, these HSC and are themselves hypoxic and express high levels of HIF-1α (122; 196). HIF-1α expression increases HSC quiescence, which renders them more radioresistant (83). Cellular metabolism is suppressed in HSC by limiting the generation of mitochondria, which results in a decrease of cellular ROS (120). In vitro, HSC lose their replicative and differentiation ability when cultured in non-hypoxic conditions (54).

Radiation Injury to the bone marrow

Radiation exposure, both low and high dose, injure the HSC and MSC populations. However, MSCs have been shown to be more radioresistant than HSC (253). These injuries significantly depress hematopoiesis, not just by damaging the HSC population, but also by damaging the supporting MSC population (18; 97).

Early Injury

Hematopoietic suppression is the most obvious consequence of bone marrow radiation-induced injury. The extent of hematopoietic suppression is dependent on the radiation dose and total volume of bone marrow exposed (111). In severe cases of ARS, the suppression of blood cell production can be lethal. The production of myeloid and lymphoid cells after injury vary with dose of radiation exposure causing a misbalance in normal blood cell counts (45). The severity of myelosuppression is dose dependent which allows clinicians to obtain a crude estimate of a patients dose of radiation exposure (111). Radiation exposure is also immunosuppressive and, in the most severe cases, individuals may die from sepsis (42). Individuals subjected to extremely high doses of total body irradiation are subject to complete hematopoietic failure and require bone marrow cell transplantation to survive (6). After radiation exposure, hematopoietic growth factors are administered to help repopulate the mature blood cell population (109; 119).

Long-term Injury

Like radiation injury to other organs, the long-term sequelae of radiation injury are insidious. In individuals who have recovered, or are recovering from radiation exposure, blood cell counts normalize, giving the appearance that hematopoietic injury has resolved (264). However, radiation-induced hematopoietic injury may never completely heal (47; 53; 177).

Long-term radiation-induced injury can result in the development of myeloproliferative neoplasms (MPN) and leukemia (243). MPNs are clonal disorders

arising from multipotent stem cells characterized by unregulated proliferation, and disparity, of trilineage myeloid cells (147). These cancers arise from genomic mutations caused by radiation-induced DNA injury (79). Interestingly, radiation exposure selects for certain leukemic mutations over others in irradiated HSC, suggesting a unique mechanism for radiation-induced leukemia (164). Over 30% of leukemias in the survivors of the atomic bombings of Hiroshima and Nagasaki developed these blood cancers (12; 29).

A serious long-term consequence of radiation exposure is the decrease of HSC self-renewal and pluripotency, also called stem cell pool failure (18; 165; 166). MSCs also suffer from decreases in self-renewal and pluripotency (18; 60; 236). These defects are long-lasting and are irreversible. Stem cells isolated from patients are still defective long after radiotherapy is completed (165). These injuries are believed to be caused by lower HSC engraftment in irradiated bone marrow in patients that have received radiotherapy (95; 264).

Mechanisms of long-term injury

Low-level radiation exposure that does not illicit apoptosis in LT-HSCs can cause accelerated senescence (242; 281). This has been observed both *in vitro* and *in vivo*. Isolated irradiated murine HSCs have increased levels of the senescence genes p16 and p19 (172). *In vitro*, low doses of radiation increase expression of p16 and senescence associated-beta galactosidase in HSC. Additionally, this increase in senescence markers occurred in the LT-HSC population verses the ST-HSC population (281). These findings

were confirmed by another study that additionally showed an increase in Arf expression after sub-lethal total body irradiation (TBI) (242).

After radiation exposure, ROS levels increase and elicit a state of persistent oxidative stress in HSC, resulting in DNA damage (280). The reduction of ROS after radiation injury has been demonstrated to decrease long-term hematopoietic injury (203; 299; 316). The use of resveratrol, an antioxidant, reduces the buildup of ROS, and inhibits senescence after nonlethal TBI. Additionally, isolated HSCs from resveratrol treated mice had higher capability for self-repair and differentiation, compared to those isolated from untreated mice (316). The connection between ROS, senescence, and decreased HSC function was also shown in a study evaluating the use of metformin in treating radiation injury (299).

There is also evidence that radiation exposure of MSCs leads to senescence (9; 56; 236; 278). Unfortunately, there is a dearth of information about the role of ROS in radiation-induced senescence in MSCs. The relationship between radiation exposure, ROS, and senescence in MSCs, has been examined in the context of autophagy. Inhibition of autophagy increases levels of ROS and senescence in isolated MSCs exposed to radiation (114).

Outside of the bone marrow

There is a robust area of research into the mechanisms of HSC and MSC radiation injury in the bone marrow. There is also information on how the changes that occur in hematopoiesis affect bone marrow injury; subsets of myeloid and lymphoid cells are suppressed at unique times after radiation exposure. It has been shown that after systemic

radiation, MSCs traffic throughout the entire body. While the response of other bone marrow derived cells has been investigated in the context of radiation injury, the response of fibrocytes, bone-marrow derived cells, has yet to be investigated.

GOAL AND AIM OF THESIS

An exponentially increasing number of diseases are associated with increased levels of fibrocytes in patients (182; 277; 294; 315). Fibrocytes are a peculiar population of leukocytes that express both hematopoietic and mesenchymal markers (36). These bone-marrow derived cells have been closely linked with a myriad of fibrotic diseases (25). Recently, evidence has been found linking fibrocytes to non-fibrotic diseases. These non-fibrotic diseases range from breast cancer to Lyme disease (68; 70; 262; 315).

The study of the relationship between bone marrow injury and fibrocytes is currently in its infancy. To thoroughly investigate the role of fibrocytes after bone marrow injury, we developed a mouse model of partial radiation-induced bone marrow injury. Total body irradiation is well established in the literature to engender bone marrow damage. After partial body irradiation, fibrocytes from non-irradiated tissue were interrogated for changes in number. Targeted injury of bone marrow will enable the investigation of the systemic response of fibrocytes after radiation-induced bone marrow injury. Elucidation of the mechanisms governing fibrocytes in diseases has identified new potential therapeutic targets. Understanding how fibrocyte levels response after bone marrow injury is the first step in development of potential therapeutics to treat bone marrow injury.

To create a mouse model of radiation-induced bone marrow injury, mice were subjected to varying doses of partial body irradiation and examined for signs of bone marrow injury. Changes in circulating and splenic fibrocyte levels were measured at various time points after partial body irradiation using flow cytometry.

This study provides a new model of bone marrow injury that can be used to investigate the mechanisms governing the response of fibrocytes after injury.

CHAPTER TWO: Study Results and Discussion

MATERIALS AND METHODS

Animals. C57BL/6J strain female mice (The Jackson Laboratory, Bar Harbor, ME, USA) weighing 17.5-21.5 g were 12–14 weeks of age at the time of irradiation. Mice were kept in a barrier facility for animals accredited by the Association for Assessment and Accreditation of Laboratory Animal Care International. Mice were housed in groups of four. Animal rooms were maintained at 21 ± 2°C, 50% ± 10% humidity, and 12-h light/dark cycle with commercial freely available rodent ration (Harlan Teklad Rodent Diet 8604, Frederick, MD, USA). Acidified water (pH = 2.5-3.0) was available ad libitum to control opportunistic infections. All animal handling procedures were performed in compliance with guidelines from the National Research Council for the ethical handling of laboratory animals, and were approved by the USUHS Institutional Animal Care and Use Committee.

Irradiation. For thoracic irradiation, mice were anesthetized with intraperitoneal injections of 150 mg/kg ketamine plus 18 mg/kg xylazine. Anesthetized mice were irradiated in the prone position in Lucite jigs (3 mm thick) (Precision Machine & Tool, Beltsville, MD) to prevent movement with forelimbs secured in the radiation field using an RS2000 small animal irradiator. Following irradiation, anesthetized animals recovered on warming pads prior to being returned to their original cages. The RS2000 provides a cone-shaped radiation field with irradiation at 12.39 to 40.50 cm from the X-ray source. For dose measurements, irradiation was performed with the following settings: 160 kVp,

25 mA, 90 sec irradiation time, and 0.3 mm Cu beam filtration. The approximate HVL provided by the manufacturer was 0.62 mm Cu. The University of Wisconsin Medical Radiation Research Center (UW MRRC) provided eight acrylic mouse phantoms with three (1×1×1mm) Harshaw TLD-100 microcubes (Thermo Electron Corp., Oakwood Village, OH) embedded in each phantom. The cylindrical phantom had a dimension of 27 mm in diameter (D) × 65 mm in length (L) and was stabilized by a cylindrical insert 15 mm (D) × 27 mm (L) with a 3mm thick stand. The custom mouse shield was placed on the floor of the irradiator with the mouse thoracic region approximately 43.75 cm from the X-ray source. The dose measurement was conducted twice to account for setup error and reproducibility. The UW MRRC is an accredited calibration laboratory and processed the TLDs using a national standard with an expanded uncertainty (k=2) of 5%. The dose rate was reported for each position 1 – 4 as absorbed dose rate to water (ADRW, Gy/min) and the two repeated measurements were averaged together. The average ADRW at any position was 0.775 Gy/min with 97% uniformity and, accounting for TLD measurement uncertainty, had an expanded uncertainty of ± 5.2%.

Histology. Sternebrae, humeri, and femurs were surgically removed from euthanized animals and fixed in 10% neutral formalin overnight. Tissues were paraffin blocked and stained using standard methods for hematoxylin and eosin. Slides were evaluated and subjectively scored by a veterinary pathologist. Bone marrow sections were digitally scanned using the Ziess Axioscan and images for publication were produced with Zen Lite software (Carl Ziess, USA).

Peripheral blood mononuclear cell (PBMC) isolation for FACS. Mice were euthanized with pentobarbital (10 mg/kg). Blood was collected via cardiocentesis using heparin-charged 25-gauge needle and syringe, and placed in EDTA-coated microtainer tubes (Becton-Dickson, Franklin Lakes, NJ). Blood was diluted to 10 ml in phosphate buffered saline (PBS), and PBMC were isolated via density gradient centrifugation using 4 ml Lymophocyte Separation media (Mediatech, Manassas, VA), then resuspended in PBS and centrifuged at 2000 rpm for 35 min at 20°C. Lymphocytes layers were recovered from the gradient and diluted up to 15 ml with PBS. Cells were centrifuged at 300 ×g and washed with 10 ml PBS twice more.

Bone marrow and spleen cell isolation. Humeri and femurs were surgically removed from euthanized animals, and flushed with sterile PBS. Collected bone marrow and spleen tissues were manually filtered to separate cells using a 40 µM cell strainer (Cell Treat, Pepperell, MA). Cells were diluted to 30 ml with PBS and centrifuged at 300 ×g for 10 mins at room temperature. After washing, red blood cells were lysed in 2 mL (for bone marrow) and 5 mL (for spleen) of ammonium-chloride-potassium (ACK) lysis buffer (Lonza, Basel, Switzerland) for 1 min for bone marrow and 5 min for spleen at room temperature. Cells were then diluted to 20 ml with PBS and pelleted as before. Cells were washed twice as before with PBS and resuspended in 1 ml PBS.

FACS staining. Cells isolated from spleen, bone marrow, and PBMCs cell were resuspended in ~200 µl and placed on 5 ml nylon cell strainer topped Falcon tubes (Corning Life Sciences, Corning, NY) and centrifuged for 10 min at 860 ×g at room

temperature. Cells were resuspended in 100 µl transferred to Falcon 96 well clear V-bottom nontreated polypropylene storage microplates (Corning). Cells were then stained with 1:40 dilution in PBS of LIVE/DEAD viability stain (Molecular Probes, Life Technology, Grand Island, NY) for 20 min in the dark. Cells were washed with FACs buffer (0.5% FBS, 0.05% NaN3 in PBS), and pelleted by centrifugation for 10 min at 860 ×g at room temperature, then blocked by the addition of 1 µl Mouse BD Fc Block (BD Bioscience, San Jose, CA) diluted in 99 µl FACS buffer, for a total of 100 µl per well, for 20 min on ice. Plates were centrifuged at 860 ×g for 5 min at room temperature, and supernatants were removed. Cells were washed once by the addition of 100 µl FACs buffer, and pelleted at 860 ×g at room temperature for 5 min. Cells were stained with Brilliant Violet 605-labeled CD45 (Cat#: 103140, Biolegend, San Diego, CA); phycoerythrin (PE) labeled CD41 (Cat#: 561850, BD Bioscience, San Jose, CA); and allophycocyanin (APC)-eFluor 780-labeled CD115 (Ref#: 47-1152-82, Affymetrix eBioscience, San Diego, CA) for 20 min on ice. Cells were then fixed and permeabilized with BD Cytofix/CytoPerm (BD Bioscience, San Jose, CA). Cells were stained with anti-Collagen type I antibody (0.5 µg/µL, Cat#: 600-406-103, Rockland Immunochemicals, Limerick, PA) in BD Perm/Wash buffer for 40 minutes at 4° C, with rocking. Cells were washed once in 100 µl BD Perm/Wash buffer (BD Bioscience, San Diego, CA) and pelleted at 860 ×g at room temperature for 5 min. Cells were then stained with anti-biotin-FITC (Miltenyi Biotech, San Diego) for 20 min on ice. After staining, cells were washed, pelleted, and resuspended in BD Perm/Wash. The following day stained cells were analyzed using a BD LSR II flow cytometer (BD, San Jose, CA). FACs data analysis was carried out with FlowJo data analysis software (FlowJo, Ashland, Oregon).

Statistical Analysis. Statistical analysis was performed using Graphpad Prism 7 (San Diego, CA). Results are represented as means ± SEM. P values of < 0.05 were considered significant. One-way ANOVA with Tukey's multiple comparison post hoc test was used for multiple comparisons.

RESULTS

Model for irradiation-induced bone marrow injury

Localized radiation has been shown to damage exposed bone marrow and effect non-irradiated tissues (102). In order to investigate the response of fibrocytes in the context of partial bone marrow radiation exposure, we developed a murine model of radiation-induced bone marrow injury. We selectively exposed the bone marrow of the sternum and humeri of adult female C57BL/6J mice by placing them inside a custom lucite jig with their humeri restrained alongside their sternum. A specialized lead shield was used to restrict the field of radiation to the thoracic cavity. This approach allowed us to ensure the bone marrow in the femur was not exposed to radiation (Figure 3).

Dose response of radiation-induced bone marrow injury.

Radiation injury is dependent on numerous factors; among them are the dose of radiation exposure and the total area of tissue exposed (161). We previously observed that 17Gy thoracic radiation depleted the bone marrow of the exposed sternum of mice at 60 days post irradiation (unpublished data). Since our new model placed the humeri in the field of radiation resulting in a larger total area of radiation exposure, we set out to determine what dose of radiation would provide bone marrow damage 60 days post irradiation.

We exposed mice to a single dose of 12Gy, 14Gy, 16Gy, or 18Gy irradiation and examined them 60 days post radiation for signs of bone marrow damage (Figure 3). The bone marrow is a complex organ. Identification of potential damage is done with the use

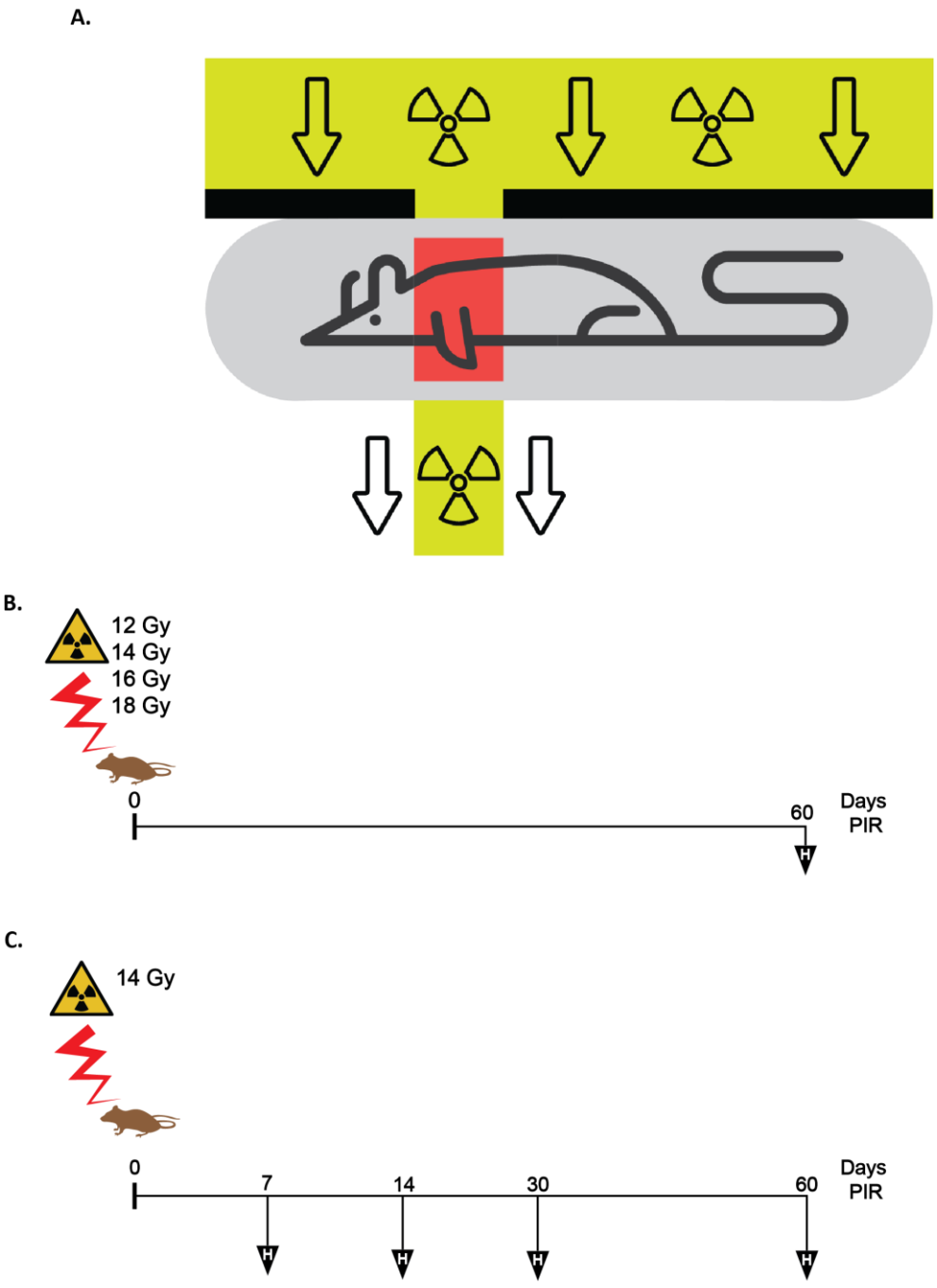

Figure 3. Model for irradiation-induced bone marrow injury.
A. Female C57BL/6J were placed in a lucite jig (gray area) with forelimbs placed parallel to the thoracic cavity, and irradiated in the prone position (red area). Targeted thoracic irradiation was achieved by positioning a custom lead shield over the radiation source (black line). **B.** Mice were exposed to varying dosages of irradiation to determine a suitable dose to illicit bone marrow damage at 60 days post irradiation. **C.** Mice were sacrificed and examined at the indicated time points after irradiation.

of histological stains to examine changes in cellular composition and the bone marrow stroma (268). Accordingly, the harvested sternum, humeri, and femur from irradiated mice were stained with H&E and examined for abnormalities in cellularity and cellular composition. There was no apparent damage to the bone marrow outside of the field of radiation of 12Gy, 14Gy, 16Gy, or 18Gy irradiation doses (Supplemental Figure 1).

We next examined the bone marrow of the sternum and humerus for any indications of radiation-induced damage. We found that radiation exposure resulted in varying degrees of bone marrow depletion. Bone marrow was scored based on degree of cellular depletion (Supplemental Figure 2-3). We first examined the humerus of the irradiated mice. We found varying degrees of depletion at all doses of radiation exposure (Figure 4). This depletion was most marked in the spongy marrow in the proximal and distal epiphysis. We further examined the bone marrow in the distal epiphysis and observed a paucity of osteoblasts and osteoclasts along the endosteum at all doses of radiation exposure (Figure 4D-E). Osteoblasts are readily seen in the bone marrow of sham-irradiated mice (Figure 4C, black arrows). We did observe a limited number of osteoblasts in the bone marrow of 18Gy irradiated mice (Figure 4G, black arrow). Additionally, macrophages laden with hemosiderin, an iron-storage complex (16), were present in depleted areas of bone marrow (Figure 4D-F, green arrow). This pigmentation is the result of the phagocytosis of surrounding red blood cells. Bone marrow from 12Gy and 14Gy irradiated mice showed a pronounced breakdown of the sinusoid compared to bone marrow from 16Gy and 18Gy irradiated mice (Figure 4C-G). The degradation of the sinusoidal network appeared to be correlated with the severity of bone marrow depletion.

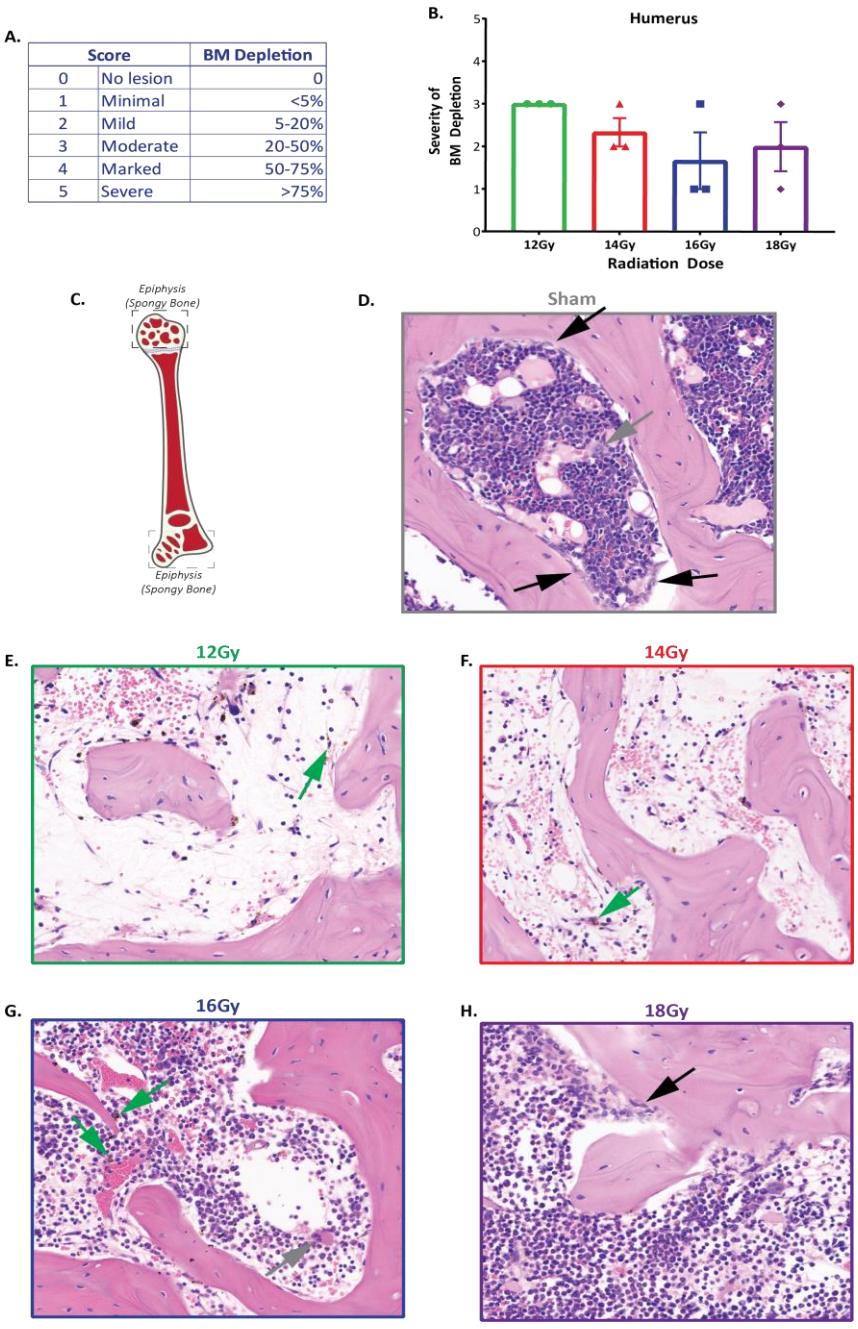

Figure 4. Dose response of radiation-induced bone marrow injury in the humerus, 60 days post injury.

At 60 days post irradiation mice were sacrificed and their bone marrow was stained with H&E and examined for any outstanding histological features. **A**. Criteria used for grading the severity of bone marrow depletion. Qualitative grading system of 0-5 was based on the overall percentage of bone marrow depletion veterinary pathologist **B.** Severity of bone marrow depletion after irradiation. **C.** Cartoon of humerus bone marrow cavity highlighting the location of spongy bone marrow areas examined. **D-H.** Histological examination of irradiated bone marrow for any outstanding features. Black arrows point to osteoblast and osteoclasts lining the endosteum. Gray arrows point to megakaryocytes. Green arrows point to hemosiderin laden macrophages.

Interestingly, we did not observe any correlation between severity of bone marrow depletion and dose of radiation exposure (Figure 4A, Supplementary Figure 4).

We proceeded to examine the bone marrow of the sternum. Unexpectedly, we found that only 14Gy and 16Gy, but not 12Gy and 18Gy irradiation elicited depletion of the sternum bone marrow (Figure 5A-B). Additionally, bone marrow depletion was not uniform among cavities within individual sternums (Figure 5B). Similar to the depleted areas of bone marrow in the humerus, macrophages containing hemosiderin were identified in the depleted areas of bone marrow in the sternum cavities (Figure 5C, green arrows). These pigmented macrophages are responsible for the phagocytosis of red blood cells that have escaped the sinusoid network in the bone marrow. 14Gy and 16Gy irradiation also diminished the sinusoids throughout the areas of depleted bone marrow in the sternum (Figure 5C). In the bony sections (trabecula) of the sternum bone marrow cavities, the osteoblasts and osteoclasts lining the endosteum were ablated (Figure 6D, black arrows).

Our histological examination of the humerus and sternum showed that all doses of radiation caused bone marrow depletion. However, we found no correlation between the dose of radiation exposure and the severity of depletion (Figure 4A, Figure 5A). Additionally, within groups of irradiated mice, there was no relationship to damage found in the bone marrow of the humerus and the bone marrow of the sternum. There was also variability in individual bone marrow cavities of the sternum (Figure 5B).

We found that 14Gy and 16Gy irradiation exposure elicited the depletion of the bone marrow in both the sternum and the humerus. Since the severity of bone marrow

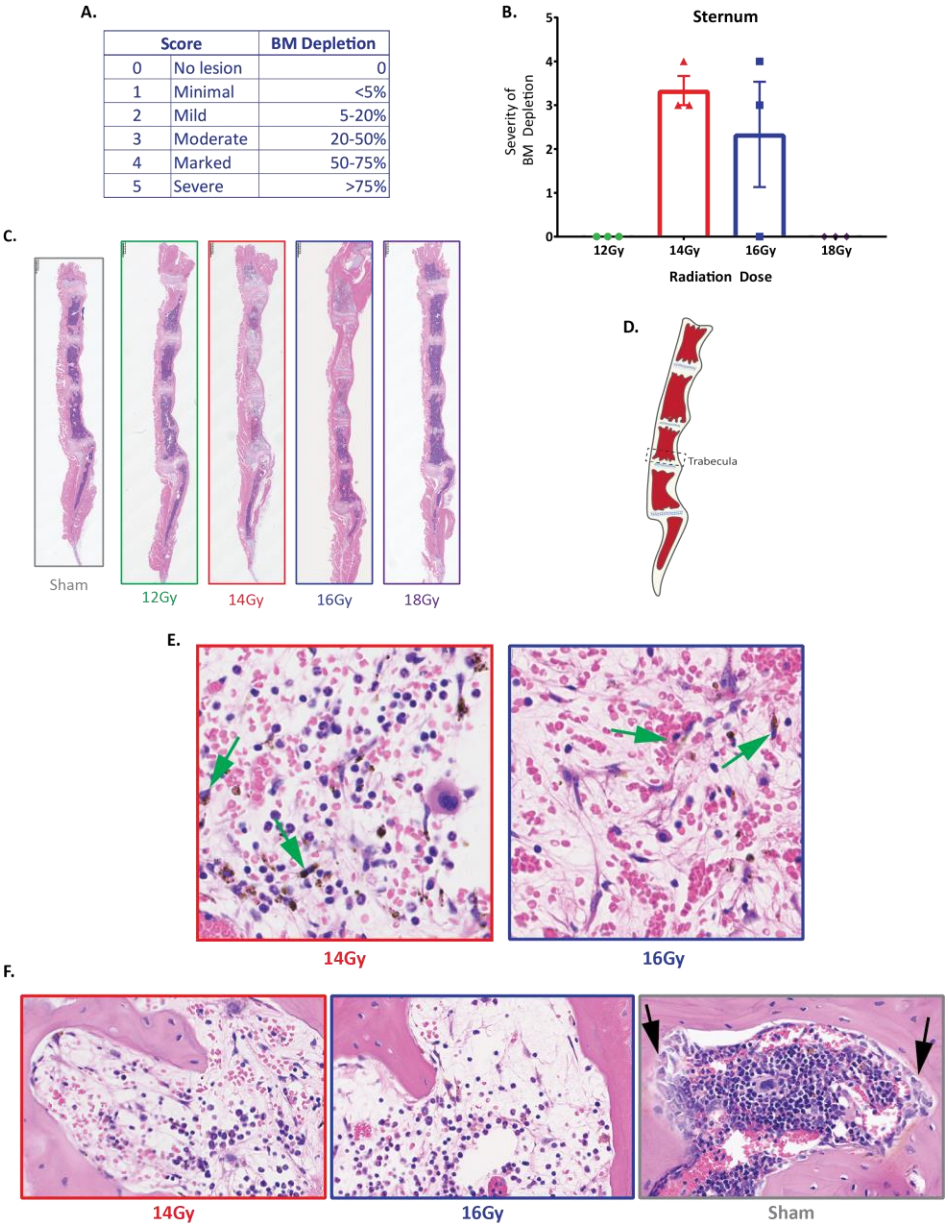

Figure 5. Dose response of radiation-induced bone marrow injury in the sternum, 60 days post injury.

At 60 days post irradiation mice were sacrificed and their bone marrow was stained with H&E and examined for any outstanding histological features. **A.** Criteria used for grading the severity of bone marrow depletion. Qualitative grading system of 0-5 was based on the overall percentage of bone marrow depletion veterinary pathologist **B.** Severity of bone marrow depletion was graded by a veterinary pathologist at a scale of 0-5. **C.** Representative images of sternums demonstrating varied severity of bone marrow depletion within individual sternums. **D.** Magnified view of the depleted areas of sternum bone marrow from 14Gy and 16Gy irradiated mice. **E.** Cartoon of sternum bone marrow cavity highlighting the trabecular areas of sternum bone marrow examined. **F.** Examination of 14Gy and 16Gy irradiated bone marrow for outstanding histological features. Black arrows point to osteoblast and osteoclasts lining the endosteum. Gray arrows point to megakaryocytes. Green arrows point to hemosiderin laden macrophages.

depletion was greater in the group of 14Gy irradiated mice, this was the dose used in our model of partial bone marrow irradiation.

Circulating fibrocytes increase in collagen expression 14 days post irradiation, and increase in frequency 30 days post irradiation

Fibrocytes contribute to the development of numerous fibrotic and non-fibrotic diseases, and increased numbers have been correlated with disease progression and severity (36; 233; 313). Characterization of human and murine fibrocytes has shown that fibrocytes do not express CD115, the receptor for colony stimulating factor expressed primarily on macrophages (194; 207; 215). Based on these data, circulating fibrocytes were identified as $CD115^{-}$ $CD45^{+}$ $ColI^{+}$ cells. The gate for identifying collagen expressing fibrocytes was determined using collagen unstained PBMCs (Figure 6A, Supplemental Figure 7).

To investigate the levels of circulating fibrocytes in irradiated mice at different time points, PBMCs were isolated 14, 30, and 60 days post irradiation, and analyzed using flow cytometry. A significant increase in the level of circulating fibrocytes occurred 30 days post irradiation. Sixty days post irradiation, the frequency of circulating fibrocytes returned to near baseline level (Figure 6B). In fibrotic disease, collagen expression in fibrocytes has been shown to increase over time (206). To examine potential changes in collagen expression, we calculated the mean fluoresce intensity (MFI) to determine the relative expression of collagen in isolated fibrocytes. We saw an increase in the relative expression of collagen 14 days post irradiation (Figure 6C). Additionally, a small but distinct population of collagen high expressing fibrocytes was seen 14 days post irradiation (Figure 6D). Thus, these data suggest that circulating fibrocytes increase after radiation-induced bone marrow injury.

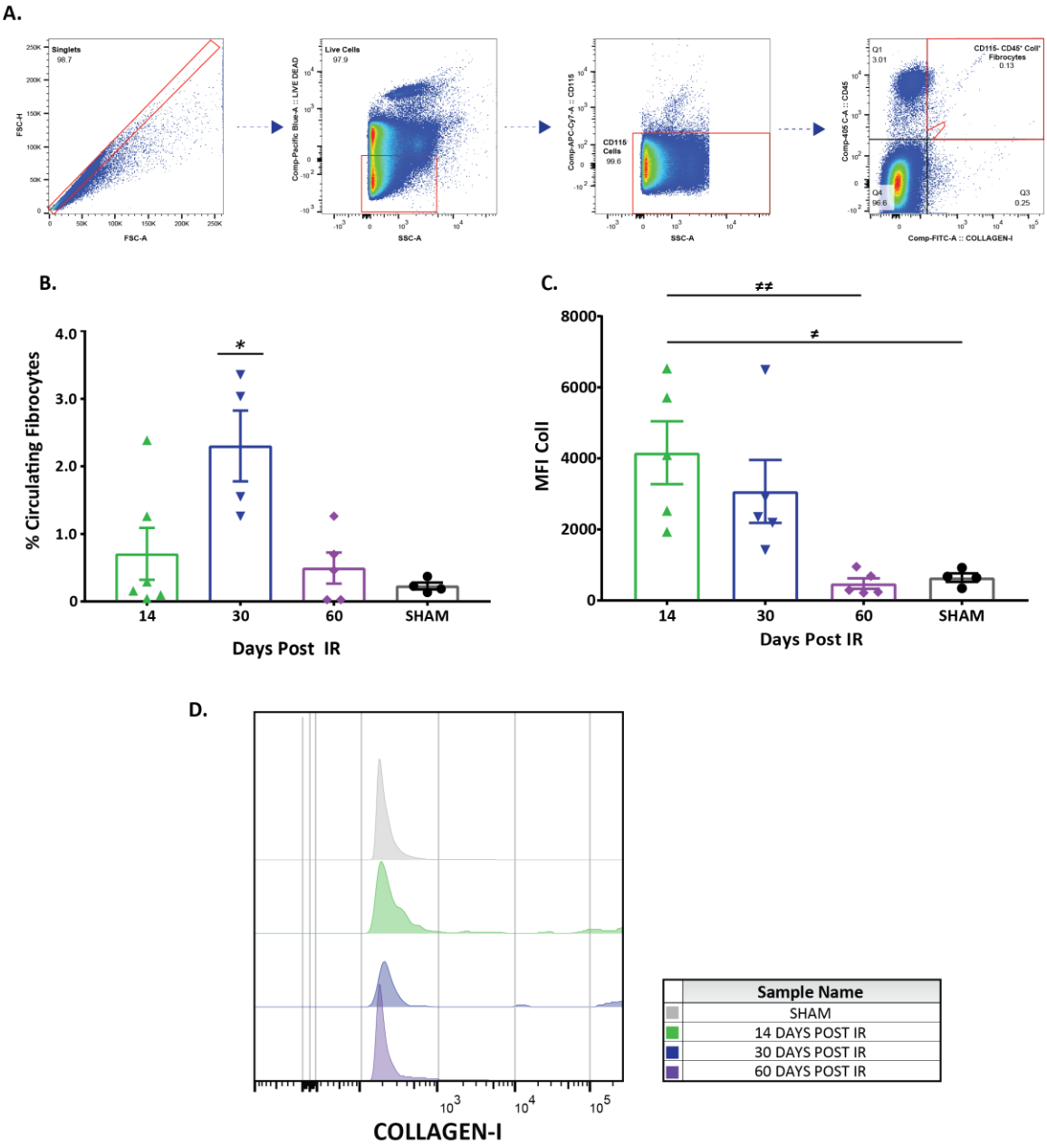

Figure 6. **The percent of circulating fibrocytes at various time points after 14Gy thoracic and partial bone marrow irradiation.**
Flow cytometry was used to determine the frequency of $CD115^{-}$ $CD45^{+}$ $ColI^{+}$ fibrocytes in mouse PBMCs. **A**. Gating strategy used to identify $CD115^{-}$ $CD45^{+}$ $ColI^{+}$ fibrocytes. B. The percent of circulating fibrocytes in isolated PBMCs post 14Gy irradiation. C. Graph of collagen MFI in isolated PBMC fibrocytes. D. Representative histogram of collagen I expression, (MFI) in PBMC fibrocytes post 14Gy irradiation in irradiated mice. Data represent mean ± SEM of at least four mice per treatment group and time point. $*p < 0.05$ vs. Sham, $\neq p < 0.05$, $\neq\neq p < 0.005$. One-way ANOVA with Tukey's multiple comparison

Frequency and collagen expression of bone marrow $CD45^+ColI^+$ fibrocyte precursors in non-irradiated bone marrow increase post irradiation, indicative of a radiation bystander effect

In response to lung, liver, and kidney injury, the frequency of bone marrow $CD45^+$ $ColI^+$ cells increase in frequency (133; 134). These cells can migrate to injured tissue and differentiate into "mature" fibrocytes (133; 185). HSC from non-irradiated bone marrow can migrate to injured bone marrow and restore hematopoiesis (137). We wished to determine if $CD45^+$ $ColI^+$ cells in non-irradiated bone marrow increased following irradiation. We isolated bone marrow cells from the non-irradiated femurs and quantified the frequency of $CD45^+ColI^+$ cells using flow cytometry at 7, 14, and 30 days post irradiation.

The flow cytometry gate for identifying $CD45^+$ $ColI^+$ cells was determined using collagen unstained bone marrow cells (Figure 7A, Supplementary Figure 7). We calculated the frequency of $CD45^+$ $ColI^+$ cells present in $CD45^+$ bone marrow cells. The frequency of fibrocyte precursors in the bone marrow was significantly increased 30 days post irradiation when compared to the levels of fibrocyte precursors in the bone marrow 7 and 14 days post irradiation (Figure 7B). The expression of collagen in $CD45^+$ $ColI^+$ bone marrow cells is significantly increased 14 days post irradiation compared to 7 and 30 days post irradiation (Figure 7C). We were fascinated with the heterogeneity of collagen expression in $CD45^+$ $ColI^+$ cells 7 and 14 days after irradiation (Figure 7D). These eclectic populations of $CD45^+$ $ColI^+$ cells were no longer present 30 days post irradiation. These data show that $CD45^+$ $ColI^+$ precursors increase in frequency in non-irradiated bone marrow sites.

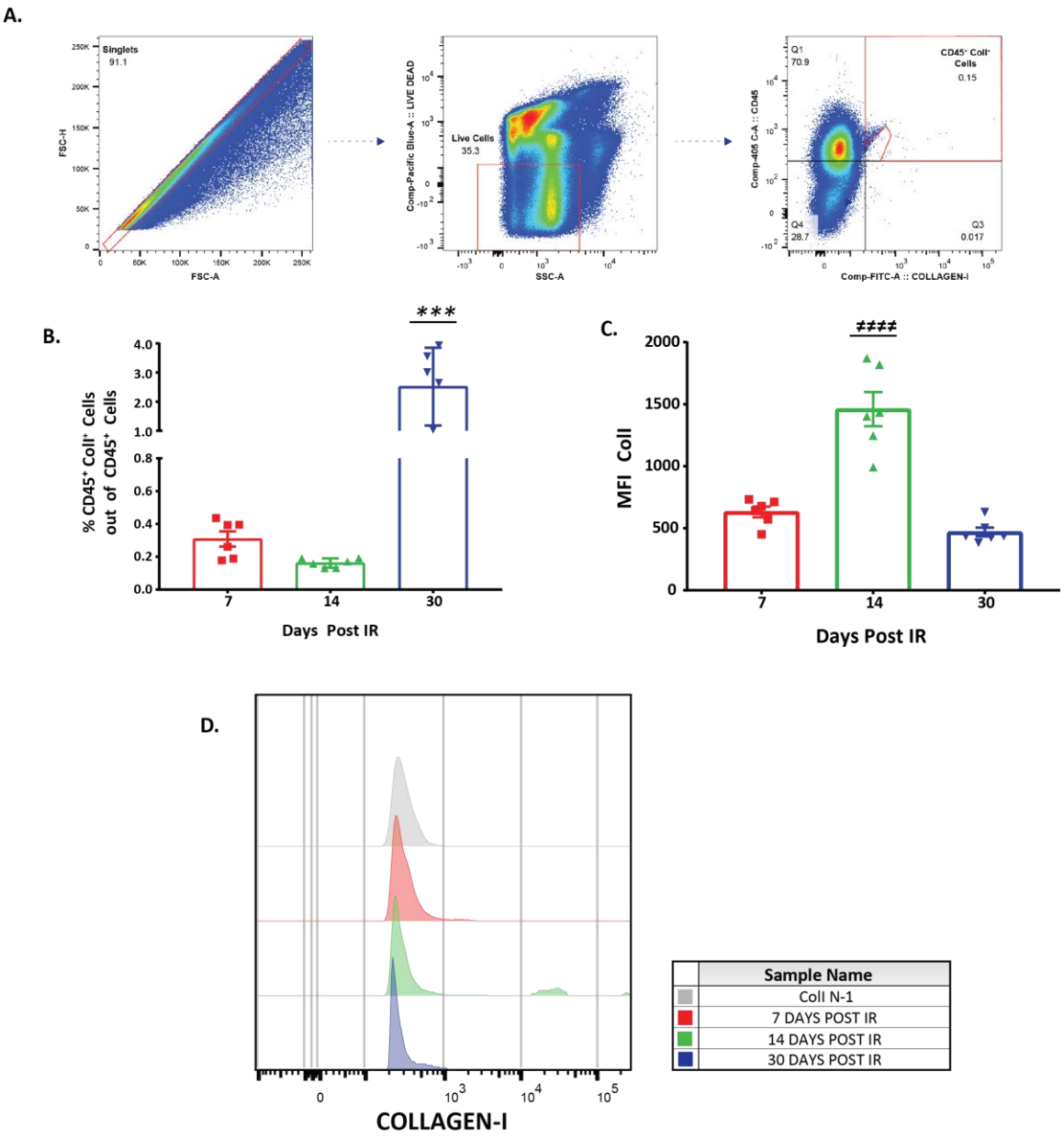

Figure 7. Number of CD45$^+$ColI$^+$ shielded femur bone marrow cells increases post irradiation.

Number of CD45$^+$ ColI$^+$ bone marrow cells were quantified using flow cytometry. **A.** Gating strategy used to identify CD45$^+$ ColI$^+$ in isolated bone marrow cells. **B.** The percentage of CD45$^+$ Col$^+$ cells in the CD45$^+$ population of femur bone marrow increases 30 days post irradiation. **C.** Graph of collagen MFI in isolated femur CD45$^+$ColI$^+$ cells post irradiation shows increased and variable expression of collagen post irradiation. **D.** Representative histogram of collagen I expression (MFI) CD45$^+$ ColI$^+$ cells. ***$p < 0.0002$ *vs*. 7D and 14D PIR, ###$p < 0.0001$ vs. 7D and 30D PIR. One-way ANOVA with Tukey's multiple comparison

Splenomegaly occurring 60 days post irradiation

The spleen's response to bone marrow injury has been well documented (105; 142). After hematopoietic damage the spleen becomes a site of extramedullary hematopoiesis and can increase in size, causing splenomegaly (139; 224). To assesses if splenomegaly occurred in our model of irradiation-induced bone marrow injury, spleen weights were recorded 7, 14, 30, and 60 days post irradiation. We did indeed observe a gradual, but sustained, increase in spleen weight that became significant 60 days post irradiation (Figure 8E).

Frequency of fibrocytes in the spleen decreases 7 days after radiation exposure and heterogenous populations of splenic fibrocytes arise after radiation exposure

Like bone marrow $CD45^{+}ColI^{+}$ cells, fibrocytes in the spleen have been shown to increase in response to kidney and liver injury (133; 215). In order to investigate the response of spleen fibrocytes after radiation-induced bone marrow injury, we measured the frequency of $CD115^{-}$ $CD45^{+}$ $ColI^{+}$ fibrocytes in the total $CD45^{+}$ cells in the shielded spleens of irradiated mice. The gate for identifying collagen-expressing cells was determined using unstained spleen cells (Figure 8A, Supplementary Figure 7). Interestingly, the number of splenic fibrocytes decreased 7 days post irradiation (Figure 8B). However, collagen expression was still increased in this small population of splenic fibrocytes and increased out to 14 days post irradiation (Figure 8C). These data show splenic fibrocytes are subject to the non-targeted effects of radiation-induced bone

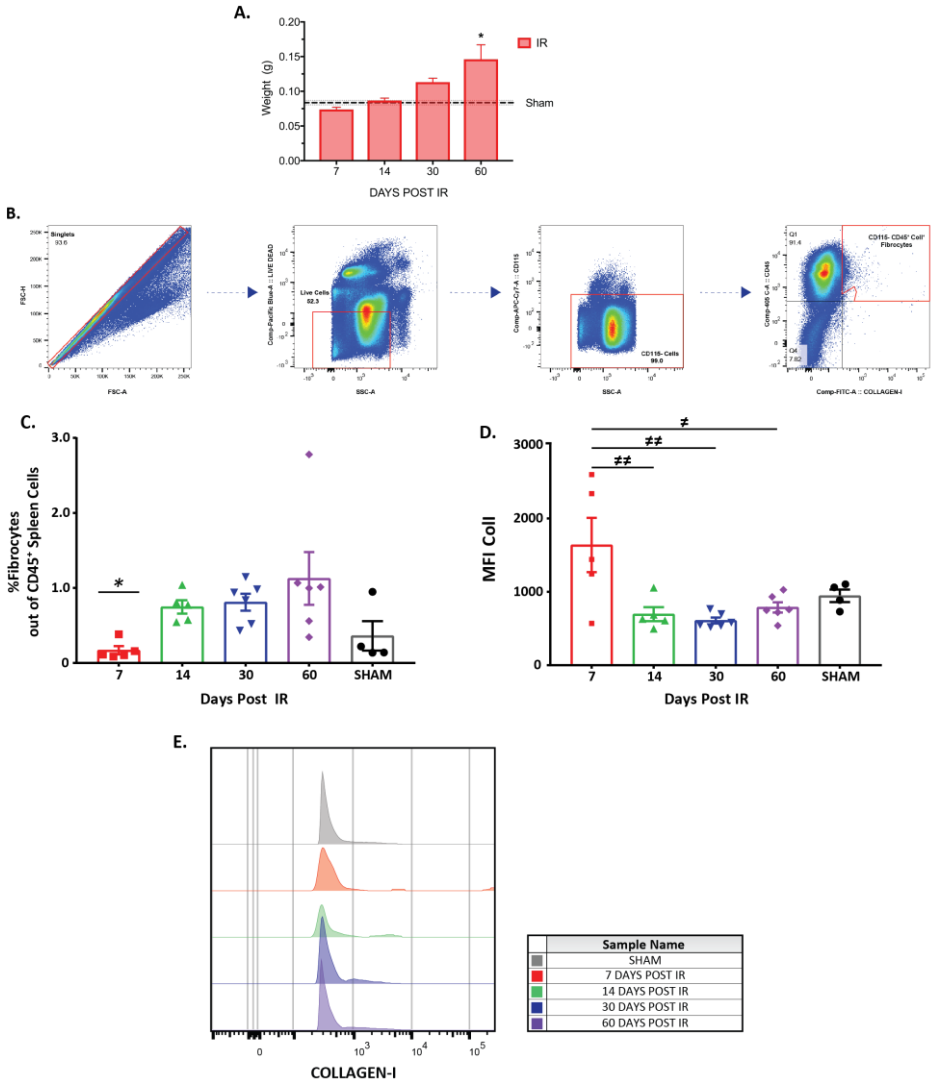

Figure 8. A significant decrease in levels of spleen fibrocytes and concomitant increase of collagen I expression occurs 7 days post irradiation.
After 14Gy irradiation, mice were sacrificed at various time points and the frequency of $CD115^{-}$ $CD45^{+}$ $ColI^{+}$ spleen fibrocytes was analyzed using flow cytometry. **A.** Gating strategy used to identify $CD115^{-}$ $CD45^{+}$ $ColI^{+}$ fibrocytes. **B.** The frequency of $CD115^{-}$ $CD45^{+}$ $ColI^{+}$ spleen fibrocytes is significantly reduced post irradiation. **C**. Graph of collagen I MFI of spleen fibrocytes post irradiation. **D.** Representative histogram of collagen expression (MFI) in spleen fibrocytes. **E.** 60 days post irradiation spleen weights of mice are significantly increased. Data represent mean ± SEM of at least four mice per treatment group and time point. *$p < 0.05$ vs. Sham. ≠$p < 0.05$, ≠≠$p < 0.005$, ≠≠≠$p < 0.0002$. One-way ANOVA with Tukey's multiple comparison

marrow injury. Like in the circulating fibrocytes and $CD45^{+}ColI^{+}$ cells, we observed a difference in the expression of collagen in spleen fibrocytes (Figure 8D).

DISCUSSION

Fibrocytes are bone marrow derived leukocytes that express both mesenchymal and hematopoietic markers (36; 174). Fibrocytes are primarily identified by their dual expression of CD45 and collagen I (110). These pleotropic cells have been demonstrated to be involved in numerous fibrotic diseases in both man and mouse (174; 227; 300). Research on the participation of fibrocytes in non-fibrotic diseases has demonstrated that their role in disease is not limited to fibrotic disease (315). Research examining fibrocytes in the context of radiation injury is in its infancy. Radiation exposure to the bone marrow is a major concern during radiotherapy (38; 102; 161; 234)(72). Therapy-related myeloproliferative neoplasms have been known to occur after radiation exposure to the bone marrow (4; 143; 146; 266). In order to investigate fibrocytes after radiation exposure, we used a model of targeted thoracic and forelimb irradiation. This allowed us to study the effects of partial bone marrow irradiation. After determining an optimal dose to illicit radiation-induced bone marrow damage, we quantified changes in circulating and splenic fibrocytes after bone marrow irradiation. We also measured changes to the $CD45^{+}ColI^{+}$ cell population in unexposed bone marrow. We found that fibrocytes do respond to thoracic and partial bone marrow irradiation. These findings pave the way for continued research into the participation of fibrocytes in radiation-induced injury.

Thoracic and partial bone marrow irradiation deplete exposed bone marrow cavities

Using a modified version of the model of thoracic irradiation performed routinely used in our laboratory we determined the optimal dose of radiation to illicit bone marrow injury 60 days post irradiation. By placing the humeri in the field of radiation, we were able to expose additional bone marrow in the field of radiation. While examining the bone marrow of the exposed sternum and humeri, we found varying degrees of bone marrow depletion in response to radiation exposure (Figure 5-6). Interestingly, we observed that the severity of injury in the form of bone marrow depletion was not correlated with increased dose of radiation exposure. This was interesting and a bit paradoxical at first. However, it has been demonstrated that in response to partial bone marrow radiation exposure, a secondary 'wave' of bone marrow depletion occurs after the initial recovery of the irradiated bone marrow (58; 137). Examination of the relationship between radiation dose and hematopoietic recovery after partial bone marrow irradiation has shown that increased dosages of radiation correspond to faster rates of hematopoietic recovery (232). The sharp decrease in the number of CFU-GMs in the bone marrow caused by high doses of radiation exposure is countered by an equally sharp increase in bone marrow regeneration (232). Our examination of the irradiated bone marrow was performed at a single time point. It is probable that the bone marrow exposed to 18Gy radiation was already recovering from its secondary injury. This would indicate that there is positive relationship between dose of radiation and bone marrow damage in our model of bone marrow injury, but since we only examined a single time point, we cannot definitively confirm this.

The discordance between bone marrow injury in the sternum marrow and the humeri of irradiated mice was another unexpected result (Figure 5-6). This could be attributed to the method of irradiation. The radiation source used by the RS2000 small animal irradiator is overhead, meaning that the radiation waves pass through the backside of the animal (Figure 4). The energy from the X-radiation photons is absorbed as it travels through the body of the mouse. The absorbed dose of radiation may have differed between the sternum bone marrow and humeri bone marrow, explaining the differences in irradiation damage within individual mice.

Close examination of depleted bone marrow spaces revealed changes in osteoblast populations after radiation exposure. Osteoblasts make up the endosteal niche of the bone marrow microenvironment (132). In concert with megakaryocytes, osteoblasts regulate the proliferation and quiescence of HSCs (190). It has been demonstrated that after total body irradiation, osteoblasts proliferate and help regulate the repopulation of the depleted bone marrow (67). A dearth in osteoblasts lining the endosteum in the spongy marrow of the humerus was seen 60 days post 12Gy and 14Gy irradiation (Figure 5D-E). However, osteoblasts could be seen lining the endosteum at 60 days post 18Gy irradiation (Figure 5G). This observation lends credence to our supposition that the lack of dose to injury relationship observed was owed in part to the temporal nature of bone marrow depletion and recovery.

The 14Gy dose of radiation was used because it provided the most consistent bone marrow damage in the sternum and humerus at 60 days post irradiation. However, it should be noted that other doses of radiation can be used to examine radiation-induced bone marrow damage at different time points.

The level of circulating fibrocytes is altered after radiation exposure

Fibrocytes can be identified using multiple combinations of expression markers (207). We used a combination of CD115, CD45 and ColI to identify circulating fibrocytes in PBMC (Figure 7A). CD115, which is also referred to as macrophage colony-stimulating factor receptor (M-CSFR), is routinely used to identify monocytes (35; 311). CD115 expression is lost during the differentiation of fibrocytes from $Gr1^{+}$ splenocytes (194). Additionally, CD115 is not present in tissue-isolated fibrocytes or cultured PBMC fibrocytes (215). Accordingly, we used CD115 as an exclusion marker in our flow cytometry panel to identify fibrocytes in circulating PBMCs and the spleen.

We found that circulating fibrocytes increase in response to thoracic and humoral bone marrow irradiation (Figure 7B). This increase of circulating fibrocytes is in step with the reported increases of fibrocytes in the context of numerous other diseases (110; 174). Interestingly, this increase in fibrocytes was observed well after irradiation exposure (Figure 7). Unfortunately, we were not able to collect enough PBMCs from irradiated mice 7 days after exposure, which was believed to be because of the depletion of the bone marrow soon after radiation exposure. By 60 days post irradiation, the level of circulating fibrocytes had returned to the levels of sham-irradiated mice. The 60-day time point corresponds to the time we observed irradiation-induced bone marrow damage in mice. This is contrary to what is seen in other models of disease where increases in fibrocytes occur concomitantly to the development of disease (206; 215). A positive correlation between circulating fibrocyte levels and disease severity is also found in patients suffering from a range of maladies (129; 138; 179; 277; 308). Total body and partial radiation exposure disrupts the balance of hematopoietic cell subsets (81; 111). A change in the proportion of monocytes to lymphocytes could explain the absence of an

overall increase in fibrocyte levels at 60 days post irradiation when radiation-induced bone marrow damage occurs.

While the level of circulating fibrocytes peaked at 30 days post irradiation, the relative expression of collagen per cell was greatest at 14 days post irradiation (Figure 7C). It has been demonstrated that in response to TGF-β and other pro-fibrotic cytokines, fibrocytes increase their level of collagen expression (28; 241). Increases in TGF-β are found in irradiated mice and patients receiving radiotherapy is common (94; 225). The elevated levels of collagen expression in early fibrocytes may be due in part to stimulation by TGF-β (163). We attempted to measure the gene expression levels of TGF-β in both non-irradiated and irradiated bone marrow of these mice but were unable to obtain reproducible data.

Examination of the histogram representing the expression of collagen in PBMC fibrocytes reveals what could be different subpopulations of fibrocytes. Fibrocytes have been shown to be a very heterogenous population of cells. Fibrocytes have been found to compose a subset of MDSC (244; 315), behave as effective antigen presenting cells (16), and transdifferentiate into adipocytes (112). Fibrocytes are very malleable and adapt to their surroundings. Radiation exposure triggers a complex cascade of events resulting in a milieu of chemokines, cytokines and growth factors (42; 64; 108; 115). These factors can manipulate the phenotype of fibrocytes, which has been shown numerous times *in vitro* (134; 285; 286)

An increase in $CD45^{+}ColI^{+}$ bone marrow cells outside the field of radiation

There is some debate on what constitutes a 'true fibrocyte'. $CD45^+ColI^+$ have been regarded to as "fibrocyte-like" (134; 216) cells and $CD45^+ColI^+$ cells have also been regarded as true fibrocytes (185). In the context of this study, bone marrow $CD45^+ColI^+$ cells were regarded as fibrocyte precursors. Also, due to lack of sham bone marrow, the only suppositions that can be made are within the isolated bone marrow cells. Relative to the populations of bone marrow $CD45^+ColI^+$ cells, the $CD45^+ColI^+$ do not exhibit changes in percentage nor collagen expression at 7 days post irradiation (Figure 8B-D). Examination of $CD45^+ColI^+$bone marrow cells at 14 and 30 days reveals a potential inverse relationship between level of bone marrow fibrocytes and expression of collagen. The relative increase in collagen expression in $CD45^+ColI^+$ bone marrow cells at 14 days post irradiation may also be caused by an increase in the level of TGF-β after irradiation (163). Relative to one another, the stark increase in $CD45^+ColI^+$ cells that occurs at 30 days is interesting due to how long after exposure it occurs. Studies that have examined the changes in $CD45^+ColI^+$ cells in the bone marrow after injury have demonstrated that the level of $CD45^+$ $ColI^+$ bone marrow cells increase close to the time of injury or development of fibrosis (134; 206). This relatively late increase could be linked to the bone marrow injury that occurs 60 days post irradiation or could be in response to injury in another tissue. However, as stated before no firm conclusions can be made about the potential meanings of these observations without the knowledge of the levels of $CD45^+ColI^+$ bone marrow cells in non-irradiated mice.

Shortly after thoracic and bone marrow irradiation the level of splenic fibrocytes is significantly reduced

Shortly after radiation there is a significant decrease of fibrocytes in the spleen. This is in contrast to the increase in spleen fibrocytes in response to various types of injury that have been reported in the literature (134; 215). However, it needs to be noted that these observations were made at a single time point after injury, meaning that the events preceding and following the time of examination may show changes in fibrocyte numbers in the spleen. Interestingly, there has been a study demonstrating a reservoir of spleen monocytes that are quickly recruited to the site of the heart after MI in mice causing a depletion of splenic monocytes (257). A similar mechanism might be occurring with respect to fibrocytes after irradiation. Additionally, the spleen has a heterogenous population of fibrocytes with different levels of collagen expression out to 60 days post irradiation. The peak of collagen expression in spleen fibrocytes coincides with the dramatic decrease of splenic fibrocytes. This could be indicative of a rapidly depleting population of 'mature' fibrocytes that are being deployed to sites of injury.

Splenomegaly occurs 60 days post irradiation

The spleen is a site of extramedullary hematopoiesis in mice. After bone marrow injury, the spleen also becomes a sight of extramedullary hematopoiesis in humans (213). The observed increase in spleen weight at 60 days post irradiation suggests that this radiation by-stander effect may also occur in our system of thoracic and partial bone marrow irradiation.

Potential communication between fibrocytes from different sources

After radiation exposure, our results indicate a series of potentially connected events that occur in PBMCs, shielded bone marrow and the shielded spleen. It could be possible that high levels of circulating PBMC fibrocytes at 30 days could be en route to the spleen explaining the increase, albeit not significant, of fibrocytes in the spleen. It may also be that the high levels of bone marrow $CD45^{+}ColI^{+}$ cells maybe on their way to the spleen to further mature and then enter circulation. This migration of $CD45^{+}$ $ColI^{+}$ cells from bone marrow to the spleen has been shown to occur in response to liver injury (235). At the early time points after irradiation the decrease of fibrocytes in the spleen could indicate that these spleen fibrocytes have entered circulation and are en route to sites of tissue injury. Splenic monocytes exhibit this particular pattern of migration after myocardial injury (257). This study highlights the benefits of conducting experiments on fibrocytes in disease over time. Many potential relationships between the $CD45^{+}ColI^{+}$ cells in the bone marrow, circulating PBMC fibrocytes, sites of injury, and the spleen are overlooked when examining spleen levels at single time points after or during injury.

An important caveat regarding this study

Lastly, a very important detail needs to be pointed out. The lungs of the irradiated mice are in the field of radiation. Radiation is known to cause injury to the lungs that often culminates in radiation-induced fibrosis (3; 66). The response to radiation-induced bone marrow injury overlaps with the response to radiation-induced lung injury and fibrosis. A study investigating the role of fibrocytes in radiation-induced lung injury found a sustained increase in the number of fibrocytes in the lungs of thoracically irradiated mice (303). The increase of lung fibrocytes was sustained throughout the

development of lung fibrosis at 6 months post irradiation. However, the initial time point examined was one month after radiation exposure. A follow up study investigated changes in fibrocytes early after radiation exposure and continued until 6 months post irradiation. This thorough and interesting study uncovered a unique mechanism governing the development of radiation-induced lung fibrosis (298). The authors found that the Tregs mediated the level of lung fibrocytes after radiation exposure. The depletion of Tregs abrogated increases in fibrocytes post radiation exposure, which was concomitant with a decrease in lung fibrosis. This study also found that the depletion of Tregs resulted in higher levels of INF-γ and IL-12 and decreased levels of IL-4 in the lung. Th1 cytokines have been shown to inhibit the differentiation of fibrocytes in human PBMC cultures, while Th2 cytokines have been found to promote fibrocyte differentiation in human PBMC cultures (241). The relationship between fibrocytes and T-cells is well documented in the literature (16; 49; 194), but this is one of the first studies examining the relationship between fibrocytes and T-cells in the setting of radiation-induced pulmonary fibrosis.

FINAL THOUGHTS

Fibrocytes are very interesting cells that have been shown to serve various roles in numerous diseases. These cells also interact with numerous organs and cell types during the initiation and development of disease. Systemic examination of fibrocytes in the context of different diseases will provide new insights on the pathogenic mechanism governing numerous diseases.

SUPPLEMENTAL FIGURES

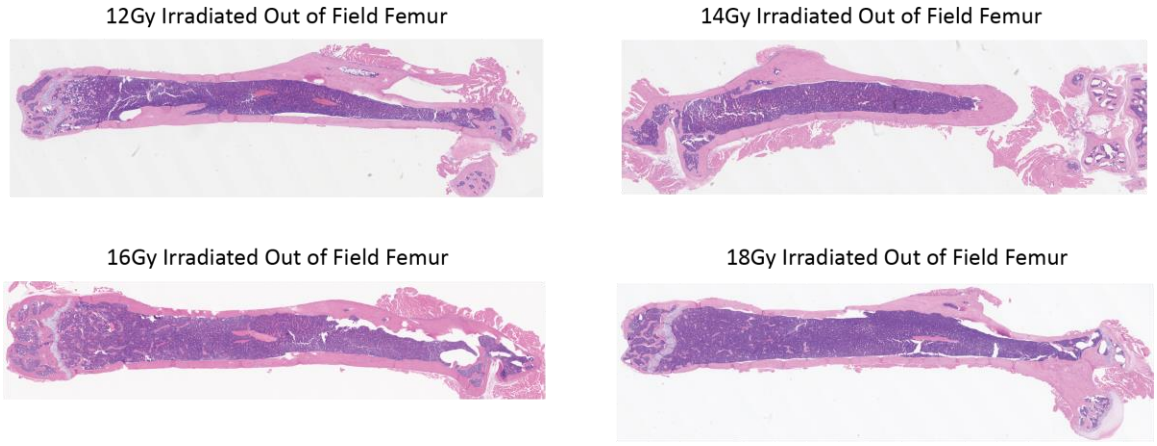

Supplementary Figure 1. Out of field bone marrow is not injured after irradiation of distal bone marrow.

Femurs were harvested and stained with H&E to examine over all cellular composition

A.

Score		BM Depletion
0	No lesion	0
1	Minimal	<5%
2	Mild	5-20%
3	Moderate	20-50%
4	Marked	50-75%
5	Severe	>75%

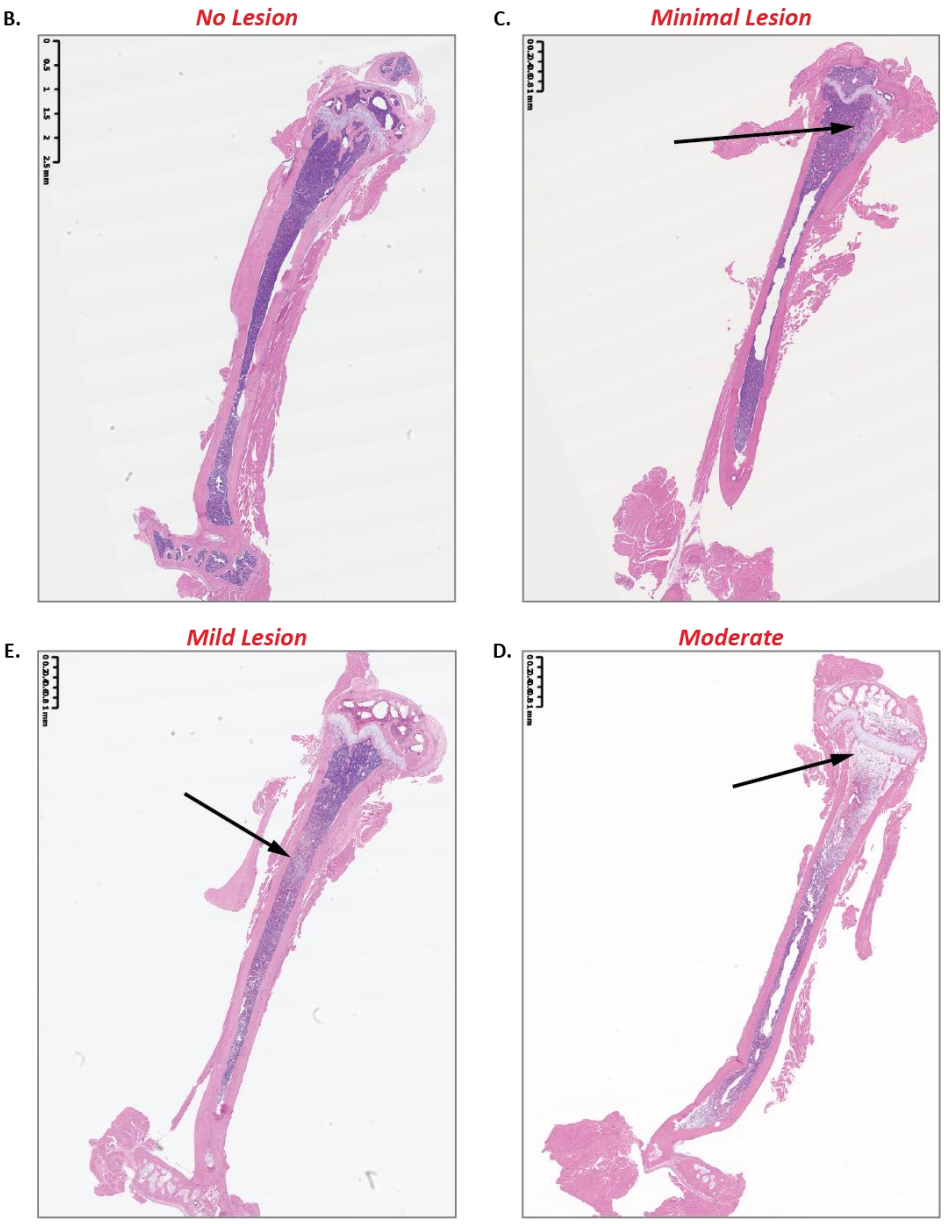

Supplementary Figure 2. Grading of bone marrow depletion in the irradiated humerus.

A. Criteria used for grading the severity of bone marrow depletion. **B-D** Images of bone marrow injury depletion scores. Black arrows point to the areas representing the lesions.

A.

Score		BM Depletion
0	No lesion	0
1	Minimal	<5%
2	Mild	5-20%
3	Moderate	20-50%
4	Marked	50-75%
5	Severe	>75%

B.

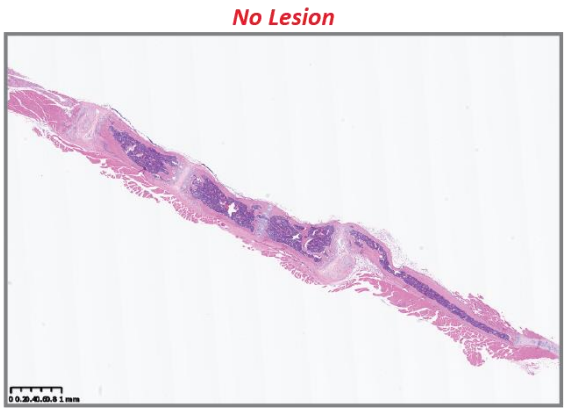

C.

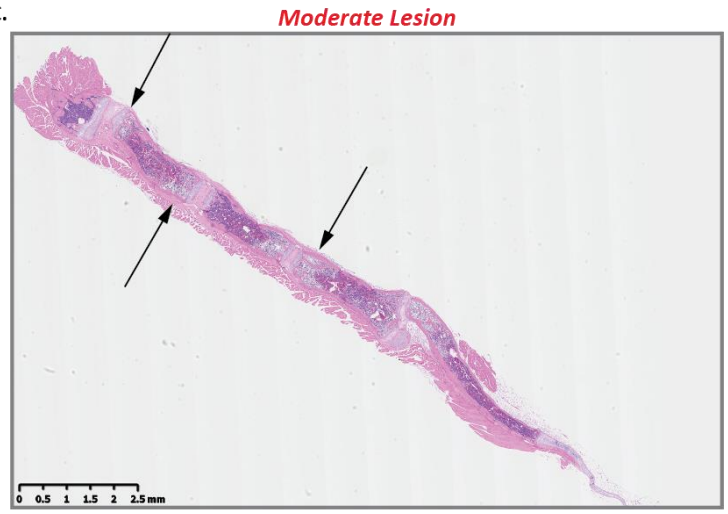

D.

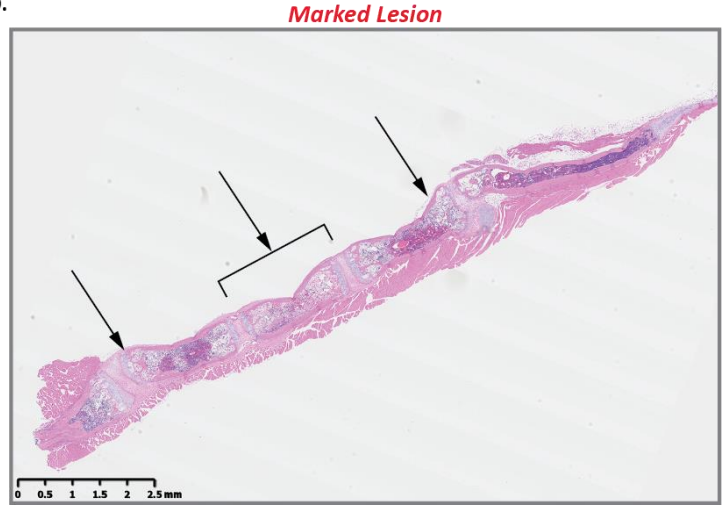

Supplementary Figure 3. Grading of bone marrow depletion in the irradiated sternum.

A. Criteria used for grading the severity of bone marrow depletion. **B-D**. Images of bone marrow injury depletion scores. Black arrows point to the areas representing the lesions.

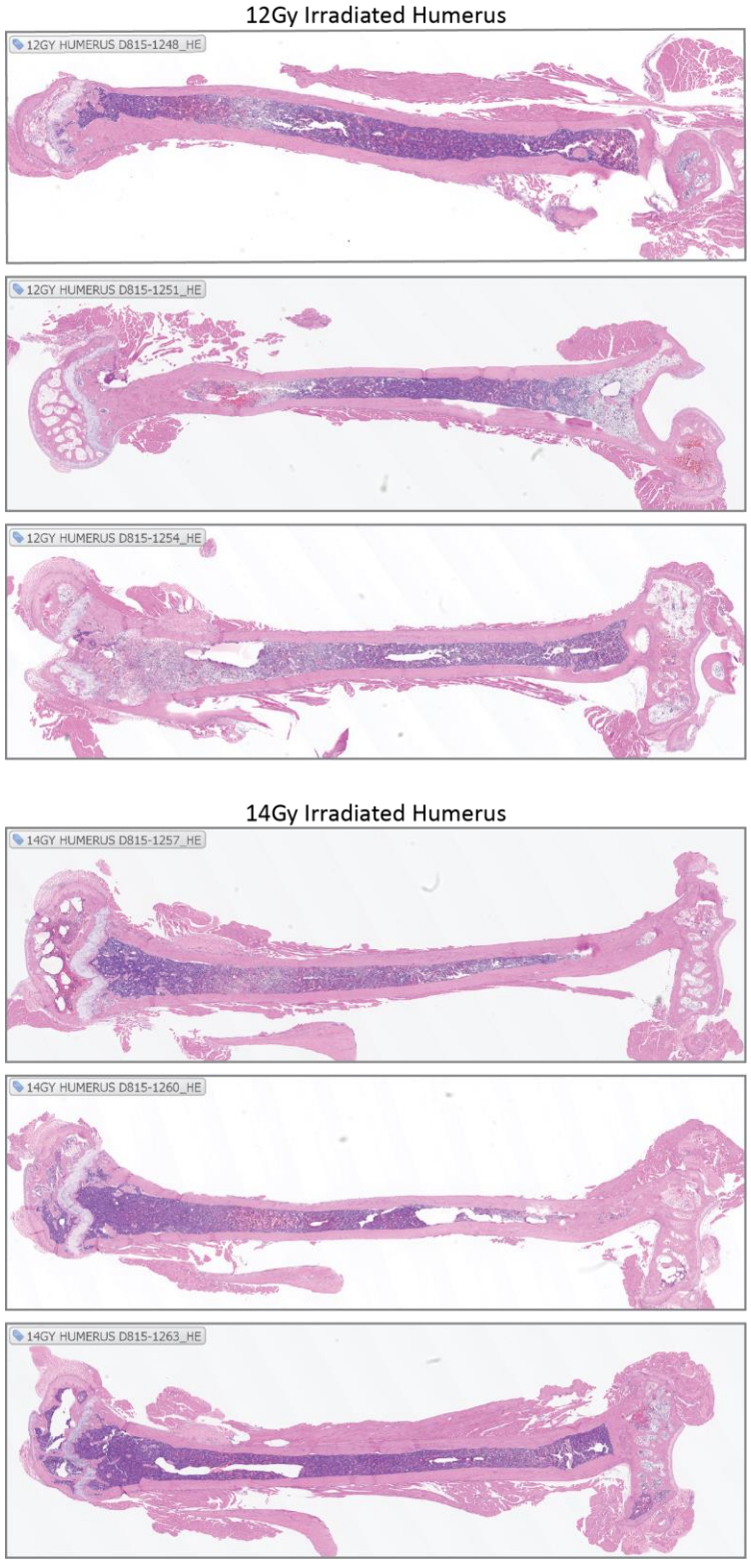

Supplementary Figure 4. Isolated humeri from all the animals used in the study. Each irradiation group consisted of 3 mice. Image continued on following page.

16Gy Irradiated Humerus

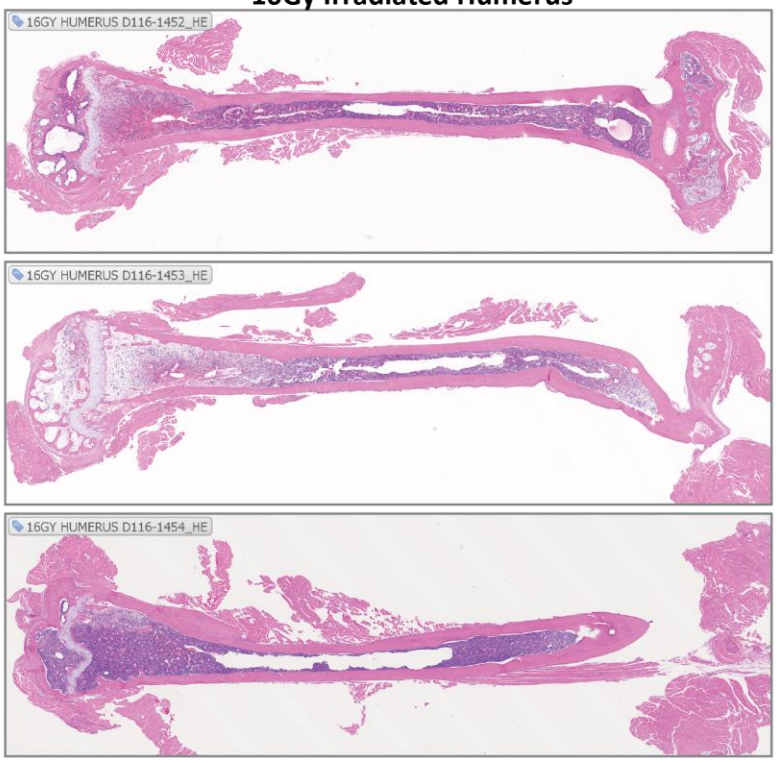

18Gy Irradiated Humerus

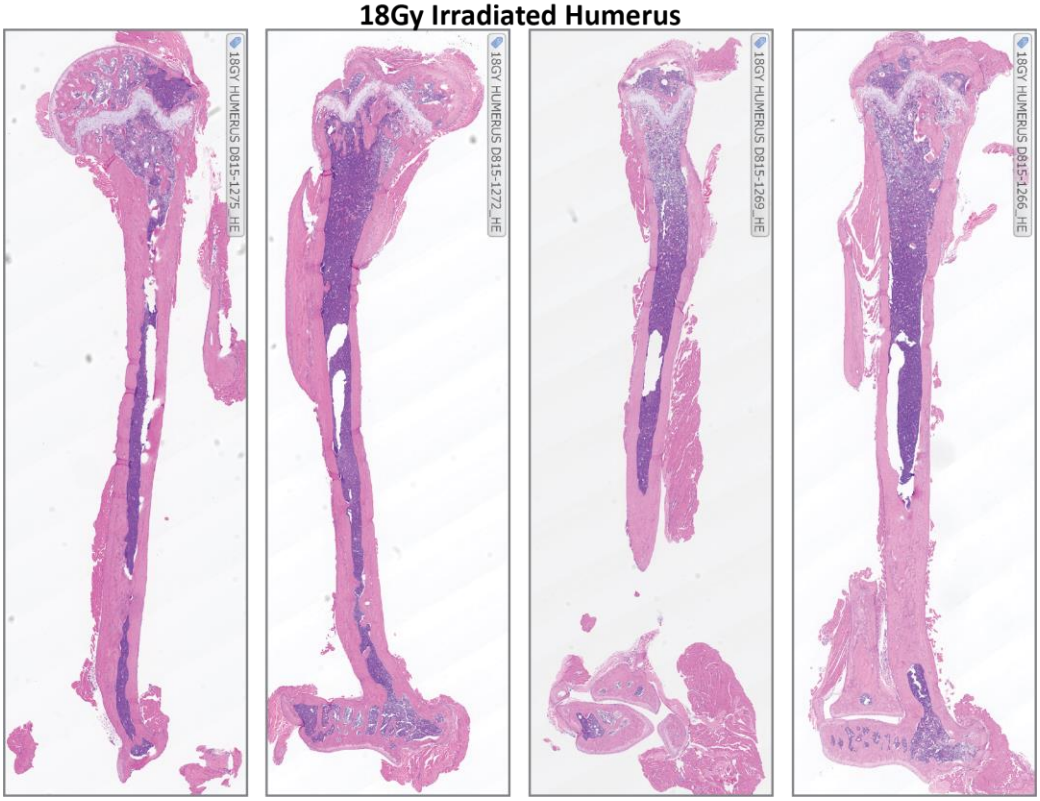

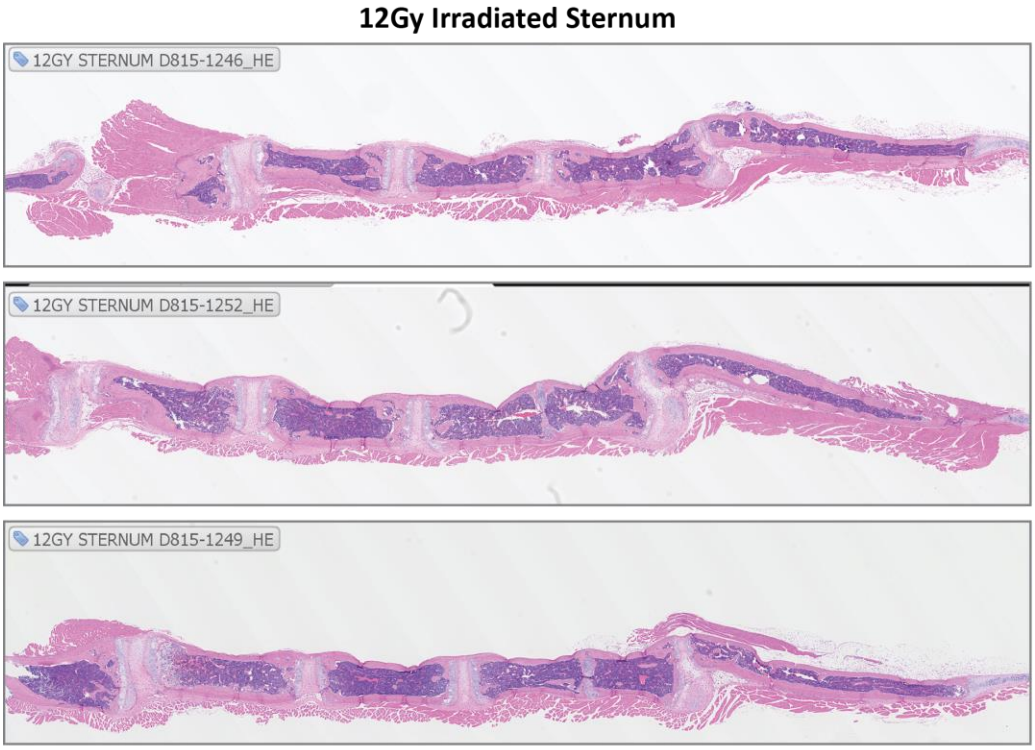

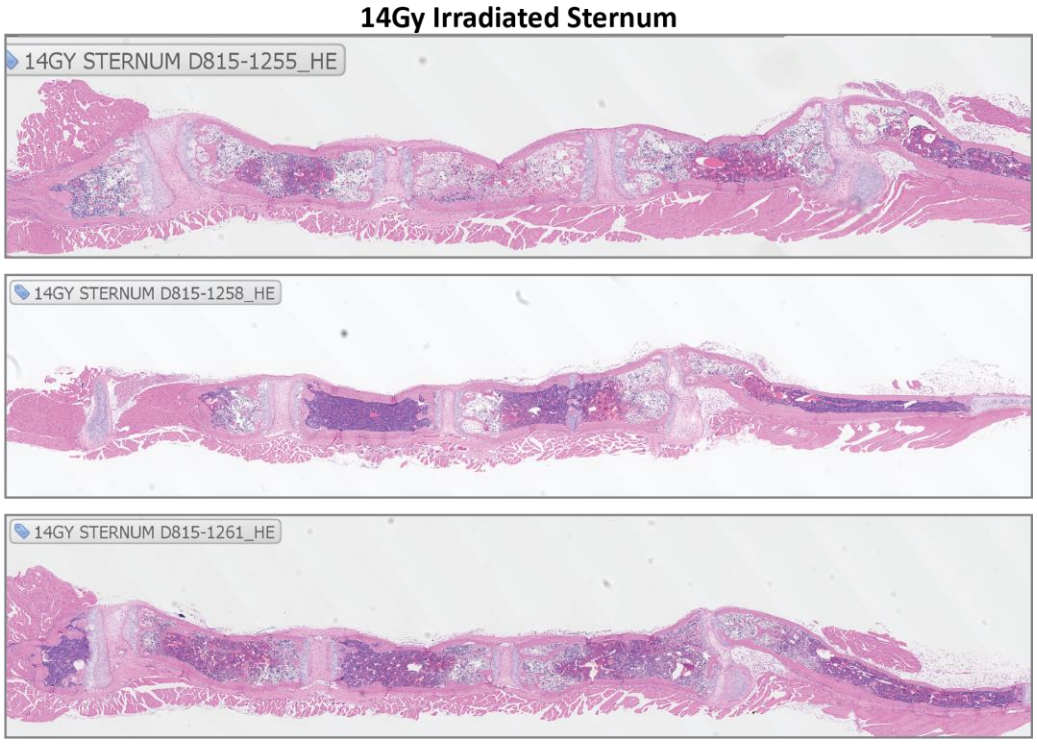

Supplementary Figure 4. Isolated sternums from all the animals used in the study. Each irradiation group consisted of 3 mice. Imaged continued on following page.

16Gy Irradiated Sternum

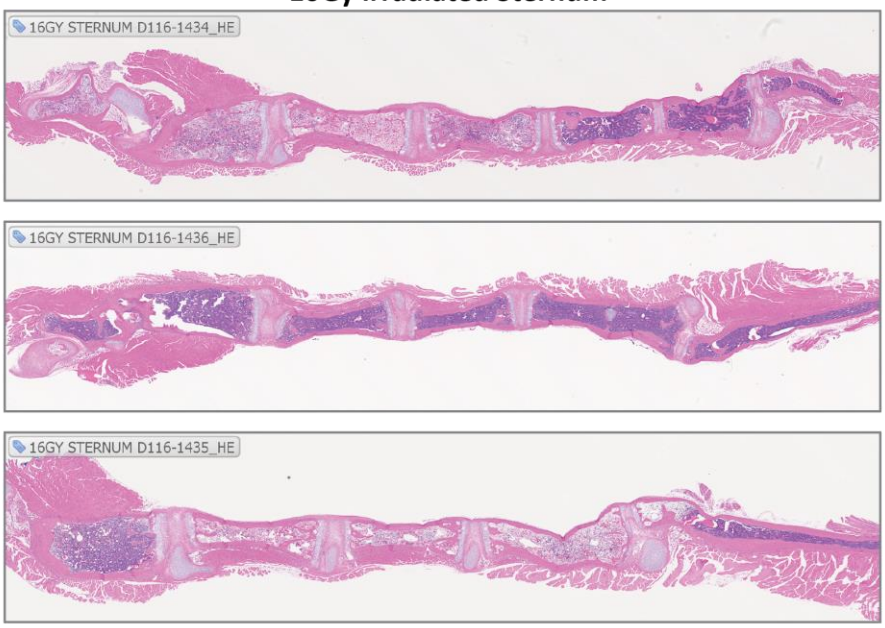

18Gy Irradiated Sternum

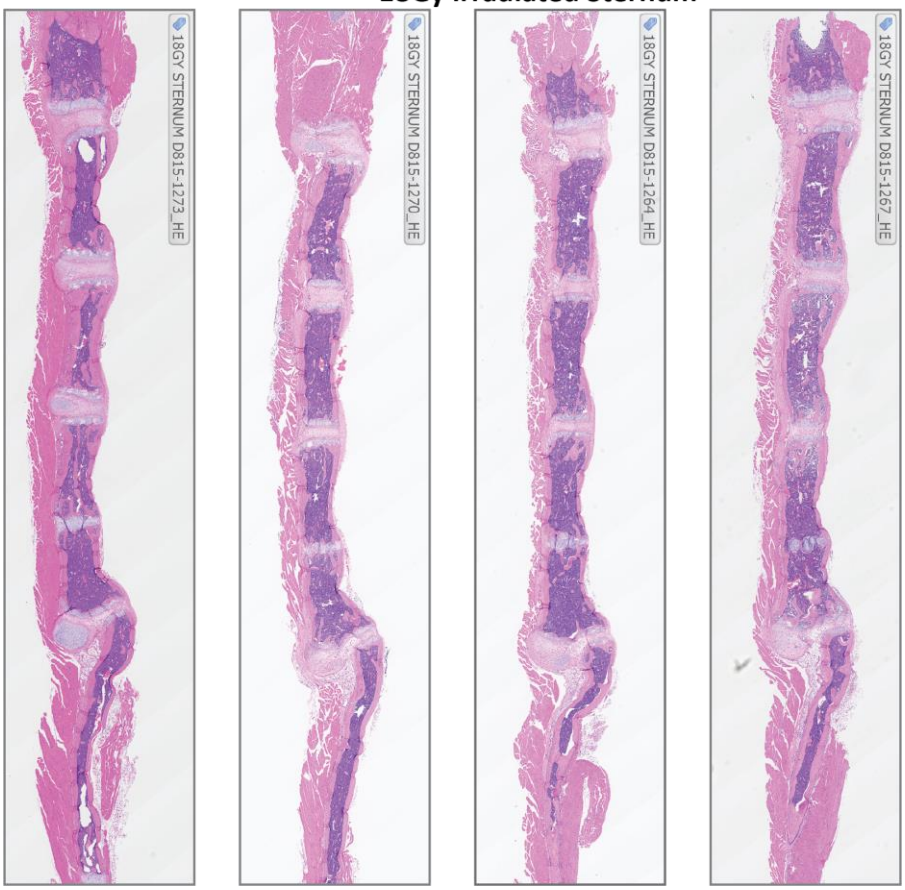

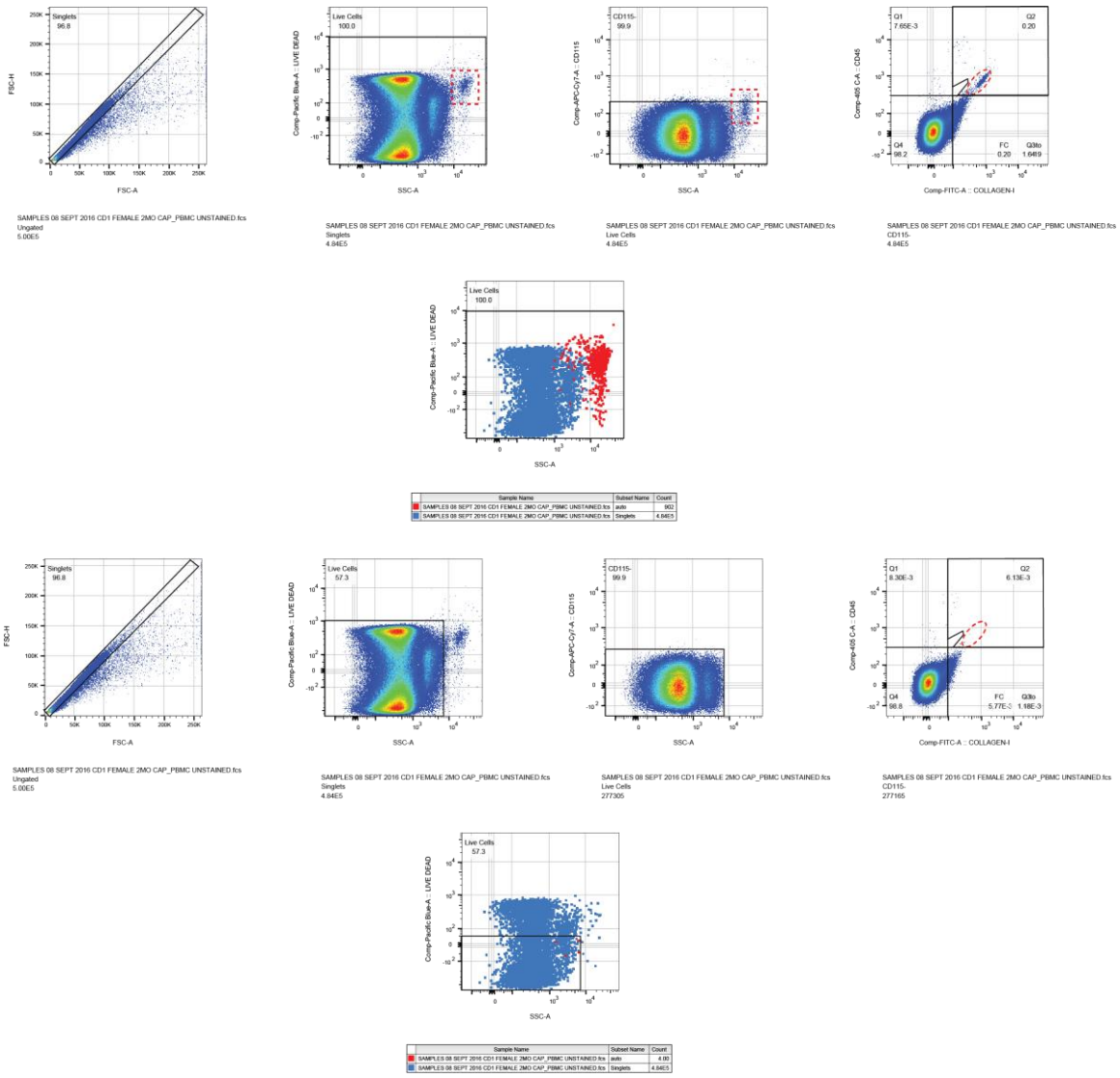

Supplementary Figure 5. Setting the gates to identify fibrocytes in PBMCs. Unstained cells were used set the gate parameters to detect $CD115^{-}$ $CD45^{+}$ $ColI^{+}$ fibrocytes. **A.** A group of auto fluorescent cells (red dashed circle) was identified in the total population of PBMCs. **B.** This population was back-gated to determine where this population of cells resided in the total population of cells. **C.** The autofluorescent group of cells was gated out and gates were determined using unstained cells. **D.** Confirmation that the population of autofluorescent cells were removed from the population of $CD115^{-}$ $CD45^{+}$ $ColI^{+}$ fibrocytes.

A.

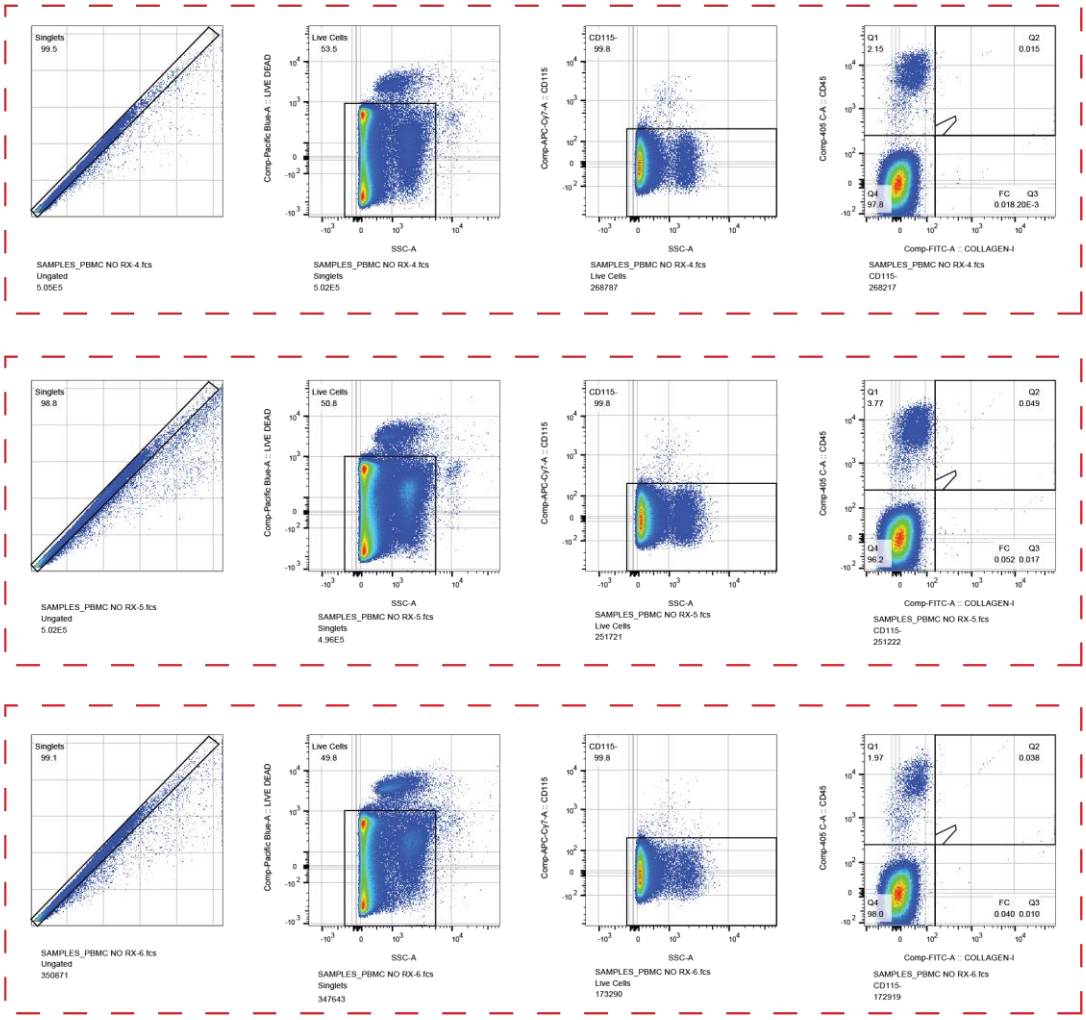
Singlets
99.5
SAMPLES_PBMC NO RX-4.fcs
Ungated
5.05E5
Live Cells
53.5
Comp-Pacific Blue-A :: LIVE DEAD
SSC-A
SAMPLES_PBMC NO RX-4.fcs
Singlets
5.02E5
CD115-
99.8
Comp-APC-Cy7-A :: CD115
SSC-A
SAMPLES_PBMC NO RX-4.fcs
Live Cells
268787
Q1
2.15
Q2
0.015
Q4
97.8
FC
0.018
Q3
20E-3
Comp-405 C-A :: CD45
Comp-FITC-A :: COLLAGEN-I
SAMPLES_PBMC NO RX-4.fcs
CD115-
268217
Singlets
98.8
SAMPLES_PBMC NO RX-5.fcs
Ungated
5.02E5
Live Cells
50.8
Comp-Pacific Blue-A :: LIVE DEAD
SSC-A
SAMPLES_PBMC NO RX-5.fcs
Singlets
4.96E5
CD115-
99.8
Comp-APC-Cy7-A :: CD115
SSC-A
SAMPLES_PBMC NO RX-5.fcs
Live Cells
251721
Q1
3.77
Q2
0.049
Q4
96.2
FC
0.052
Q3
0.017
Comp-405 C-A :: CD45
Comp-FITC-A :: COLLAGEN-I
SAMPLES_PBMC NO RX-5.fcs
CD115-
251222
Singlets
99.1
SAMPLES_PBMC NO RX-6.fcs
Ungated
350871
Live Cells
49.8
Comp-Pacific Blue-A :: LIVE DEAD
SSC-A
SAMPLES_PBMC NO RX-6.fcs
Singlets
347643
CD115-
99.8
Comp-APC-Cy7-A :: CD115
SSC-A
SAMPLES_PBMC NO RX-6.fcs
Live Cells
173290
Q1
1.97
Q2
0.038
Q4
98.0
FC
0.040
Q3
0.010
Comp-405 C-A :: CD45
Comp-FITC-A :: COLLAGEN-I
SAMPLES_PBMC NO RX-6.fcs
CD115-
172919

A.

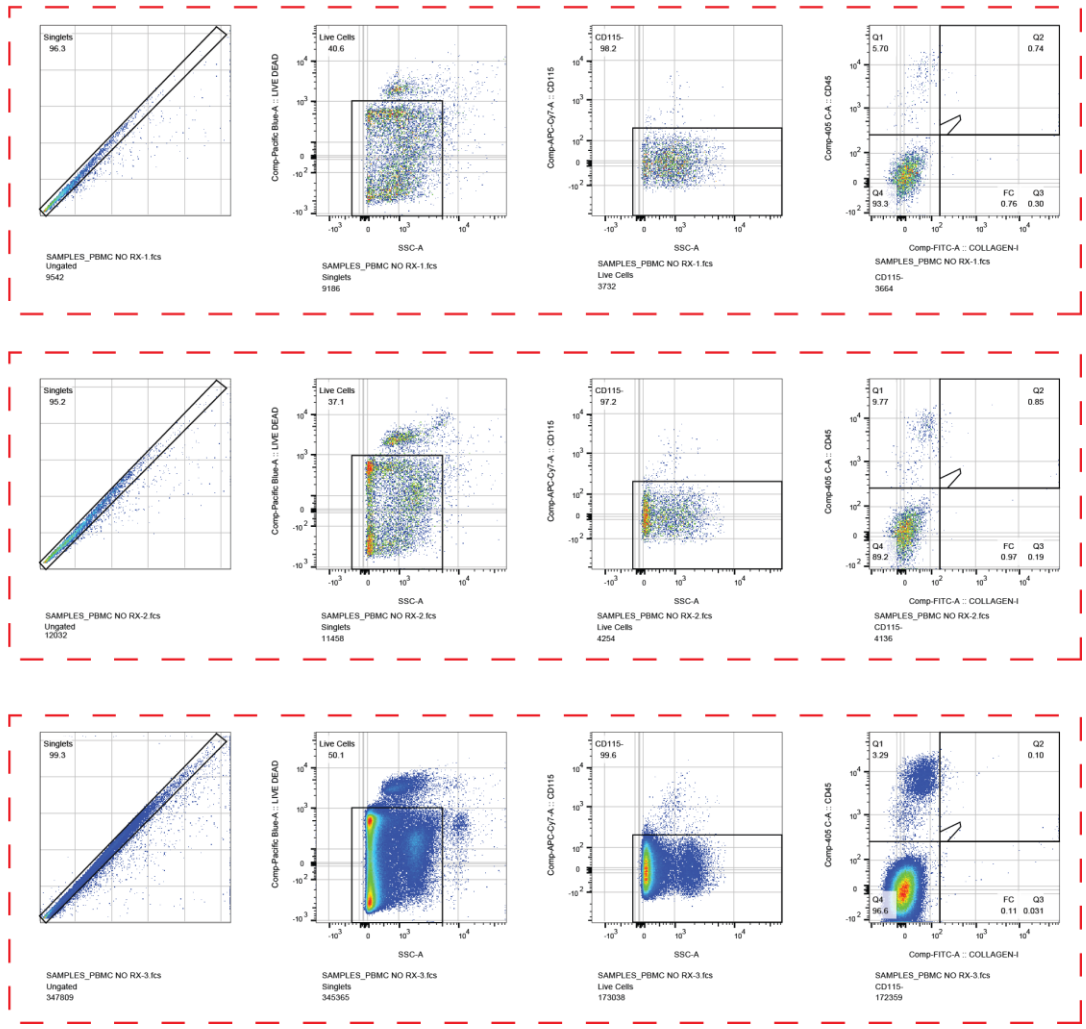
Singlets
96.3
SAMPLES_PBMC NO RX-1.fcs
Ungated
9542
Live Cells
40.6
Comp-Pacific Blue-A :: LIVE DEAD
SSC-A
SAMPLES_PBMC NO RX-1.fcs
Singlets
9186
CD115-
98.2
Comp-APC-Cy7-A :: CD115
SSC-A
SAMPLES_PBMC NO RX-1.fcs
Live Cells
3732
Q1
5.70
Q2
0.74
Q4
93.3
FC
0.76
Q3
0.30
Comp-405 C-A :: CD45
Comp-FITC-A :: COLLAGEN-I
SAMPLES_PBMC NO RX-1.fcs
CD115-
3664
Singlets
95.2
SAMPLES_PBMC NO RX-2.fcs
Ungated
12632
Live Cells
37.1
Comp-Pacific Blue-A :: LIVE DEAD
SSC-A
SAMPLES_PBMC NO RX-2.fcs
Singlets
11458
CD115-
97.2
Comp-APC-Cy7-A :: CD115
SSC-A
SAMPLES_PBMC NO RX-2.fcs
Live Cells
4254
Q1
9.77
Q2
0.85
Q4
89.2
FC
0.97
Q3
0.19
Comp-405 C-A :: CD45
Comp-FITC-A :: COLLAGEN-I
SAMPLES_PBMC NO RX-2.fcs
CD115-
4136
Singlets
99.3
SAMPLES_PBMC NO RX-3.fcs
Ungated
347809
Live Cells
50.1
Comp-Pacific Blue-A :: LIVE DEAD
SSC-A
SAMPLES_PBMC NO RX-3.fcs
Singlets
345365
CD115-
99.6
Comp-APC-Cy7-A :: CD115
SSC-A
SAMPLES_PBMC NO RX-3.fcs
Live Cells
173038
Q1
3.29
Q2
0.10
Q4
96.6
FC
0.11
Q3
0.031
Comp-405 C-A :: CD45
Comp-FITC-A :: COLLAGEN-I
SAMPLES_PBMC NO RX-3.fcs
CD115-
172359

B.

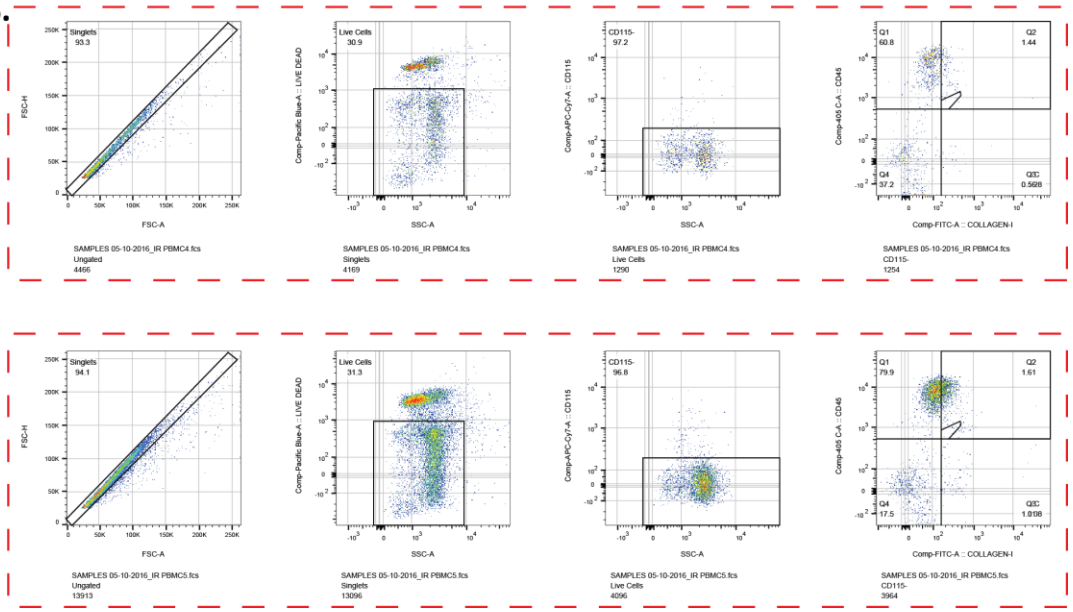
Singlets
93.3
FSC-H
FSC-A
SAMPLES 05-10-2016_IR PBMC4.fcs
Ungated
4466
Live Cells
30.9
Comp-Pacific Blue-A :: LIVE DEAD
SSC-A
SAMPLES 05-10-2016_IR PBMC4.fcs
Singlets
4169
CD115-
97.2
Comp-APC-Cy7-A :: CD115
SSC-A
SAMPLES 05-10-2016_IR PBMC4.fcs
Live Cells
1290
Q1
60.8
Q2
1.44
Q4
37.2
Q3
0.528
Comp-405 C-A :: CD45
Comp-FITC-A :: COLLAGEN-I
SAMPLES 05-10-2016_IR PBMC4.fcs
CD115-
1254
Singlets
94.1
FSC-H
FSC-A
SAMPLES 05-10-2016_IR PBMC5.fcs
Ungated
13913
Live Cells
31.3
Comp-Pacific Blue-A :: LIVE DEAD
SSC-A
SAMPLES 05-10-2016_IR PBMC5.fcs
Singlets
13096
CD115-
96.8
Comp-APC-Cy7-A :: CD115
SSC-A
SAMPLES 05-10-2016_IR PBMC5.fcs
Live Cells
4096
Q1
79.9
Q2
1.61
Q4
17.5
Q3
1.098
Comp-405 C-A :: CD45
Comp-FITC-A :: COLLAGEN-I
SAMPLES 05-10-2016_IR PBMC5.fcs
CD115-
3964

B.

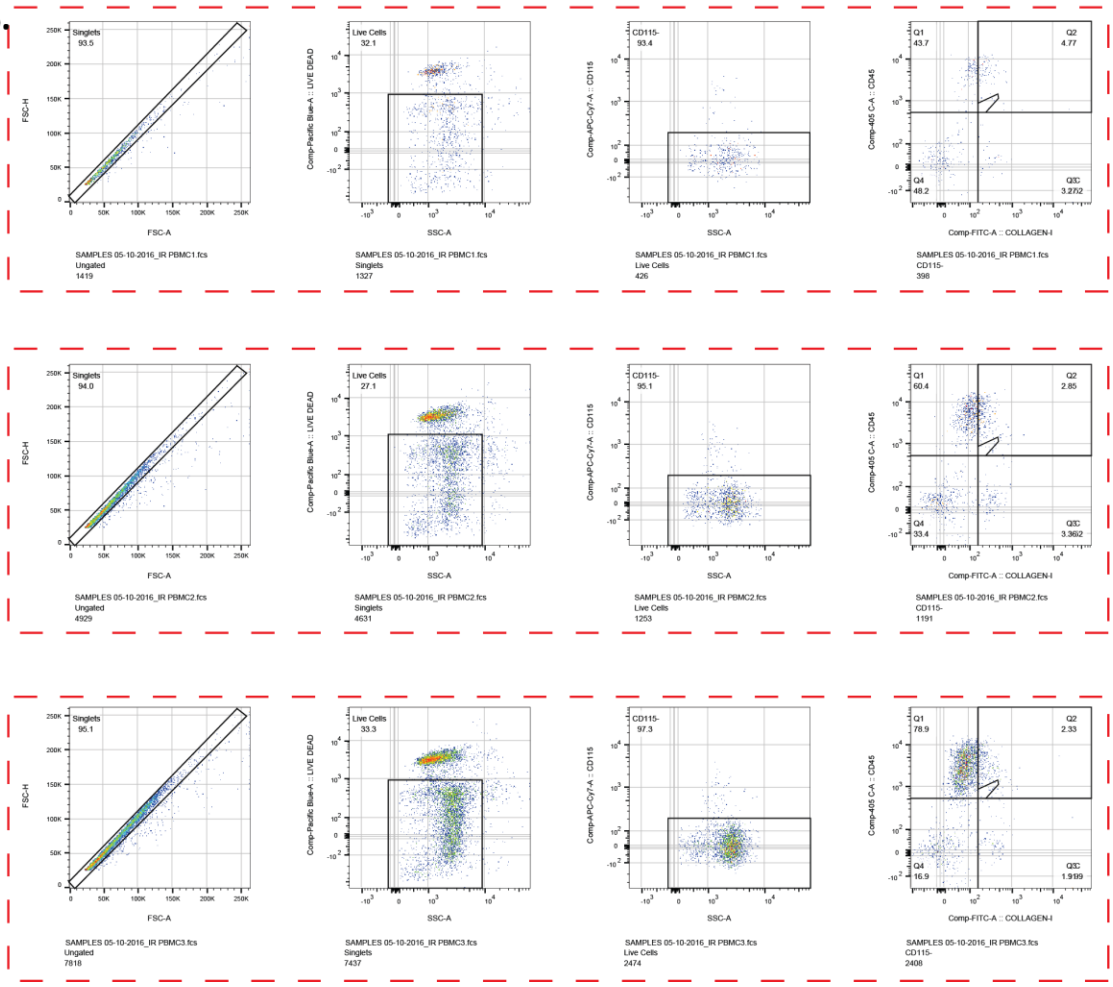
Singlets
93.5
FSC-H
FSC-A
SAMPLES 05-10-2016_IR PBMC1.fcs
Ungated
1419
Live Cells
32.1
Comp-Pacific Blue-A :: LIVE DEAD
SSC-A
SAMPLES 05-10-2016_IR PBMC1.fcs
Singlets
1327
CD115-
93.4
Comp-APC-Cy7-A :: CD115
SSC-A
SAMPLES 05-10-2016_IR PBMC1.fcs
Live Cells
426
Q1
43.7
Q2
4.77
Q4
48.2
Q3
3.272
Comp-405 C-A :: CD45
Comp-FITC-A :: COLLAGEN-I
SAMPLES 05-10-2016_IR PBMC1.fcs
CD115-
398
Singlets
94.0
FSC-H
FSC-A
SAMPLES 05-10-2016_IR PBMC2.fcs
Ungated
4929
Live Cells
27.1
Comp-Pacific Blue-A :: LIVE DEAD
SSC-A
SAMPLES 05-10-2016_IR PBMC2.fcs
Singlets
4631
CD115-
95.1
Comp-APC-Cy7-A :: CD115
SSC-A
SAMPLES 05-10-2016_IR PBMC2.fcs
Live Cells
1253
Q1
60.4
Q2
2.85
Q4
33.4
Q3
3.362
Comp-405 C-A :: CD45
Comp-FITC-A :: COLLAGEN-I
SAMPLES 05-10-2016_IR PBMC2.fcs
CD115-
1191
Singlets
95.1
FSC-H
FSC-A
SAMPLES 05-10-2016_IR PBMC3.fcs
Ungated
7818
Live Cells
33.3
Comp-Pacific Blue-A :: LIVE DEAD
SSC-A
SAMPLES 05-10-2016_IR PBMC3.fcs
Singlets
7437
CD115-
97.3
Comp-APC-Cy7-A :: CD115
SSC-A
SAMPLES 05-10-2016_IR PBMC3.fcs
Live Cells
2474
Q1
78.9
Q2
2.33
Q4
16.9
Q3
1.919
Comp-405 C-A :: CD45
Comp-FITC-A :: COLLAGEN-I
SAMPLES 05-10-2016_IR PBMC3.fcs
CD115-
2408

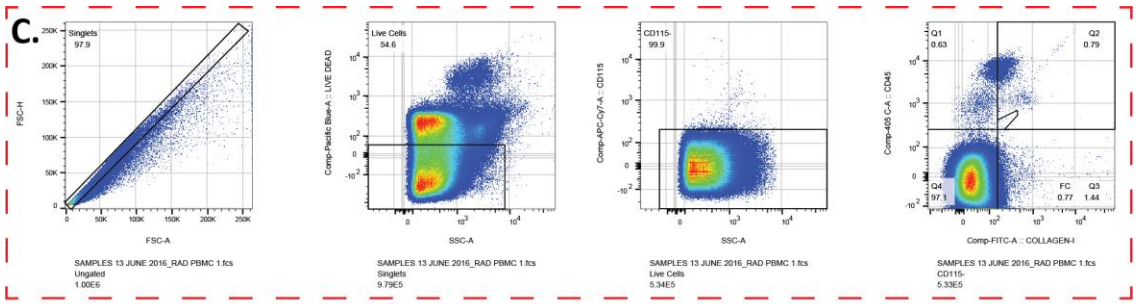
C.
Singlets
97.9
FSC-H
FSC-A
SAMPLES 13 JUNE 2016_RAD PBMC 1.fcs
Ungated
1.00E6
Live Cells
54.6
Comp-Pacific Blue-A :: LIVE DEAD
SSC-A
SAMPLES 13 JUNE 2016_RAD PBMC 1.fcs
Singlets
9.79E5
CD115-
99.9
Comp-APC-Cy7-A :: CD115
SSC-A
SAMPLES 13 JUNE 2016_RAD PBMC 1.fcs
Live Cells
5.34E5
Q1
0.63
Q2
0.79
Q4
97.1
FC
0.77
Q3
1.44
Comp-405 C-A :: CD45
Comp-FITC-A :: COLLAGEN-I
SAMPLES 13 JUNE 2016_RAD PBMC 1.fcs
CD115-
5.33E5

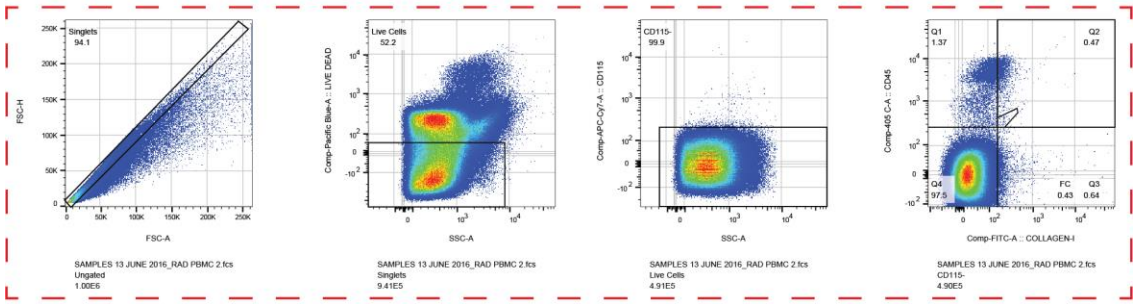
Singlets
94.1
FSC-H
FSC-A
SAMPLES 13 JUNE 2016_RAD PBMC 2.fcs
Ungated
1.00E6
Live Cells
52.2
Comp-Pacific Blue-A :: LIVE DEAD
SSC-A
SAMPLES 13 JUNE 2016_RAD PBMC 2.fcs
Singlets
9.41E5
CD115-
99.9
Comp-APC-Cy7-A :: CD115
SSC-A
SAMPLES 13 JUNE 2016_RAD PBMC 2.fcs
Live Cells
4.91E5
Q1
1.37
Q2
0.47
Q4
97.5
FC
0.43
Q3
0.64
Comp-405 C-A :: CD45
Comp-FITC-A :: COLLAGEN-I
SAMPLES 13 JUNE 2016_RAD PBMC 2.fcs
CD115-
4.90E5

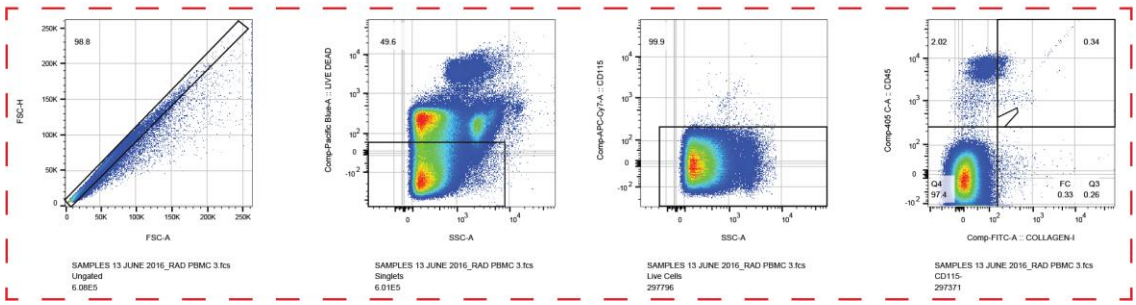
98.8
FSC-H
FSC-A
SAMPLES 13 JUNE 2016_RAD PBMC 3.fcs
Ungated
6.08E5
49.6
Comp-Pacific Blue-A :: LIVE DEAD
SSC-A
SAMPLES 13 JUNE 2016_RAD PBMC 3.fcs
Singlets
6.01E5
99.9
Comp-APC-Cy7-A :: CD115
SSC-A
SAMPLES 13 JUNE 2016_RAD PBMC 3.fcs
Live Cells
297796
2.02
0.34
Q4
97.4
FC
0.33
Q3
0.26
Comp-405 C-A :: CD45
Comp-FITC-A :: COLLAGEN-I
SAMPLES 13 JUNE 2016_RAD PBMC 3.fcs
CD115-
297371

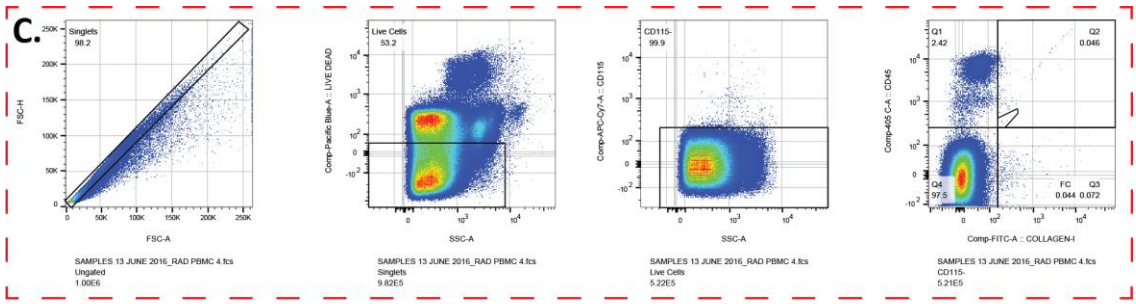
C.
Singlets
98.2
FSC-H
FSC-A
SAMPLES 13 JUNE 2016_RAD PBMC 4.fcs
Ungated
1.00E6
Live Cells
53.2
Comp-Pacific Blue-A :: LIVE DEAD
SSC-A
SAMPLES 13 JUNE 2016_RAD PBMC 4.fcs
Singlets
9.82E5
CD115-
99.9
Comp-APC-Cy7-A :: CD115
SSC-A
SAMPLES 13 JUNE 2016_RAD PBMC 4.fcs
Live Cells
5.22E5
Q1
2.42
Q2
0.046
Q4
97.5
FC
0.044
Q3
0.072
Comp-405 C-A :: CD45
Comp-FITC-A :: COLLAGEN-I
SAMPLES 13 JUNE 2016_RAD PBMC 4.fcs
CD115-
5.21E5

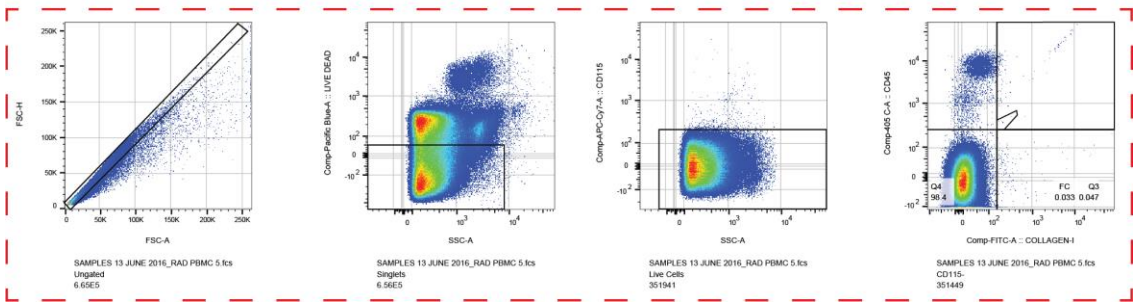
FSC-H
FSC-A
SAMPLES 13 JUNE 2016_RAD PBMC 5.fcs
Ungated
6.65E5
Comp-Pacific Blue-A :: LIVE DEAD
SSC-A
SAMPLES 13 JUNE 2016_RAD PBMC 5.fcs
Singlets
6.56E5
Comp-APC-Cy7-A :: CD115
SSC-A
SAMPLES 13 JUNE 2016_RAD PBMC 5.fcs
Live Cells
351941
Q4
98.4
FC
0.033
Q3
0.047
Comp-405 C-A :: CD45
Comp-FITC-A :: COLLAGEN-I
SAMPLES 13 JUNE 2016_RAD PBMC 5.fcs
CD115-
351449

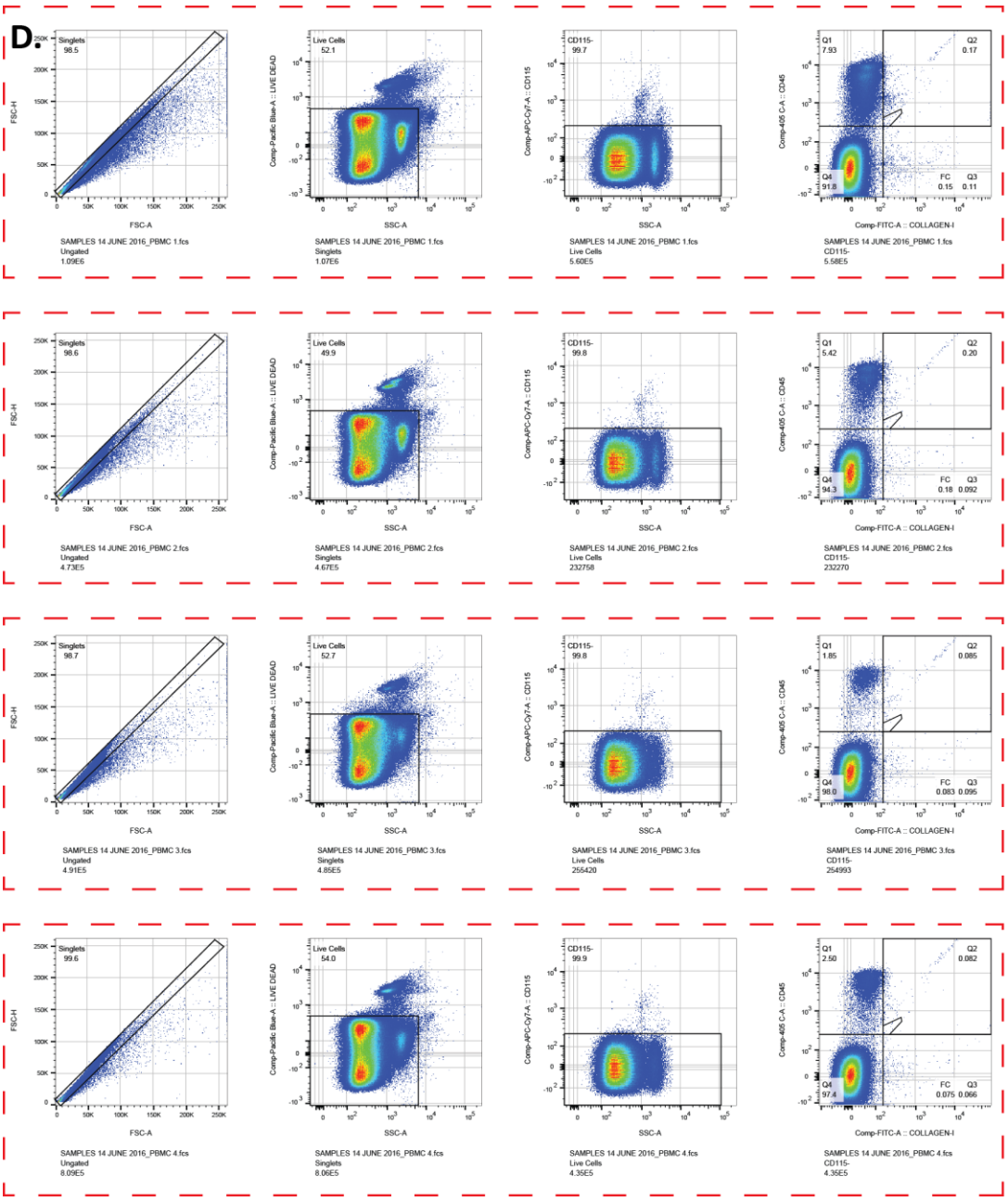

Supplementary Figure 6. Isolated PBMCs flow cytometry data.

Full gating strategy and data are shown for each experimental animal. Red dashed box corresponds to samples isolated from an individual animal. **A.** PBMCs analyzed 14 days post irradiation. **B.** PBMCs analyzed 30 days post irradiation. **C.** PBMCs analyzed 60 days post irradiation. **D.** Sham animal analyzed PBMCs.

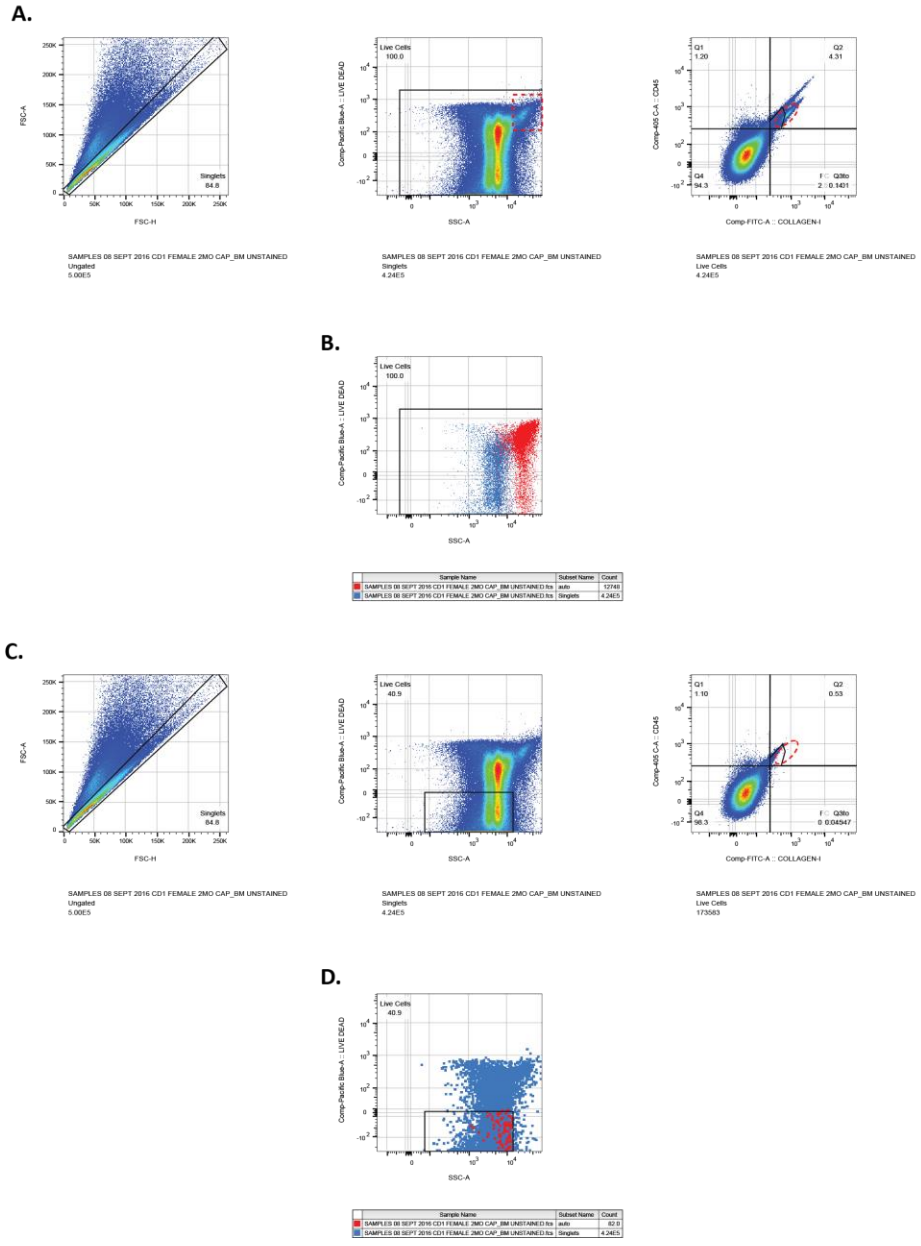

Supplementary Figure 7. Setting the gates to identify CD45$^+$ ColI$^+$ cells in bone marrow cells.

Unstained cells were used set the gate parameters to detect CD45$^+$ ColI$^+$ cells. **A.** A group of autofluorescent cells (red dashed circle). was identified in the total population of bone marrow cells **B.** This population was back-gated to determine where this population of cells resided in the total population of cells. **C.** The autofluorescent group of cells was gated out and gates were determined using unstained cells. **D.** Confirmation that the population of autofluorescent cells were removed from the population of CD45$^+$ ColI$^+$ cells.

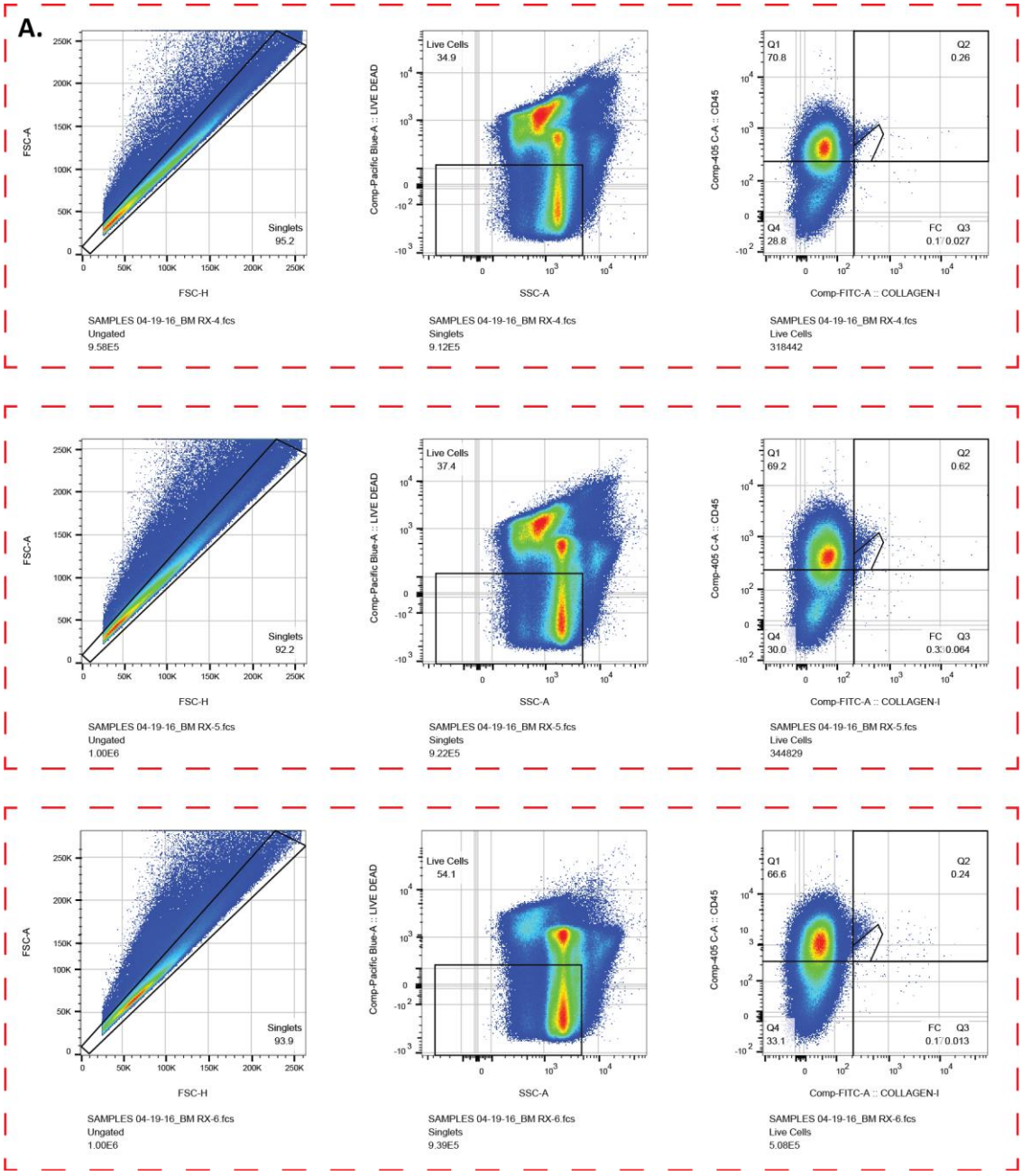
A.
FSC-A
FSC-H
Singlets
95.2
SAMPLES 04-19-16_BM RX-4.fcs
Ungated
9.58E5
Comp-Pacific Blue-A :: LIVE DEAD
SSC-A
Live Cells
34.9
SAMPLES 04-19-16_BM RX-4.fcs
Singlets
9.12E5
Comp-405 C-A :: CD45
Comp-FITC-A :: COLLAGEN-I
Q1
70.8
Q2
0.26
Q4
28.8
FC Q3
0.1 0.027
SAMPLES 04-19-16_BM RX-4.fcs
Live Cells
318442
FSC-A
FSC-H
Singlets
92.2
SAMPLES 04-19-16_BM RX-5.fcs
Ungated
1.00E6
Comp-Pacific Blue-A :: LIVE DEAD
SSC-A
Live Cells
37.4
SAMPLES 04-19-16_BM RX-5.fcs
Singlets
9.22E5
Comp-405 C-A :: CD45
Comp-FITC-A :: COLLAGEN-I
Q1
69.2
Q2
0.62
Q4
30.0
FC Q3
0.3 0.064
SAMPLES 04-19-16_BM RX-5.fcs
Live Cells
344829
FSC-A
FSC-H
Singlets
93.9
SAMPLES 04-19-16_BM RX-6.fcs
Ungated
1.00E6
Comp-Pacific Blue-A :: LIVE DEAD
SSC-A
Live Cells
54.1
SAMPLES 04-19-16_BM RX-6.fcs
Singlets
9.39E5
Comp-405 C-A :: CD45
Comp-FITC-A :: COLLAGEN-I
Q1
66.6
Q2
0.24
Q4
33.1
FC Q3
0.1 0.013
SAMPLES 04-19-16_BM RX-6.fcs
Live Cells
5.08E5

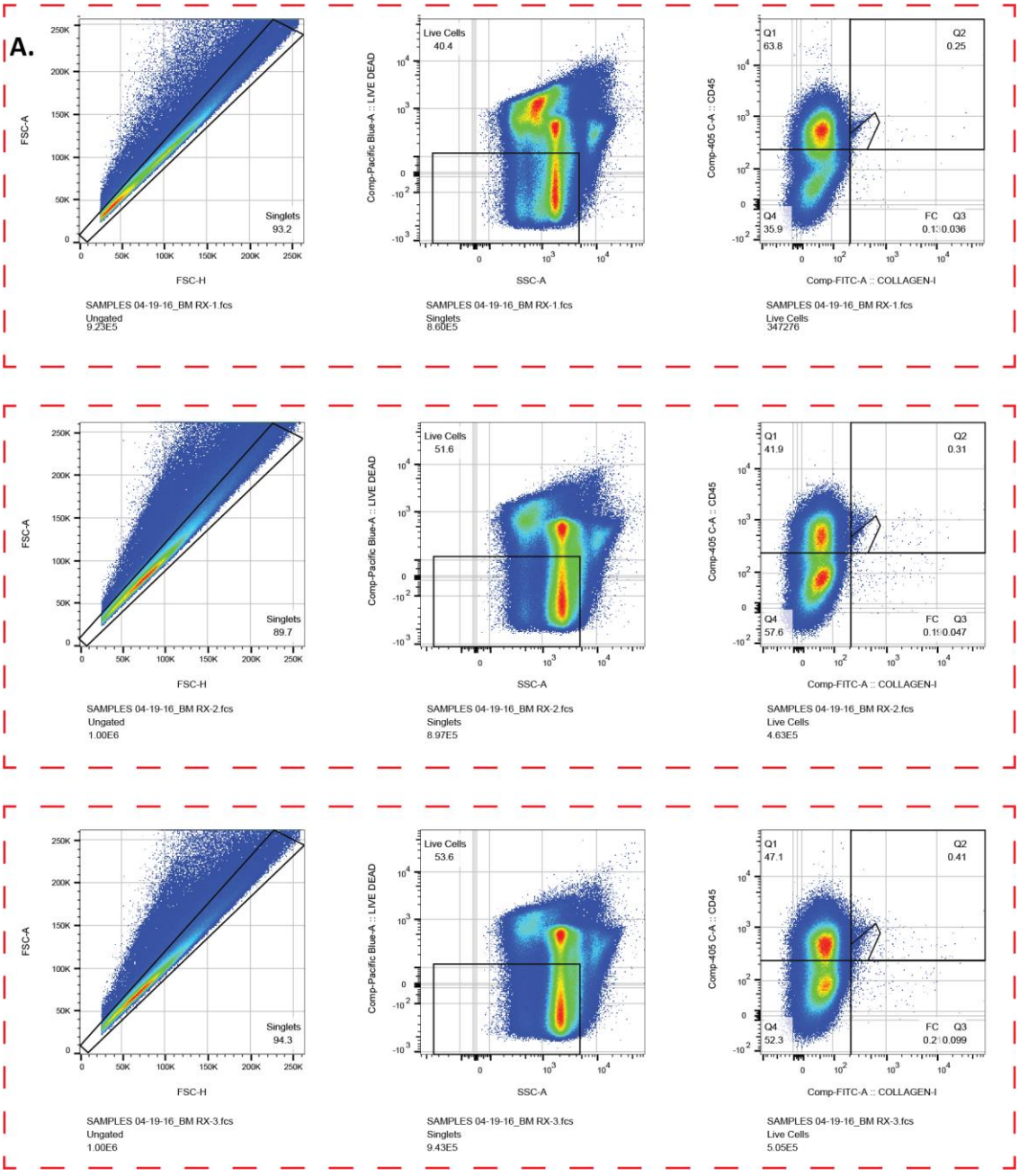
A.
FSC-A
FSC-H
Singlets
93.2
SAMPLES 04-19-16_BM RX-1.fcs
Ungated
9.23E5
Comp-Pacific Blue-A :: LIVE DEAD
SSC-A
Live Cells
40.4
SAMPLES 04-19-16_BM RX-1.fcs
Singlets
8.60E5
Comp-405 C-A :: CD45
Comp-FITC-A :: COLLAGEN-I
Q1
63.8
Q2
0.25
Q4
35.9
FC
0.1
Q3
0.036
SAMPLES 04-19-16_BM RX-1.fcs
Live Cells
347276
FSC-A
FSC-H
Singlets
89.7
SAMPLES 04-19-16_BM RX-2.fcs
Ungated
1.00E6
Comp-Pacific Blue-A :: LIVE DEAD
SSC-A
Live Cells
51.6
SAMPLES 04-19-16_BM RX-2.fcs
Singlets
8.97E5
Comp-405 C-A :: CD45
Comp-FITC-A :: COLLAGEN-I
Q1
41.9
Q2
0.31
Q4
57.6
FC
0.1
Q3
0.047
SAMPLES 04-19-16_BM RX-2.fcs
Live Cells
4.63E5
FSC-A
FSC-H
Singlets
94.3
SAMPLES 04-19-16_BM RX-3.fcs
Ungated
1.00E6
Comp-Pacific Blue-A :: LIVE DEAD
SSC-A
Live Cells
53.6
SAMPLES 04-19-16_BM RX-3.fcs
Singlets
9.43E5
Comp-405 C-A :: CD45
Comp-FITC-A :: COLLAGEN-I
Q1
47.1
Q2
0.41
Q4
52.3
FC
0.2
Q3
0.099
SAMPLES 04-19-16_BM RX-3.fcs
Live Cells
5.05E5

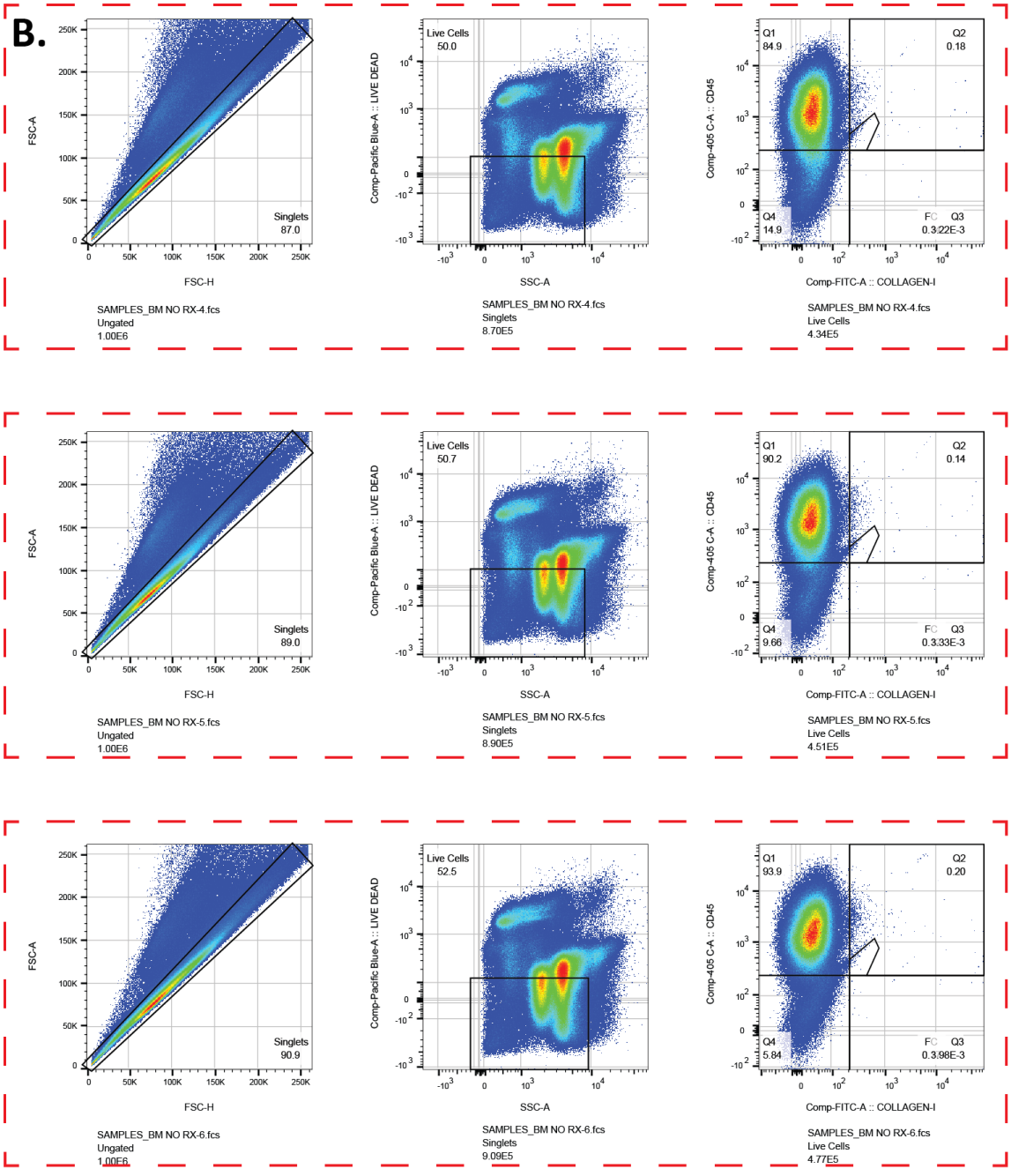
B.
FSC-A
FSC-H
Singlets
87.0
SAMPLES_BM NO RX-4.fcs
Ungated
1.00E6
Comp-Pacific Blue-A :: LIVE DEAD
SSC-A
Live Cells
50.0
SAMPLES_BM NO RX-4.fcs
Singlets
8.70E5
Comp-405 C-A :: CD45
Comp-FITC-A :: COLLAGEN-I
Q1
84.9
Q2
0.18
Q4
14.9
Q3
0.322E-3
SAMPLES_BM NO RX-4.fcs
Live Cells
4.34E5
FSC-A
FSC-H
Singlets
89.0
SAMPLES_BM NO RX-5.fcs
Ungated
1.00E6
Comp-Pacific Blue-A :: LIVE DEAD
SSC-A
Live Cells
50.7
SAMPLES_BM NO RX-5.fcs
Singlets
8.90E5
Comp-405 C-A :: CD45
Comp-FITC-A :: COLLAGEN-I
Q1
90.2
Q2
0.14
Q4
9.66
Q3
0.333E-3
SAMPLES_BM NO RX-5.fcs
Live Cells
4.51E5
FSC-A
FSC-H
Singlets
90.9
SAMPLES_BM NO RX-6.fcs
Ungated
1.00E6
Comp-Pacific Blue-A :: LIVE DEAD
SSC-A
Live Cells
52.5
SAMPLES_BM NO RX-6.fcs
Singlets
9.09E5
Comp-405 C-A :: CD45
Comp-FITC-A :: COLLAGEN-I
Q1
93.9
Q2
0.20
Q4
5.84
Q3
0.398E-3
SAMPLES_BM NO RX-6.fcs
Live Cells
4.77E5

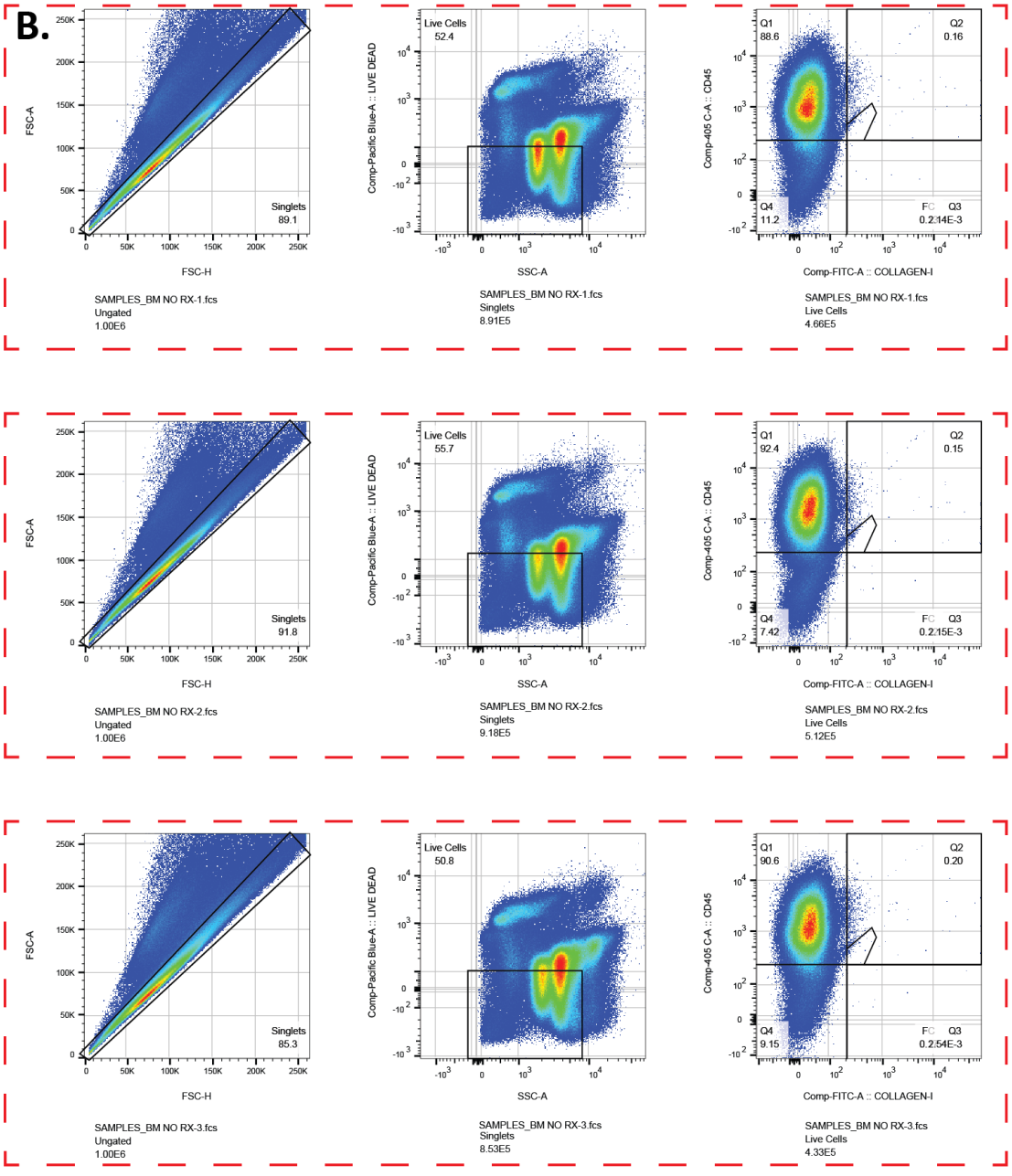
B.
FSC-A
FSC-H
Singlets
89.1
SAMPLES_BM NO RX-1.fcs
Ungated
1.00E6
Comp-Pacific Blue-A :: LIVE DEAD
SSC-A
Live Cells
52.4
SAMPLES_BM NO RX-1.fcs
Singlets
8.91E5
Comp-405 C-A :: CD45
Comp-FITC-A :: COLLAGEN-I
Q1
88.6
Q2
0.16
Q4
11.2
Q3
0.214E-3
SAMPLES_BM NO RX-1.fcs
Live Cells
4.66E5
FSC-A
FSC-H
Singlets
91.8
SAMPLES_BM NO RX-2.fcs
Ungated
1.00E6
Comp-Pacific Blue-A :: LIVE DEAD
SSC-A
Live Cells
55.7
SAMPLES_BM NO RX-2.fcs
Singlets
9.18E5
Comp-405 C-A :: CD45
Comp-FITC-A :: COLLAGEN-I
Q1
92.4
Q2
0.15
Q4
7.42
Q3
0.215E-3
SAMPLES_BM NO RX-2.fcs
Live Cells
5.12E5
FSC-A
FSC-H
Singlets
85.3
SAMPLES_BM NO RX-3.fcs
Ungated
1.00E6
Comp-Pacific Blue-A :: LIVE DEAD
SSC-A
Live Cells
50.8
SAMPLES_BM NO RX-3.fcs
Singlets
8.53E5
Comp-405 C-A :: CD45
Comp-FITC-A :: COLLAGEN-I
Q1
90.6
Q2
0.20
Q4
9.15
Q3
0.254E-3
SAMPLES_BM NO RX-3.fcs
Live Cells
4.33E5

C.

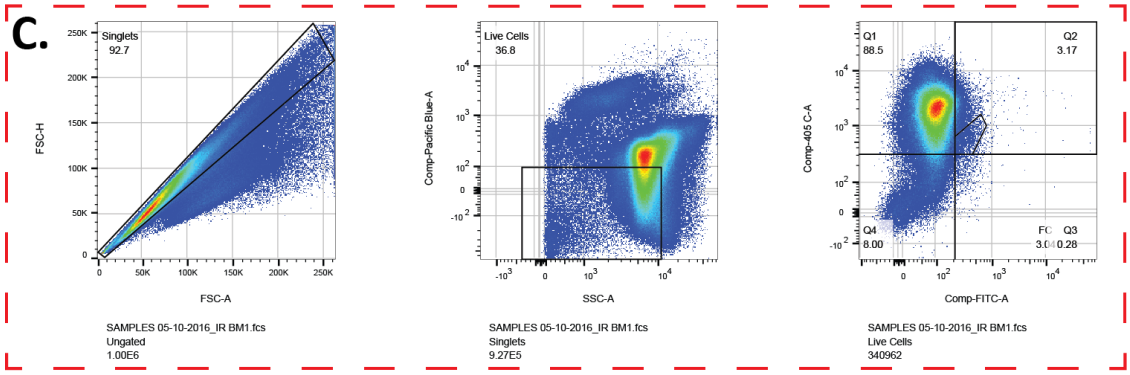
Singlets
92.7
FSC-H
FSC-A
SAMPLES 05-10-2016_IR BM1.fcs
Ungated
1.00E6
Live Cells
36.8
Comp-Pacific Blue-A
SSC-A
SAMPLES 05-10-2016_IR BM1.fcs
Singlets
9.27E5
Q1
88.5
Q2
3.17
Q4
8.00
Q3
Comp-405 C-A
Comp-FITC-A
SAMPLES 05-10-2016_IR BM1.fcs
Live Cells
340962

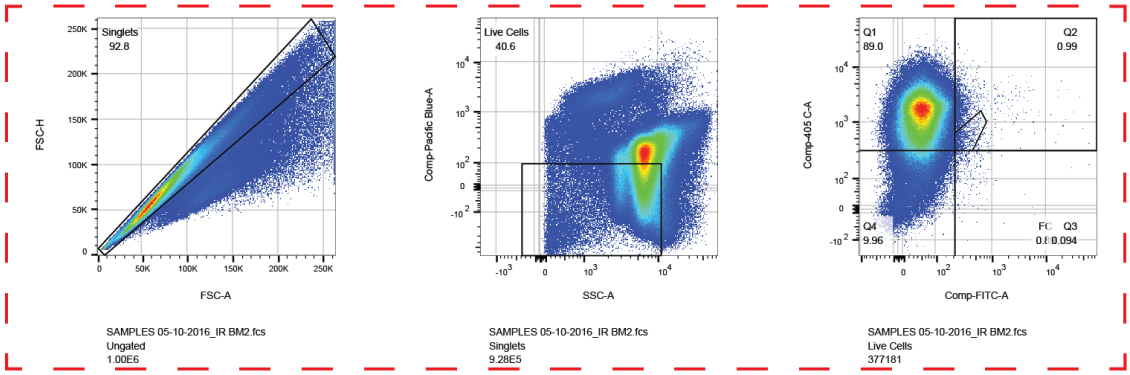
Singlets
92.8
FSC-H
FSC-A
SAMPLES 05-10-2016_IR BM2.fcs
Ungated
1.00E6
Live Cells
40.6
Comp-Pacific Blue-A
SSC-A
SAMPLES 05-10-2016_IR BM2.fcs
Singlets
9.28E5
Q1
89.0
Q2
0.99
Q4
9.96
Q3
Comp-405 C-A
Comp-FITC-A
SAMPLES 05-10-2016_IR BM2.fcs
Live Cells
377181

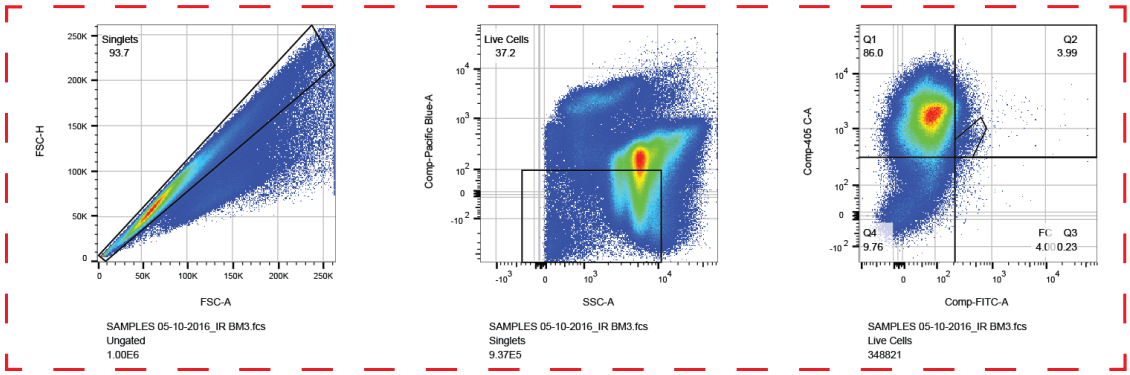
Singlets
93.7
FSC-H
FSC-A
SAMPLES 05-10-2016_IR BM3.fcs
Ungated
1.00E6
Live Cells
37.2
Comp-Pacific Blue-A
SSC-A
SAMPLES 05-10-2016_IR BM3.fcs
Singlets
9.37E5
Q1
86.0
Q2
3.99
Q4
9.76
Q3
Comp-405 C-A
Comp-FITC-A
SAMPLES 05-10-2016_IR BM3.fcs
Live Cells
348821

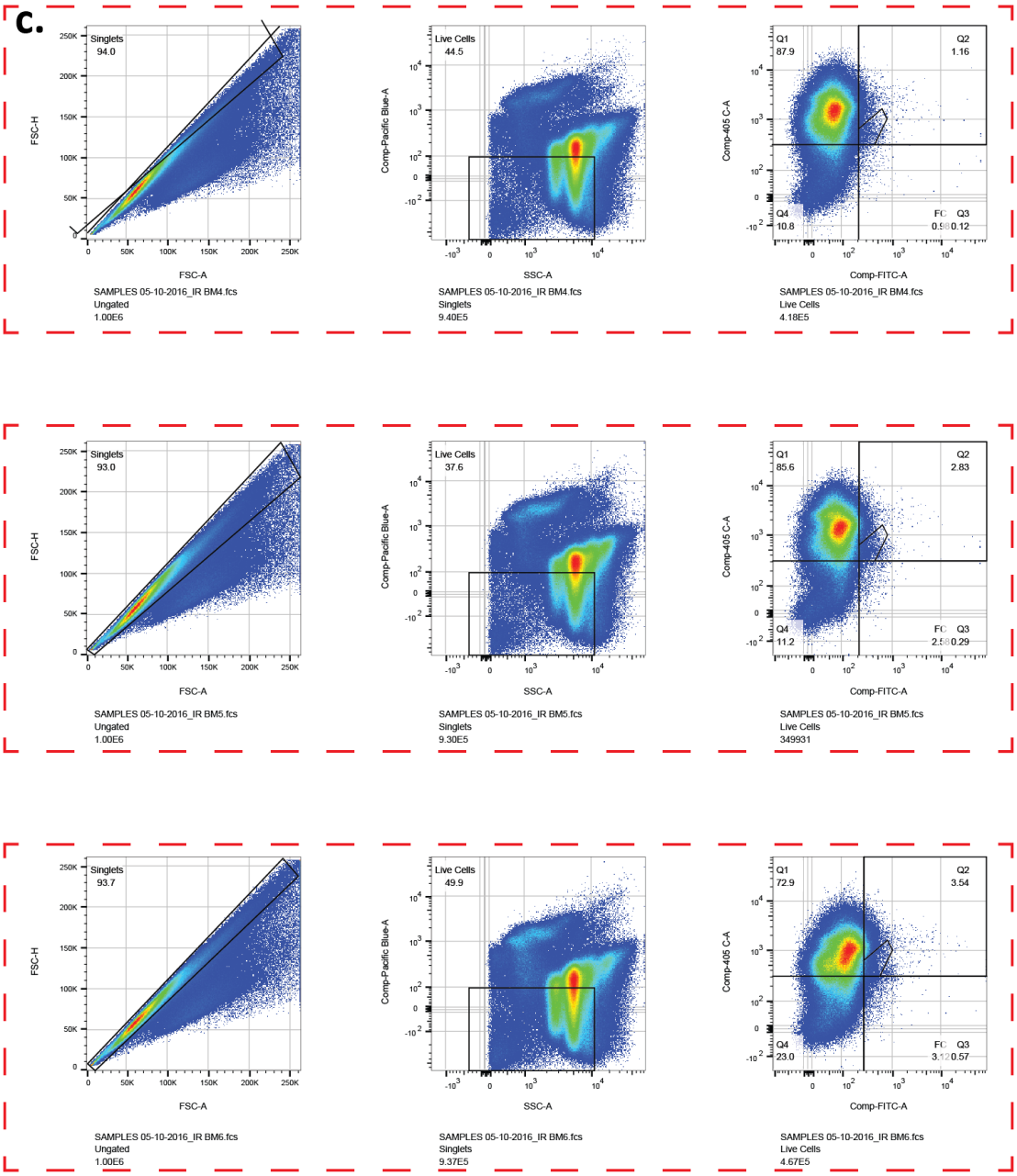

Supplementary Figure 8. Isolated bone marrow cells flow cytometry data. Full gating strategy and data are shown for each experimental animal. Red dashed box corresponds to samples isolated from an individual animal. **A.** Bone marrow cells isolated and analyzed 7 days post irradiation. **B.** Bone marrow cells isolated and analyzed 14 days post irradiation. **C.** Bone marrow cells isolated and analyzed 30 days post irradiation.

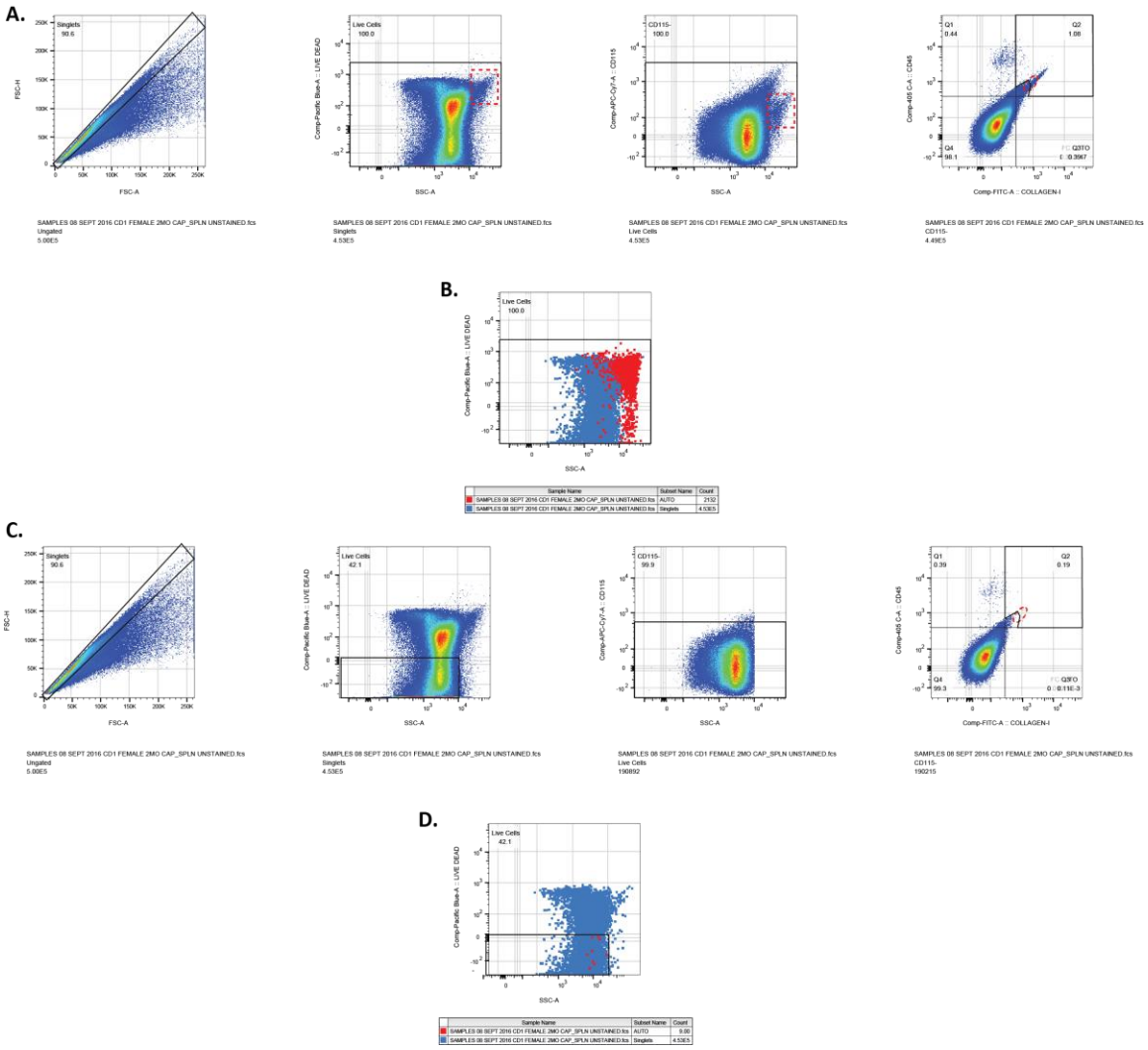

Supplementary Figure 9. Setting the gates to identify fibrocytes in spleen cells. Unstained cells were used set the gate parameters to detect $CD115^{-}$ $CD45^{+}$ $ColI^{+}$ fibrocytes. **A.** A group of autofluorescent cells (red dashed circle) was identified in the total population of spleen cells. **B.** This population was back-gated to determine where this population of cells resided in the total population of cells. **C.** The autofluorescent group of cells was gated out and gates were determined using unstained cells. **D.** Confirmation that the population of autofluorescent cells were removed from the population of $CD115^{-}$ $CD45^{+}$ $ColI^{+}$ fibrocytes.

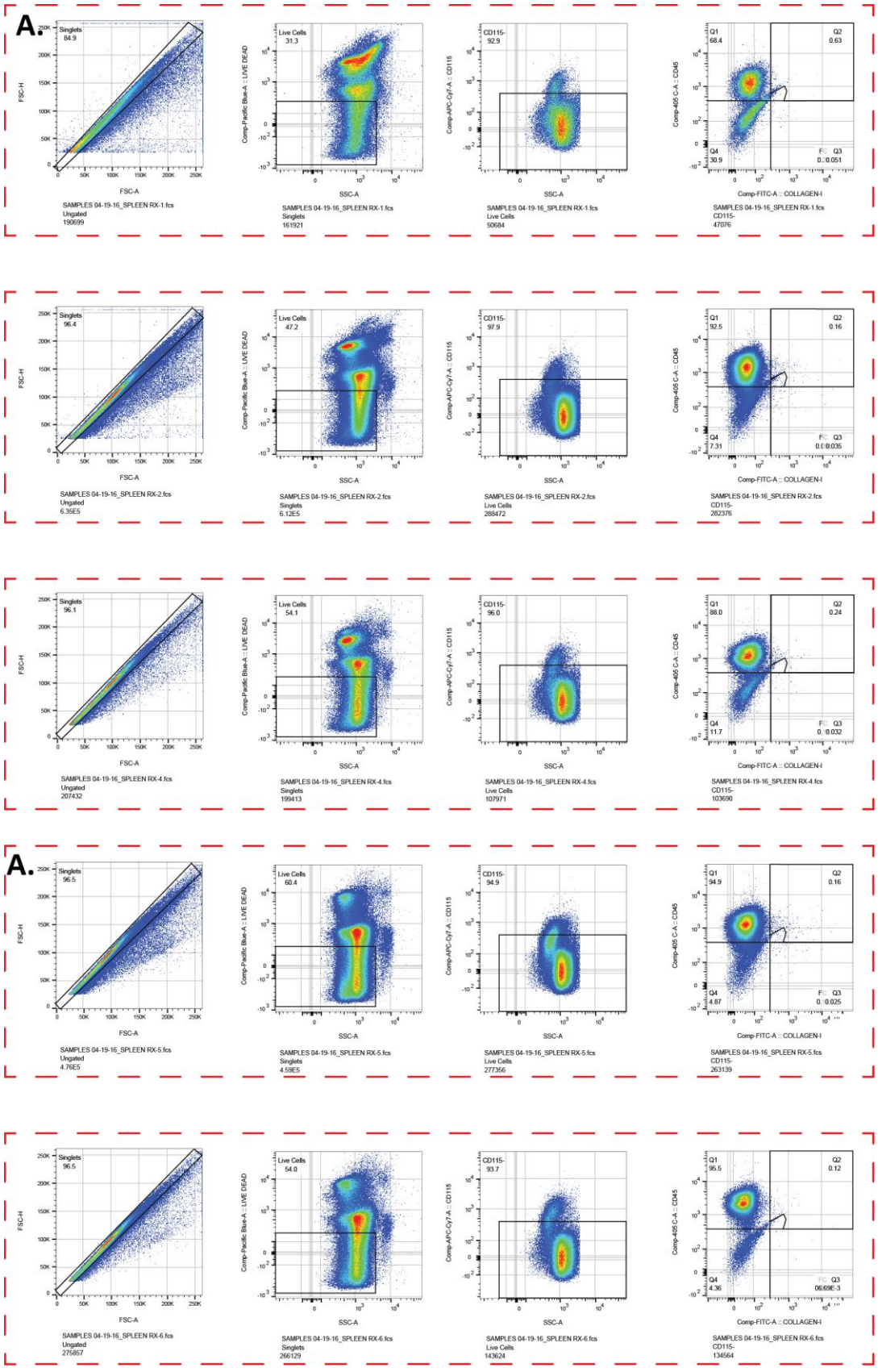
A.
Singlets
84.9
FSC-H
FSC-A
SAMPLES 04-19-16_SPLEEN RX-1.fcs
Ungated
190699
Live Cells
31.3
Comp-Pacific Blue-A :: LIVE DEAD
SSC-A
SAMPLES 04-19-16_SPLEEN RX-1.fcs
Singlets
161921
CD115-
92.9
Comp-APC-Cy7-A :: CD115
SSC-A
SAMPLES 04-19-16_SPLEEN RX-1.fcs
Live Cells
50684
Q1
68.4
Q2
0.63
Q4
30.9
Q3
0.0:0.051
Comp-405 C-A :: CD45
Comp-FITC-A :: COLLAGEN-I
SAMPLES 04-19-16_SPLEEN RX-1.fcs
CD115-
47076
Singlets
96.4
SAMPLES 04-19-16_SPLEEN RX-2.fcs
Ungated
6.35E5
Live Cells
47.2
SAMPLES 04-19-16_SPLEEN RX-2.fcs
Singlets
6.12E5
CD115-
97.9
SAMPLES 04-19-16_SPLEEN RX-2.fcs
Live Cells
288472
Q1
92.5
Q2
0.16
Q4
7.31
Q3
0.0:0.035
SAMPLES 04-19-16_SPLEEN RX-2.fcs
CD115-
282376
Singlets
96.1
SAMPLES 04-19-16_SPLEEN RX-4.fcs
Ungated
207432
Live Cells
54.1
SAMPLES 04-19-16_SPLEEN RX-4.fcs
Singlets
199413
CD115-
96.0
SAMPLES 04-19-16_SPLEEN RX-4.fcs
Live Cells
107971
Q1
88.0
Q2
0.24
Q4
11.7
Q3
0.0:0.032
SAMPLES 04-19-16_SPLEEN RX-4.fcs
CD115-
103690
A.
Singlets
96.5
SAMPLES 04-19-16_SPLEEN RX-5.fcs
Ungated
4.76E5
Live Cells
60.4
SAMPLES 04-19-16_SPLEEN RX-5.fcs
Singlets
4.59E5
CD115-
94.9
SAMPLES 04-19-16_SPLEEN RX-5.fcs
Live Cells
277356
Q1
94.9
Q2
0.16
Q4
4.87
Q3
0.0:0.025
SAMPLES 04-19-16_SPLEEN RX-5.fcs
CD115-
263139
Singlets
96.5
SAMPLES 04-19-16_SPLEEN RX-6.fcs
Ungated
275857
Live Cells
54.8
SAMPLES 04-19-16_SPLEEN RX-6.fcs
Singlets
266129
CD115-
93.7
SAMPLES 04-19-16_SPLEEN RX-6.fcs
Live Cells
143624
Q1
95.5
Q2
0.12
Q4
4.36
Q3
05.69E-3
SAMPLES 04-19-16_SPLEEN RX-6.fcs
CD115-
134564

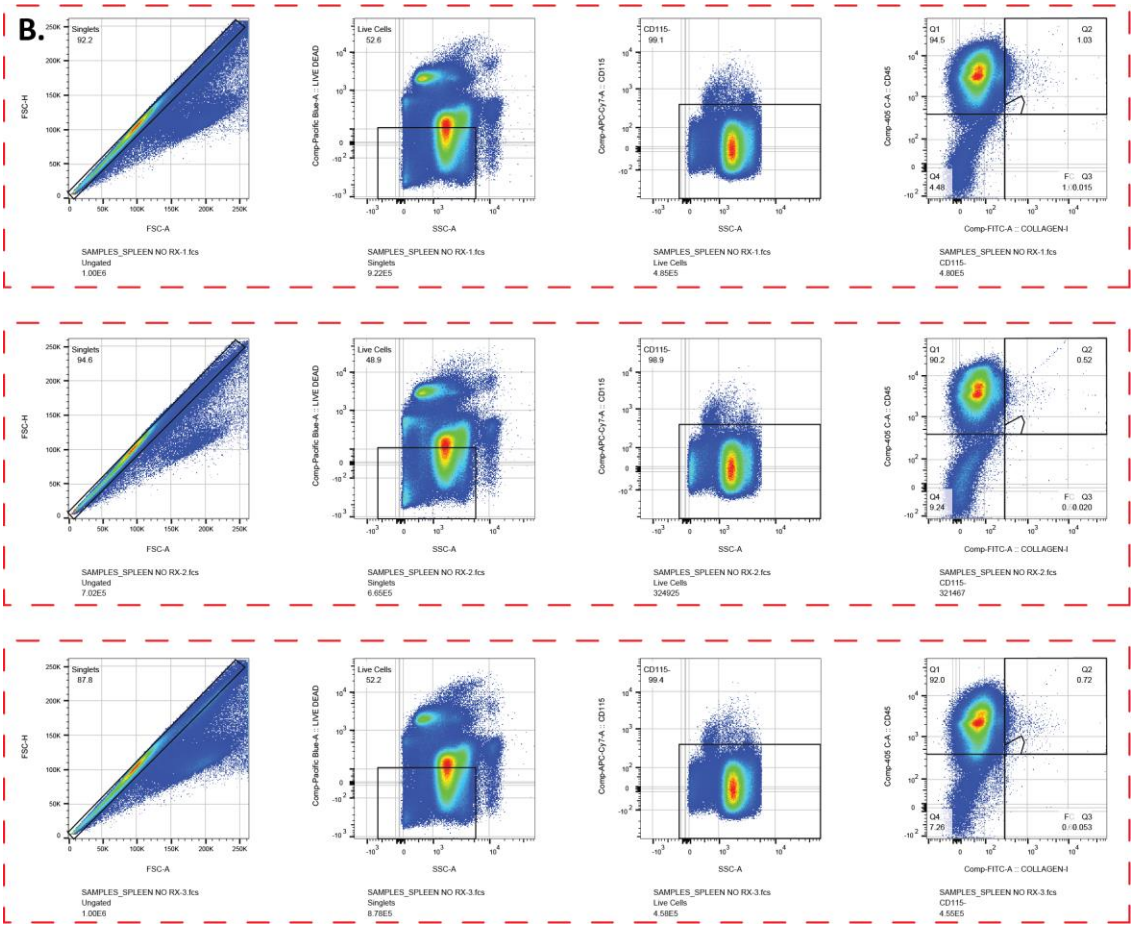
B.
Singlets
92.2
FSC-H
FSC-A
SAMPLES_SPLEEN NO RX-1.fcs
Ungated
1.00E6
Live Cells
52.6
Comp-Pacific Blue-A :: LIVE DEAD
SSC-A
SAMPLES_SPLEEN NO RX-1.fcs
Singlets
9.22E5
CD115-
99.1
Comp-APC-Cy7-A :: CD115
SSC-A
SAMPLES_SPLEEN NO RX-1.fcs
Live Cells
4.85E5
Q1
94.5
Q2
1.03
Q4
4.48
Q3
1.01
Comp-405 C-A :: CD45
Comp-FITC-A :: COLLAGEN-I
SAMPLES_SPLEEN NO RX-1.fcs
CD115-
4.80E5
Singlets
94.6
FSC-H
FSC-A
SAMPLES_SPLEEN NO RX-2.fcs
Ungated
7.02E5
Live Cells
48.9
Comp-Pacific Blue-A :: LIVE DEAD
SSC-A
SAMPLES_SPLEEN NO RX-2.fcs
Singlets
6.65E5
CD115-
98.9
Comp-APC-Cy7-A :: CD115
SSC-A
SAMPLES_SPLEEN NO RX-2.fcs
Live Cells
324925
Q1
90.2
Q2
0.52
Q4
9.24
Q3
0.020
Comp-405 C-A :: CD45
Comp-FITC-A :: COLLAGEN-I
SAMPLES_SPLEEN NO RX-2.fcs
CD115-
321467
Singlets
87.8
FSC-H
FSC-A
SAMPLES_SPLEEN NO RX-3.fcs
Ungated
1.00E6
Live Cells
52.2
Comp-Pacific Blue-A :: LIVE DEAD
SSC-A
SAMPLES_SPLEEN NO RX-3.fcs
Singlets
8.78E5
CD115-
99.4
Comp-APC-Cy7-A :: CD115
SSC-A
SAMPLES_SPLEEN NO RX-3.fcs
Live Cells
4.58E5
Q1
92.0
Q2
0.72
Q4
7.26
Q3
0.053
Comp-405 C-A :: CD45
Comp-FITC-A :: COLLAGEN-I
SAMPLES_SPLEEN NO RX-3.fcs
CD115-
4.55E5

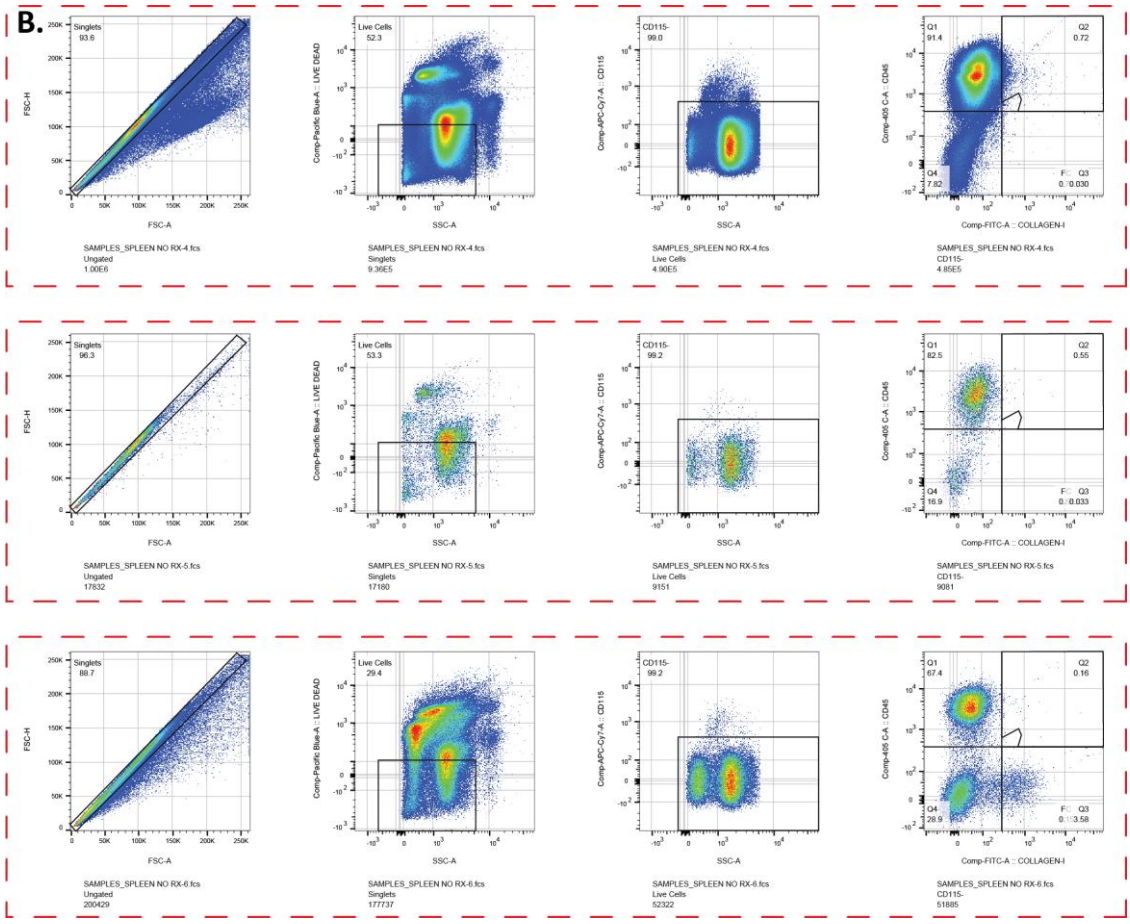
B.
Singlets
93.6
FSC-H
FSC-A
SAMPLES_SPLEEN NO RX-4.fcs
Ungated
1.00E6
Live Cells
52.3
Comp-Pacific Blue-A :: LIVE DEAD
SSC-A
SAMPLES_SPLEEN NO RX-4.fcs
Singlets
9.36E5
CD115-
99.0
Comp-APC-Cy7-A :: CD115
SSC-A
SAMPLES_SPLEEN NO RX-4.fcs
Live Cells
4.90E5
Q1
91.4
Q2
0.72
Q4
7.82
Q3
0.030
Comp-405 C-A :: CD45
Comp-FITC-A :: COLLAGEN-I
SAMPLES_SPLEEN NO RX-4.fcs
CD115-
4.85E5
Singlets
96.3
FSC-H
FSC-A
SAMPLES_SPLEEN NO RX-5.fcs
Ungated
17632
Live Cells
53.3
Comp-Pacific Blue-A :: LIVE DEAD
SSC-A
SAMPLES_SPLEEN NO RX-5.fcs
Singlets
17180
CD115-
99.2
Comp-APC-Cy7-A :: CD115
SSC-A
SAMPLES_SPLEEN NO RX-5.fcs
Live Cells
9151
Q1
82.5
Q2
0.55
Q4
16.9
Q3
0.033
Comp-405 C-A :: CD45
Comp-FITC-A :: COLLAGEN-I
SAMPLES_SPLEEN NO RX-5.fcs
CD115-
9081
Singlets
88.7
FSC-H
FSC-A
SAMPLES_SPLEEN NO RX-6.fcs
Ungated
200429
Live Cells
29.4
Comp-Pacific Blue-A :: LIVE DEAD
SSC-A
SAMPLES_SPLEEN NO RX-6.fcs
Singlets
177737
CD115-
99.2
Comp-APC-Cy7-A :: CD115
SSC-A
SAMPLES_SPLEEN NO RX-6.fcs
Live Cells
52322
Q1
67.4
Q2
0.16
Q4
28.9
Q3
3.58
Comp-405 C-A :: CD45
Comp-FITC-A :: COLLAGEN-I
SAMPLES_SPLEEN NO RX-6.fcs
CD115-
51885

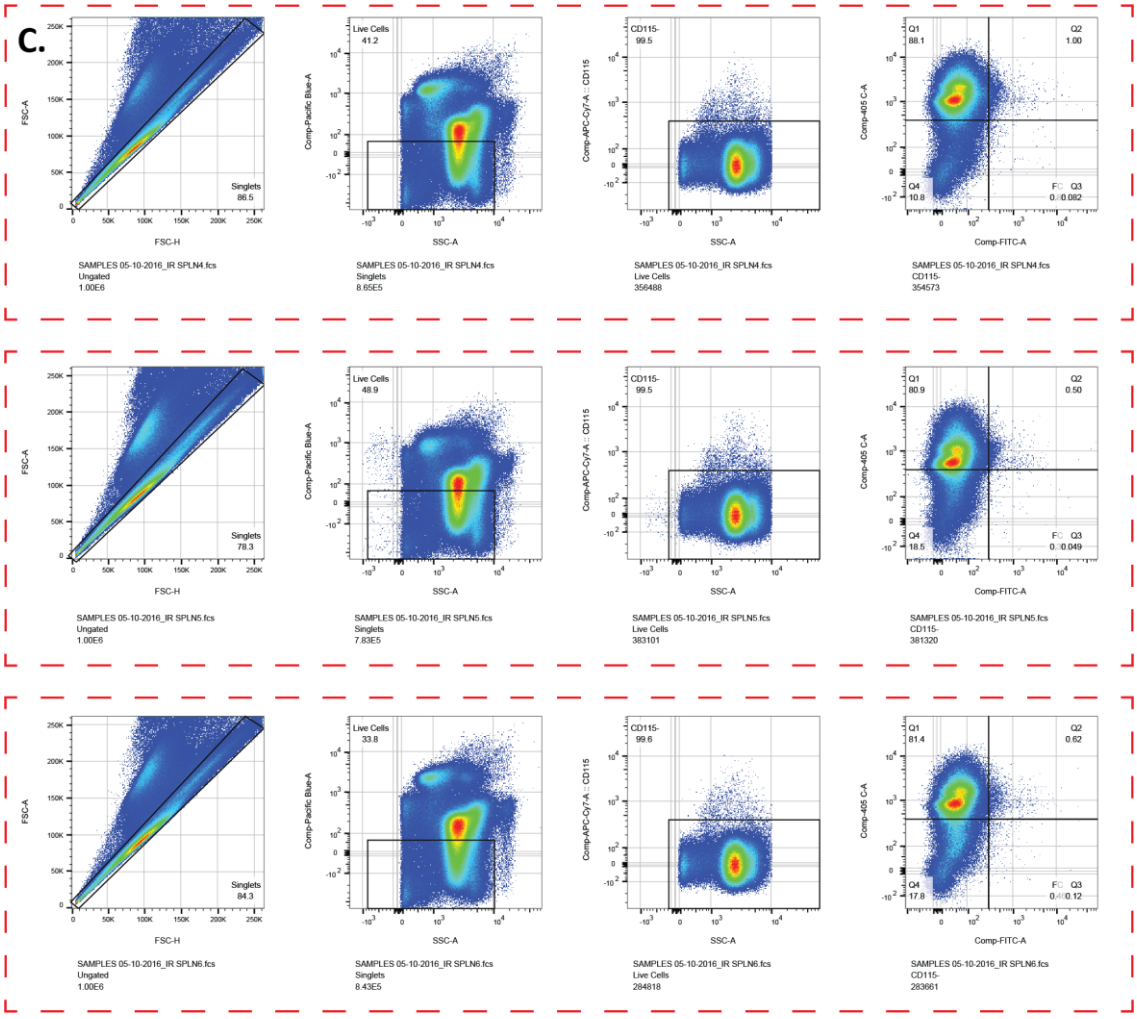
C.
FSC-A
FSC-H
Singlets
86.5
SAMPLES 05-10-2016_IR SPLN4.fcs
Ungated
1.00E6
Comp-Pacific Blue-A
SSC-A
Live Cells
41.2
SAMPLES 05-10-2016_IR SPLN4.fcs
Singlets
8.65E5
Comp-APC-Cy7-A :: CD115
SSC-A
CD115-
99.5
SAMPLES 05-10-2016_IR SPLN4.fcs
Live Cells
356488
Comp-405 C-A
Comp-FITC-A
Q1
88.1
Q2
1.00
Q4
10.8
Q3
SAMPLES 05-10-2016_IR SPLN4.fcs
CD115-
354573
FSC-A
FSC-H
Singlets
78.3
SAMPLES 05-10-2016_IR SPLN5.fcs
Ungated
1.00E6
Comp-Pacific Blue-A
SSC-A
Live Cells
48.9
SAMPLES 05-10-2016_IR SPLN5.fcs
Singlets
7.83E5
Comp-APC-Cy7-A :: CD115
SSC-A
CD115-
99.5
SAMPLES 05-10-2016_IR SPLN5.fcs
Live Cells
383101
Comp-405 C-A
Comp-FITC-A
Q1
80.9
Q2
0.50
Q4
18.5
Q3
SAMPLES 05-10-2016_IR SPLN5.fcs
CD115-
381320
FSC-A
FSC-H
Singlets
84.3
SAMPLES 05-10-2016_IR SPLN6.fcs
Ungated
1.00E6
Comp-Pacific Blue-A
SSC-A
Live Cells
33.8
SAMPLES 05-10-2016_IR SPLN6.fcs
Singlets
8.43E5
Comp-APC-Cy7-A :: CD115
SSC-A
CD115-
99.6
SAMPLES 05-10-2016_IR SPLN6.fcs
Live Cells
284818
Comp-405 C-A
Comp-FITC-A
Q1
81.4
Q2
0.62
Q4
17.8
Q3
SAMPLES 05-10-2016_IR SPLN6.fcs
CD115-
283661

C.

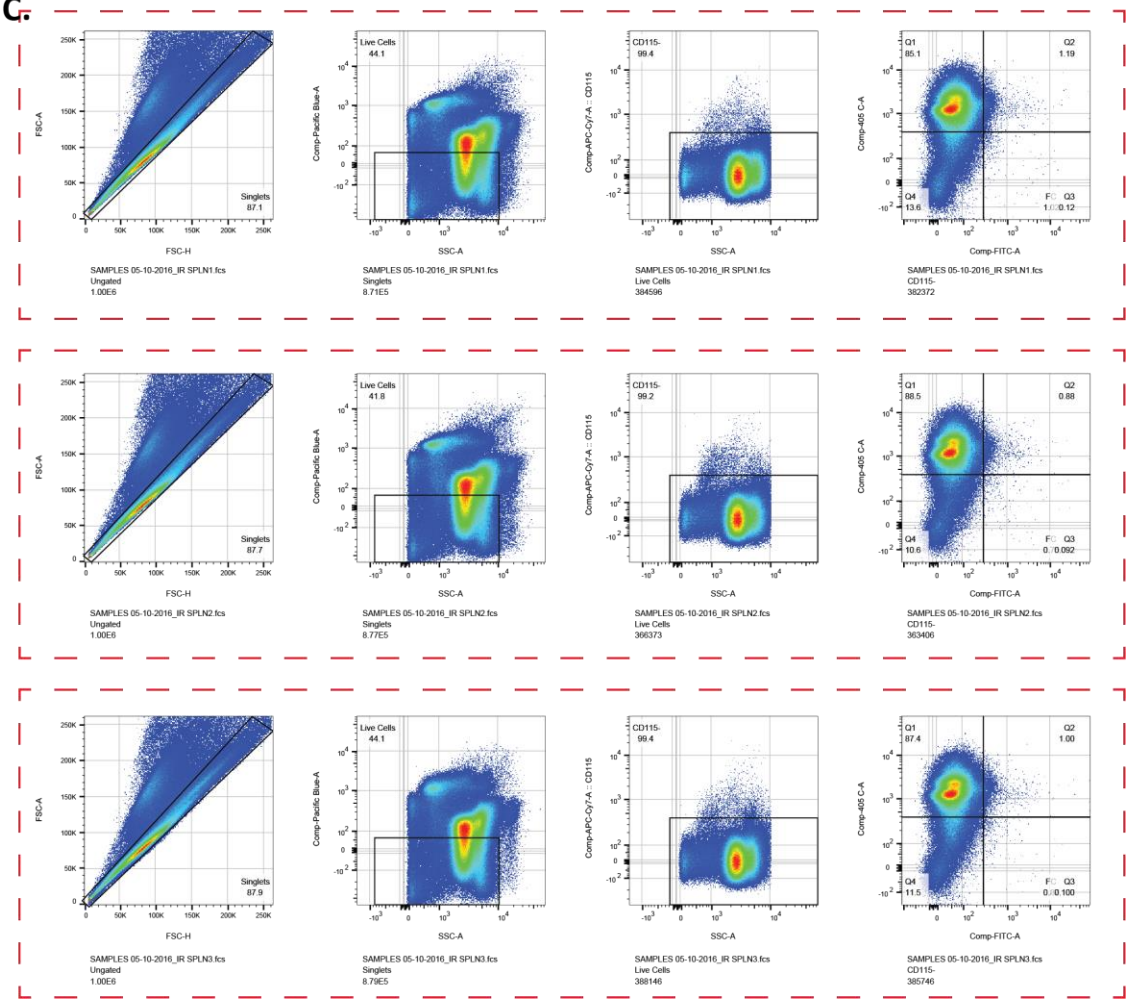
FSC-A
FSC-H
Singlets
87.1
SAMPLES 05-10-2016_IR SPLN1.fcs
Ungated
1.00E6
Comp-Pacific Blue-A
SSC-A
Live Cells
44.1
SAMPLES 05-10-2016_IR SPLN1.fcs
Singlets
8.71E5
Comp-APC-Cy7-A :: CD115
CD115-
99.4
SAMPLES 05-10-2016_IR SPLN1.fcs
Live Cells
384596
Comp-405 C-A
Comp-FITC-A
Q1
85.1
Q2
1.19
Q4
13.6
Q3
1.00
0.12
SAMPLES 05-10-2016_IR SPLN1.fcs
CD115-
382372
Singlets
87.7
SAMPLES 05-10-2016_IR SPLN2.fcs
Ungated
1.00E6
Live Cells
41.8
SAMPLES 05-10-2016_IR SPLN2.fcs
Singlets
8.77E5
CD115-
99.2
SAMPLES 05-10-2016_IR SPLN2.fcs
Live Cells
366373
Q1
88.5
Q2
0.88
Q4
10.6
Q3
0.00
0.092
SAMPLES 05-10-2016_IR SPLN2.fcs
CD115-
363406
Singlets
87.9
SAMPLES 05-10-2016_IR SPLN3.fcs
Ungated
1.00E6
Live Cells
44.1
SAMPLES 05-10-2016_IR SPLN3.fcs
Singlets
8.79E5
CD115-
99.4
SAMPLES 05-10-2016_IR SPLN3.fcs
Live Cells
388146
Q1
87.4
Q2
1.00
Q4
11.5
Q3
0.00
0.100
SAMPLES 05-10-2016_IR SPLN3.fcs
CD115-
385746

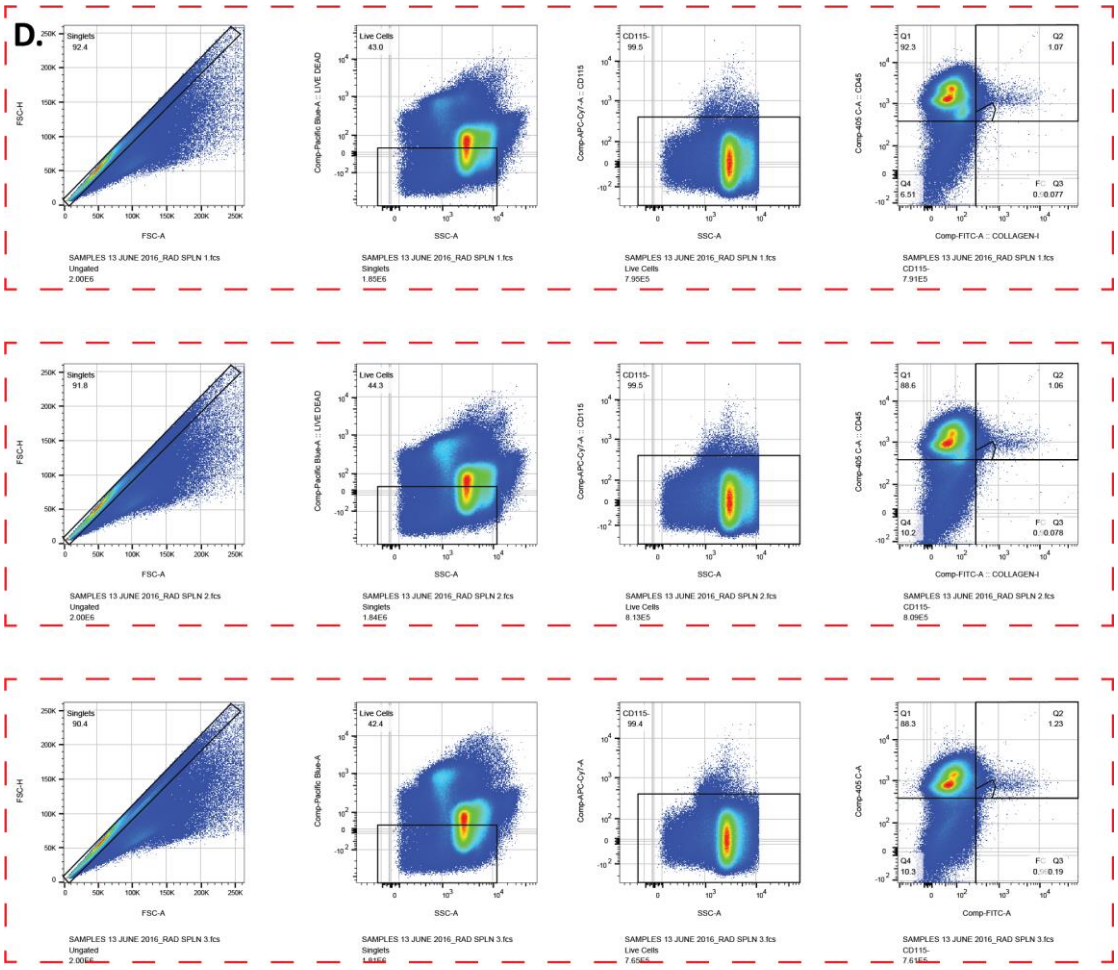
D.
Singlets
92.4
FSC-H
FSC-A
SAMPLES 13 JUNE 2016_RAD SPLN 1.fcs
Ungated
2.00E6
Live Cells
43.0
Comp-Pacific Blue-A :: LIVE DEAD
SSC-A
SAMPLES 13 JUNE 2016_RAD SPLN 1.fcs
Singlets
1.85E6
CD115-
99.5
Comp-APC-Cy7-A :: CD115
SSC-A
SAMPLES 13 JUNE 2016_RAD SPLN 1.fcs
Live Cells
7.99E5
Q1
92.3
Q2
1.07
Q4
6.51
Comp-405 C-A :: CD45
Comp-FITC-A :: COLLAGEN-I
SAMPLES 13 JUNE 2016_RAD SPLN 1.fcs
CD115-
7.91E5
Singlets
91.8
FSC-H
FSC-A
SAMPLES 13 JUNE 2016_RAD SPLN 2.fcs
Ungated
2.00E6
Live Cells
44.3
Comp-Pacific Blue-A :: LIVE DEAD
SSC-A
SAMPLES 13 JUNE 2016_RAD SPLN 2.fcs
Singlets
1.84E6
CD115-
99.5
Comp-APC-Cy7-A :: CD115
SSC-A
SAMPLES 13 JUNE 2016_RAD SPLN 2.fcs
Live Cells
8.13E5
Q1
88.6
Q2
1.06
Q4
10.2
Comp-405 C-A :: CD45
Comp-FITC-A :: COLLAGEN-I
SAMPLES 13 JUNE 2016_RAD SPLN 2.fcs
CD115-
8.09E5
Singlets
90.4
FSC-H
FSC-A
SAMPLES 13 JUNE 2016_RAD SPLN 3.fcs
Ungated
2.00E6
Live Cells
42.4
Comp-Pacific Blue-A
SSC-A
SAMPLES 13 JUNE 2016_RAD SPLN 3.fcs
Singlets
1.81E6
CD115-
99.4
Comp-APC-Cy7-A
SSC-A
SAMPLES 13 JUNE 2016_RAD SPLN 3.fcs
Live Cells
7.65E5
Q1
88.3
Q2
1.23
Q4
10.3
Comp-405 C-A
Comp-FITC-A
SAMPLES 13 JUNE 2016_RAD SPLN 3.fcs
CD115-
7.61E5

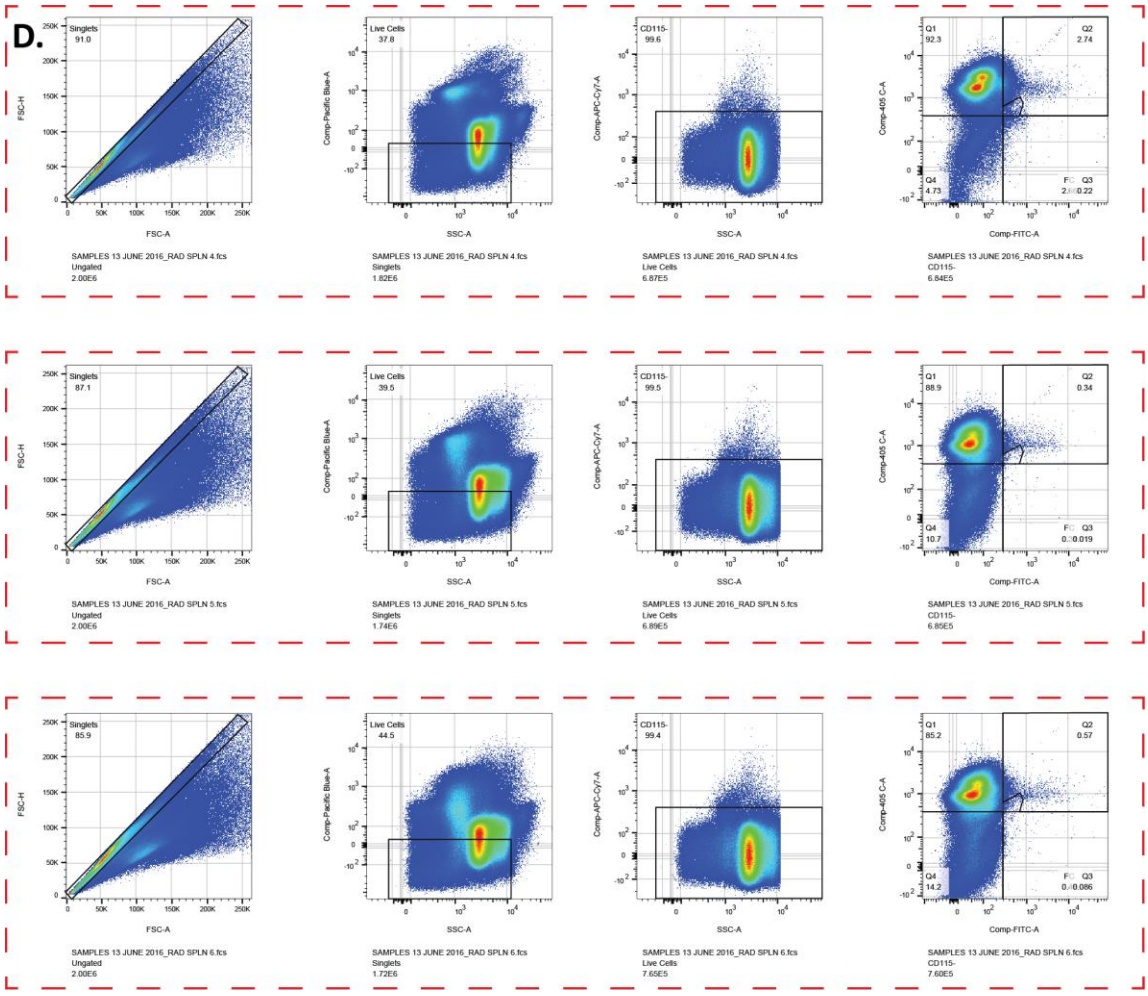
D.
Singlets
91.0
FSC-H
FSC-A
SAMPLES 13 JUNE 2016_RAD SPLN 4.fcs
Ungated
2.00E6
Live Cells
37.8
Comp-Pacific Blue-A
SSC-A
SAMPLES 13 JUNE 2016_RAD SPLN 4.fcs
Singlets
1.82E6
CD115-
99.6
Comp-APC-Cy7-A
SSC-A
SAMPLES 13 JUNE 2016_RAD SPLN 4.fcs
Live Cells
6.87E5
Q1
92.3
Q2
2.74
Q4
4.73
Comp-405 C-A
Comp-FITC-A
SAMPLES 13 JUNE 2016_RAD SPLN 4.fcs
CD115-
6.84E5
Singlets
87.1
FSC-H
FSC-A
SAMPLES 13 JUNE 2016_RAD SPLN 5.fcs
Ungated
2.00E6
Live Cells
39.5
Comp-Pacific Blue-A
SSC-A
SAMPLES 13 JUNE 2016_RAD SPLN 5.fcs
Singlets
1.74E6
CD115-
99.5
Comp-APC-Cy7-A
SSC-A
SAMPLES 13 JUNE 2016_RAD SPLN 5.fcs
Live Cells
6.89E5
Q1
88.9
Q2
0.34
Q4
10.7
Comp-405 C-A
Comp-FITC-A
SAMPLES 13 JUNE 2016_RAD SPLN 5.fcs
CD115-
6.85E5
Singlets
85.9
FSC-H
FSC-A
SAMPLES 13 JUNE 2016_RAD SPLN 6.fcs
Ungated
2.00E6
Live Cells
44.5
Comp-Pacific Blue-A
SSC-A
SAMPLES 13 JUNE 2016_RAD SPLN 6.fcs
Singlets
1.72E6
CD115-
99.4
Comp-APC-Cy7-A
SSC-A
SAMPLES 13 JUNE 2016_RAD SPLN 6.fcs
Live Cells
7.65E5
Q1
85.2
Q2
0.57
Q4
14.2
Comp-405 C-A
Comp-FITC-A
SAMPLES 13 JUNE 2016_RAD SPLN 6.fcs
CD115-
7.60E5

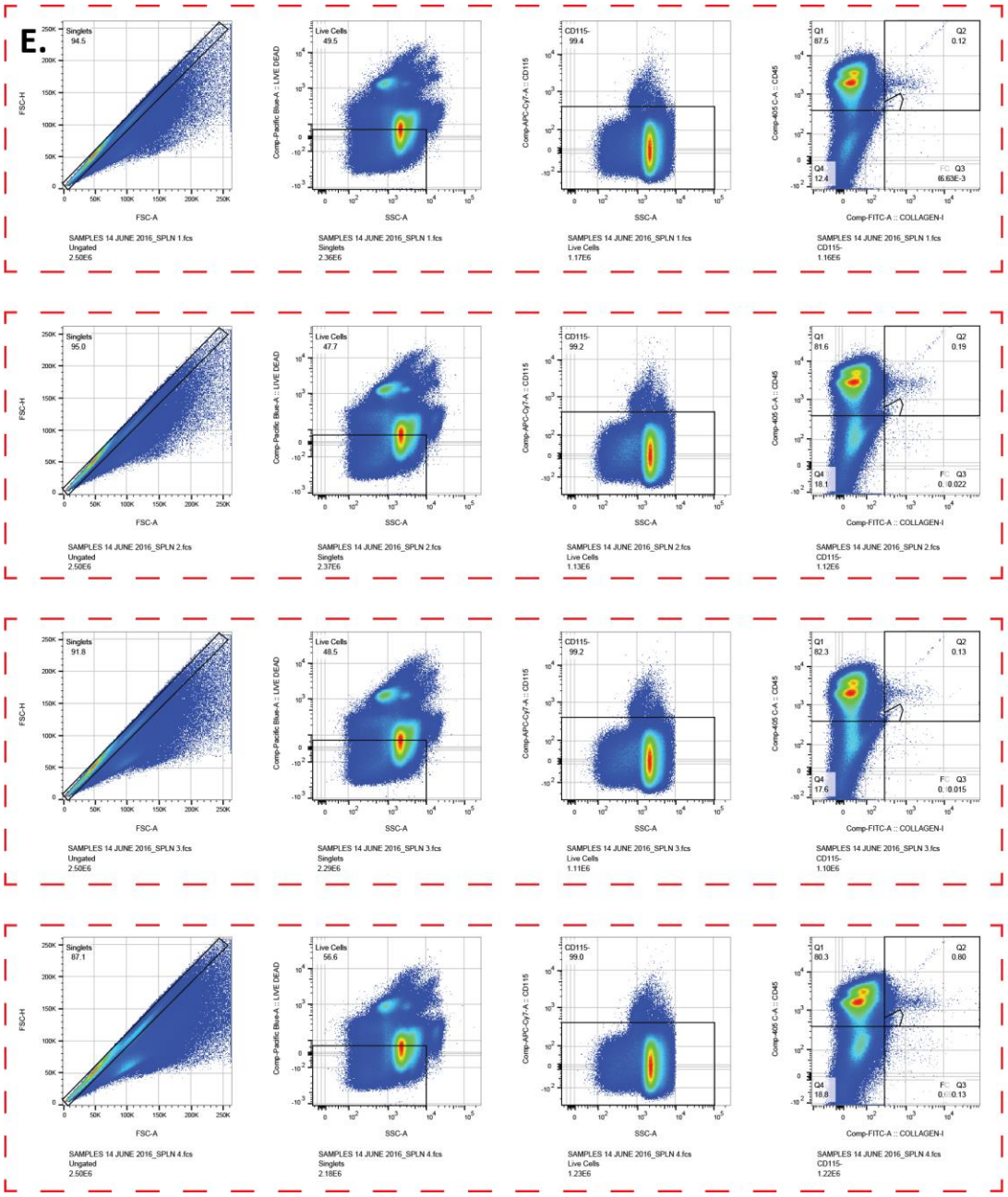

Supplementary Figure 10. Isolated spleen cells flow cytometry data.

Full gating strategy and data are shown for each experimental animal. Red dashed box corresponds to samples isolated from an individual animal. **A.** Spleen cells analyzed 14 days post irradiation. **B.** Spleen cells analyzed 14 days post irradiation. **C.** Spleen cells analyzed 30 days post irradiation. **D.** Spleen cells analyzed 60 days post irradiation. **E.** Sham animal analyzed spleen cells.

REFERENCES

1. AbdAlla S, Lother H, Abdel-tawab AM, Quitterer U. 2001. The Angiotensin II AT2 Receptor Is an AT1Receptor Antagonist. *Journal of Biological Chemistry* 276:39721-6
2. Abe R, Donnelly SC, Peng T, Bucala R, Metz CN. 2001. Peripheral blood fibrocytes: differentiation pathway and migration to wound sites. *J Immunol* 166:7556-62
3. Abid SH, Malhotra V, Perry MC. 2001. Radiation-induced and chemotherapy-induced pulmonary injury. *Curr Opin Oncol* 13:242-8
4. Abou Zahr A, Kavi AM, Mukherjee S, Zeidan AM. 2016. Therapy-related myelodysplastic syndromes, or are they? *Blood Rev*
5. Agrawala PK, Eschenbrenner A, du Penhoat M-AH, Boissiere A, Politis M-F, et al. 2008. Induction and repairability of DNA damage caused by ultrasoft X-rays: Role of core events. *International Journal of Radiation Biology* 84:1093-103
6. Akashi M, Hirama T, Tanosaki S, Kuroiwa N, Nakagawa K, et al. 2001. Initial symptoms of acute radiation syndrome in the JCO criticality accident in Tokai-mura. *J Radiat Res* 42 Suppl:S157-66
7. Akita S, Akino K, Hirano A, Ohtsuru A, Yamashita S. 2010. Noncultured Autologous Adipose-Derived Stem Cells Therapy for Chronic Radiation Injury. *Stem Cells International* 2010:8
8. Alan Mitteer R, Wang Y, Shah J, Gordon S, Fager M, et al. 2015. Proton beam radiation induces DNA damage and cell apoptosis in glioma stem cells through reactive oxygen species. *Sci Rep* 5:13961
9. Alessio N, Del Gaudio S, Capasso S, Di Bernardo G, Cappabianca S, et al. 2015. Low dose radiation induced senescence of human mesenchymal stromal cells and impaired the autophagy process. *Oncotarget* 6:8155-66
10. Alrbiaan A, Burdick M, Kadl A, Enfield KB, Mehrad B. 2016. Circulating Fibrocytes As Biomarkers Of Outcome In Acute Respiratory Distress Syndrome. In *A101. HOST DEFENSE, LUNG INJURY, AND FIBROSIS: INNATE MECHANISMS*:A2657-A: Am Thoracic Soc. Number of A2657-A pp.
11. Andarawewa KL, Paupert J, Pal A, Barcellos-Hoff MH. 2007. New rationales for using TGF beta inhibitors in radiotherapy. *International journal of radiation biology* 83:803-11
12. Anderson RE, Hoshino T, Yamamoto T. 1964. Myelofibrosis with myeloid metaplasia in survivors of the atomic bomb in Hiroshima. *Annals of internal medicine* 60:1-18
13. Anscher MS, Peters WP, Reisenbichler H, Petros WP, Jirtle RL. 1993. Transforming growth factor beta as a predictor of liver and lung fibrosis after autologous bone marrow transplantation for advanced breast cancer. *N Engl J Med* 328:1592-8

14. Arai F, Hirao A, Ohmura M, Sato H, Matsuoka S, et al. 2004. Tie2/angiopoietin-1 signaling regulates hematopoietic stem cell quiescence in the bone marrow niche. *Cell* 118:149-61
15. Augustine AD, Gondre-Lewis T, McBride W, Miller L, Pellmar TC, Rockwell S. 2005. Animal models for radiation injury, protection and therapy. *Radiat Res* 164:100-9
16. Balmelli C, Ruggli N, McCullough K, Summerfield A. 2005. Fibrocytes are potent stimulators of anti-virus cytotoxic T cells. *J Leukoc Biol* 77:923-33
17. Bancroft JD, Gamble M. 2008. *Theory and practice of histological techniques*. Elsevier Health Sciences
18. Banfi A, Bianchi G, Galotto M, Cancedda R, Quarto R. 2001. Bone marrow stromal damage after chemo/radiotherapy: occurrence, consequences and possibilities of treatment. *Leuk Lymphoma* 42:863-70
19. Barkauskas CE, Noble PW. 2014. Cellular Mechanisms of Tissue Fibrosis. 7. New insights into the cellular mechanisms of pulmonary fibrosis. *American Journal of Physiology - Cell Physiology* 306:C987-C96
20. Barrios R, Skurski P, Simons J. 2002. Mechanism for Damage to DNA by Low-Energy Electrons. *The Journal of Physical Chemistry B* 106:7991-4
21. Barth PJ, Koster H, Moosdorf R. 2005. CD34+ fibrocytes in normal mitral valves and myxomatous mitral valve degeneration. *Pathol Res Pract* 201:301-4
22. Barth PJ, Schenck zu Schweinsberg T, Ramaswamy A, Moll R. 2004. CD34+ fibrocytes, alpha-smooth muscle antigen-positive myofibroblasts, and CD117 expression in the stroma of invasive squamous cell carcinomas of the oral cavity, pharynx, and larynx. *Virchows Arch* 444:231-4
23. Barthelemy-Brichant N, Bosquée L, Cataldo D, Corhay J-L, Gustin M, et al. 2004. Increased IL-6 and TGF-β1 concentrations in bronchoalveolar lavage fluid associated with thoracic radiotherapy. *International Journal of Radiation Oncology*Biology*Physics* 58:758-67
24. Becker GJ, Hewitson TD. 2013. Animal models of chronic kidney disease: useful but not perfect. *Nephrol Dial Transplant* 28:2432-8
25. Bellini A, Mattoli S. 2007. The role of the fibrocyte, a bone marrow-derived mesenchymal progenitor, in reactive and reparative fibroses. *Lab Invest* 87:858-70
26. Benoff LJ, Schweitzer P. 1995. Radiation therapy-induced cardiac injury. *American Heart Journal* 129:1193-6
27. Berenbaum M. 2001. Rad Roaches. *American Entomologist* 47:132-3
28. Bianchetti L, Barczyk M, Cardoso J, Schmidt M, Bellini A, Mattoli S. 2012. Extracellular matrix remodelling properties of human fibrocytes. *J Cell Mol Med* 16:483-95
29. Bizzozero Jr OJ, Johnson KG, Ciocco A, Hoshino T, Itoga T, et al. 1966. Radiation-related leukemia in Hiroshima and Nagasaki, 1946–1964: distribution, incidence and appearance time. *New England Journal of Medicine* 274:1095-101
30. Blacher J, Levy BI, Mourad J-J, Safar ME, Bakris G. 2016. From epidemiological transition to modern cardiovascular epidemiology: hypertension in the 21st century. *The Lancet* 388:530-2

31. Boice JD. 2006. Thyroid disease 60 years after Hiroshima and 20 years after Chernobyl. *Jama* 295:1060-2
32. Breimer LH, Lindahl T. 1985. Thymine lesions produced by ionizing radiation in double-stranded DNA. *Biochemistry* 24:4018-22
33. Breitfeld D, Ohl L, Kremmer E, Ellwart J, Sallusto F, et al. 2000. Follicular B helper T cells express CXC chemokine receptor 5, localize to B cell follicles, and support immunoglobulin production. *Journal of Experimental Medicine* 192:1545-52
34. Brenner DJ, Curtis RE, Hall EJ, Ron E. 2000. Second malignancies in prostate carcinoma patients after radiotherapy compared with surgery. *Cancer* 88:398-406
35. Breslin W, Strohacker K, Carpenter K, Haviland D, McFarlin B. 2013. Mouse blood monocytes: standardizing their identification and analysis using CD115. *Journal of immunological methods* 390:1-8
36. Bucala R, Spiegel LA, Chesney J, Hogan M, Cerami A. 1994. Circulating fibrocytes define a new leukocyte subpopulation that mediates tissue repair. *Molecular medicine* 1:71-81
37. Burchfield JS, Xie M, Hill JA. 2013. Pathological ventricular remodeling. *Circulation* 128:388-400
38. Burnet NG, Nyman J, Turesson I, Wurm R, Yarnold JR, Peacock JH. 1994. The relationship between cellular radiation sensitivity and tissue response may provide the basis for individualising radiotherapy schedules. *Radiother Oncol* 33:228-38
39. Busch D. 1994. Genetic susceptibility to radiation and chemotherapy injury: diagnosis and management. *International Journal of Radiation Oncology* Biology* Physics* 30:997-1002
40. Calvi LM, Adams GB, Weibrecht KW, Weber JM, Olson DP, et al. 2003. Osteoblastic cells regulate the haematopoietic stem cell niche. *Nature* 425:841-6
41. Campisi J. 2000. Cancer, aging and cellular senescence. *In vivo (Athens, Greece)* 14:183-8
42. Candeias SM, Testard I. 2015. The many interactions between the innate immune system and the response to radiation. *Cancer Lett* 368:173-8
43. Canman CE, Lim DS, Cimprich KA, Taya Y, Tamai K, et al. 1998. Activation of the ATM kinase by ionizing radiation and phosphorylation of p53. *Science* 281:1677-9
44. Cao T, Rajasingh S, Rajasingh J. 2016. Circulating fibrocytes serve as a marker for clinical diagnosis. *Ann Transl Med* 4:S38
45. Chambers KA, Harrington NP, Ross WM, Filion LG. 1998. Relative alterations in blood mononuclear cell populations reflect radiation injury in mice. *Cytometry* 31:45-52
46. Chang HHY, Pannunzio NR, Adachi N, Lieber MR. 2017. Non-homologous DNA end joining and alternative pathways to double-strand break repair. *Nat Rev Mol Cell Biol* 18:495-506
47. Chang J, Feng W, Wang Y, Luo Y, Allen AR, et al. 2015. Whole-body proton irradiation causes long-term damage to hematopoietic stem cells in mice. *Radiat Res* 183:240-8

48. Chen G, Lin SC, Chen J, He L, Dong F, et al. 2011. CXCL16 recruits bone marrow-derived fibroblast precursors in renal fibrosis. *J Am Soc Nephrol* 22:1876-86
49. Chesney J, Bacher M, Bender A, Bucala R. 1997. The peripheral blood fibrocyte is a potent antigen-presenting cell capable of priming naive T cells in situ. *Proc Natl Acad Sci U S A* 94:6307-12
50. Chesney J, Metz C, Stavitsky AB, Bacher M, Bucala R. 1998. Regulated production of type I collagen and inflammatory cytokines by peripheral blood fibrocytes. *J Immunol* 160:419-25
51. Chevalier RL, Forbes MS, Thornhill BA. 2009. Ureteral obstruction as a model of renal interstitial fibrosis and obstructive nephropathy. *Kidney International* 75:1145-52
52. Childs BG, Baker DJ, Kirkland JL, Campisi J, van Deursen JM. 2014. Senescence and apoptosis: dueling or complementary cell fates? *EMBO reports* 15:1139-53
53. Chua HL, Plett PA, Sampson CH, Joshi M, Tabbey R, et al. 2012. Long-term hematopoietic stem cell damage in a murine model of the hematopoietic syndrome of the acute radiation syndrome. *Health physics* 103:356
54. Cipolleschi MG, Dello Sbarba P, Olivotto M. 1993. The role of hypoxia in the maintenance of hematopoietic stem cells. *Blood* 82:2031-7
55. Cleutjens J, Verluyten M, Smiths J, Daemen M. 1995. Collagen remodeling after myocardial infarction in the rat heart. *The American journal of pathology* 147:325
56. Cmielova J, Havelek R, Soukup T, Jiroutova A, Visek B, et al. 2012. Gamma radiation induces senescence in human adult mesenchymal stem cells from bone marrow and periodontal ligaments. *Int J Radiat Biol* 88:393-404
57. Coggle JE, Lambert BE, Moores SR. 1986. Radiation effects in the lung. *Environmental health perspectives* 70:261
58. Congdon C, Urso IS. 1957. Homologous bone marrow in the treatment of radiation injury in mice. *The American journal of pathology* 33:749
59. Crawford DC, Chobanian A, Brecher P. 1994. Angiotensin II induces fibronectin expression associated with cardiac fibrosis in the rat. *Circulation Research* 74:727-39
60. Cruet-Hennequart S, Drougard C, Shaw G, Legendre F, Demoor M, et al. 2015. Radiation-induced alterations of osteogenic and chondrogenic differentiation of human mesenchymal stem cells. *PLoS One* 10:e0119334
61. Curtis RE, Boice JD, Stovall M, Bernstein L, Holowaty E, et al. 1994. Relationship of leukemia risk to radiation dose following cancer of the uterine corpus. *Journal of the National Cancer Institute* 86:1315-24
62. Dahm-Daphi J, Sass C, Alberti W. 2000. Comparison of biological effects of DNA damage induced by ionizing radiation and hydrogen peroxide in CHO cells. *Int J Radiat Biol* 76:67-75
63. Delaney G, Jacob S, Featherstone C, Barton M. 2005. The role of radiotherapy in cancer treatment. *Cancer* 104:1129-37
64. Delanian S, Lefaix J-L. 2007. Current Management for Late Normal Tissue Injury: Radiation-Induced Fibrosis and Necrosis. *Seminars in Radiation Oncology* 17:99-107

65. Dewald O, Frangogiannis NG, Zoerlein M, Duerr GD, Klemm C, et al. 2003. Development of murine ischemic cardiomyopathy is associated with a transient inflammatory reaction and depends on reactive oxygen species. *Proceedings of the National Academy of Sciences* 100:2700-5
66. Ding N-H, Jian Li J, Sun L-Q. 2013. Molecular mechanisms and treatment of radiation-induced lung fibrosis. *Current drug targets* 14:1347-56
67. Dominici M, Rasini V, Bussolari R, Chen X, Hofmann TJ, et al. 2009. Restoration and reversible expansion of the osteoblastic hematopoietic stem cell niche after marrow radioablation. *Blood* 114:2333-43
68. Douglas RS, Afifiyan NF, Hwang CJ, Chong K, Haider U, et al. 2010. Increased Generation of Fibrocytes in Thyroid-Associated Ophthalmopathy. *The Journal of Clinical Endocrinology & Metabolism* 95:430-8
69. Dupin I, Allard B, Ozier A, Maurat E, Ousova O, et al. 2016. Blood fibrocytes are recruited during acute exacerbations of chronic obstructive pulmonary disease through a CXCR4-dependent pathway. *J Allergy Clin Immunol* 137:1036-42 e1-7
70. Ebrahimsade S, Westhoff CC, Barth PJ. 2007. CD34+ fibrocytes are preserved in most invasive lobular carcinomas of the breast. *Pathology-Research and Practice* 203:695-8
71. Eddy AA. 2014. Overview of the cellular and molecular basis of kidney fibrosis. *Kidney Int Suppl (2011)* 4:2-8
72. Eisbruch A, Gregoire V. Balancing risk and reward in target delineation for highly conformal radiotherapy in head and neck cancer. *Proc. Seminars in radiation oncology*, *2009*, 19:43-52: Elsevier
73. Emami B, Lyman J, Brown A, Cola L, Goitein M, et al. 1991. Tolerance of normal tissue to therapeutic irradiation. *International Journal of Radiation Oncology* Biology* Physics* 21:109-22
74. Falkenham A, Sopel M, Rosin N, Lee TD, Issekutz T, Legare JF. 2013. Early fibroblast progenitor cell migration to the AngII-exposed myocardium is not CXCL12 or CCL2 dependent as previously thought. *Am J Pathol* 183:459-69
75. Fang L, Beale A, Ellims AH, Moore XL, Ling LH, et al. 2013. Associations between fibrocytes and postcontrast myocardial T1 times in hypertrophic cardiomyopathy. *J Am Heart Assoc* 2:e000270
76. Fang L, Moore XL, Chan W, White DA, Chin-Dusting J, Dart AM. 2012. Decreased fibrocyte number is associated with atherosclerotic plaque instability in man. *Cardiovasc Res* 95:124-33
77. Finkelstein JN, Johnston CJ, Baggs R, Rubin P. 1994. Early alterations in extracellular matrix and transforming growth factor beta gene expression in mouse lung indicative of late radiation fibrosis. *Int J Radiat Oncol Biol Phys* 28:621-31
78. Flechsig P, Dadrich M, Bickelhaupt S, Jenne J, Hauser K, et al. 2012. LY2109761 attenuates radiation-induced pulmonary murine fibrosis via reversal of TGF-beta and BMP associated proinflammatory and proangiogenic signals. *Clinical Cancer Research*
79. Fleenor CJ, Marusyk A, DeGregori J. 2010. Ionizing radiation and hematopoietic malignancies: altering the adaptive landscape. *Cell Cycle* 9:3005-11

80. Fliedner TM, Friesecke I, Beyrer K. 2001. *Medical management of radiation accidents: manual on the acute radiation syndrome*. British Inst of Radiology
81. Fliedner TM, Graessle D, Paulsen C, Reimers K. 2002. Structure and function of bone marrow hemopoiesis: mechanisms of response to ionizing radiation exposure. *Cancer Biother Radiopharm* 17:405-26
82. Forbes SJ, Russo FP, Rey V, Burra P, Rugge M, et al. 2004. A significant proportion of myofibroblasts are of bone marrow origin in human liver fibrosis. *Gastroenterology* 126:955-63
83. Forristal CE, Winkler IG, Nowlan B, Barbier V, Walkinshaw G, Levesque JP. 2013. Pharmacologic stabilization of HIF-1alpha increases hematopoietic stem cell quiescence in vivo and accelerates blood recovery after severe irradiation. *Blood* 121:759-69
84. Forsberg EC, Bhattacharya D, Weissman IL. 2006. Hematopoietic stem cells. *Stem cell reviews* 2:23-30
85. Fu XY, Zhang DW, Li YD, Zhao PW, Tang YQ, et al. 2015. Curcumin treatment suppresses CCR7 expression and the differentiation and migration of human circulating fibrocytes. *Cell Physiol Biochem* 35:489-98
86. Fujimoto H, Kobayashi T, Azuma A. 2015. Idiopathic Pulmonary Fibrosis: Treatment and Prognosis. *Clinical Medicine Insights. Circulatory, Respiratory and Pulmonary Medicine* 9:179-85
87. Fujita J, Mori M, Kawada H, Ieda Y, Tsuma M, et al. 2007. Administration of Granulocyte Colony‐Stimulating Factor After Myocardial Infarction Enhances the Recruitment of Hematopoietic Stem Cell‐Derived Myofibroblasts and Contributes to Cardiac Repair. *Stem Cells* 25:2750-9
88. Gabbiani G. 2003. The myofibroblast in wound healing and fibrocontractive diseases. *J Pathol* 200:500-3
89. Gallagher RP, Lee TK. 2006. Adverse effects of ultraviolet radiation: A brief review. *Progress in Biophysics and Molecular Biology* 92:119-31
90. Gao X, He X, Luo B, Peng L, Lin J, Zuo Z. 2009. Angiotensin II increases collagen I expression via transforming growth factor-beta1 and extracellular signal-regulated kinase in cardiac fibroblasts. *Eur J Pharmacol* 606:115-20
91. Gibhardt CS, Roth B, Schroeder I, Fuck S, Becker P, et al. 2015. X-ray irradiation activates K+ channels via H2O2 signaling. *Scientific reports* 5
92. Gieseg SP, Simpson JA, Charlton TS, Duncan MW, Dean RT. 1993. Protein-bound 3,4-dihydroxyphenylalanine is a major reductant formed during hydroxyl radical damage to proteins. *Biochemistry* 32:4780-6
93. Gilpin SE, Lung K, de Couto GT, Cypel M, Sato M, et al. 2013. Bone marrow-derived progenitor cells in end-stage lung disease patients. *BMC pulmonary medicine* 13:48
94. Giotopoulos G, Symonds RP, Foweraker K, Griffin M, Peat I, et al. 2007. The late radiotherapy normal tissue injury phenotypes of telangiectasia, fibrosis and atrophy in breast cancer patients have distinct genotype-dependent causes. *Br J Cancer* 96:1001-7
95. Gluckman E. 1990. Influence of conditioning on the outcome of allogeneic bone marrow transplantation. *Int J Radiat Oncol Biol Phys* 19:1325-7

96. Greenbaum A, Hsu Y-MS, Day RB, Schuettpelz LG, Christopher MJ, et al. 2013. Cxcl12 production by early mesenchymal progenitors is required for hematopoietic stem cell maintenance. *Nature* 495:227
97. Guo CY, Luo L, Urata Y, Goto S, Huang WJ, et al. 2015. Sensitivity and dose dependency of radiation-induced injury in hematopoietic stem/progenitor cells in mice. *Sci Rep* 5:8055
98. Gyenes G. 1998. Radiation-induced ischemic heart disease in breast cancer--a review. *Acta Oncol* 37:241-6
99. Hall J, Angèle S. 1999. Radiation, DNA damage and cancer. *Molecular Medicine Today* 5:157-64
100. Hamill WH. 1969. Model for the radiolysis of water. *The Journal of Physical Chemistry* 73:1341-7
101. Haston CK, Zhou X, Gumbiner-Russo L, Irani R, Dejournett R, et al. 2002. Universal and radiation-specific loci influence murine susceptibility to radiation-induced pulmonary fibrosis. *Cancer research* 62:3782-8
102. Hatzi VI, Laskaratou DA, Mavragani IV, Nikitaki Z, Mangelis A, et al. 2015. Non-targeted radiation effects in vivo: a critical glance of the future in radiobiology. *Cancer Lett* 356:34-42
103. Haudek SB, Cheng J, Du J, Wang Y, Hermosillo-Rodriguez J, et al. 2010. Monocytic fibroblast precursors mediate fibrosis in angiotensin-II-induced cardiac hypertrophy. *Journal of molecular and cellular cardiology* 49:499-507
104. Haudek SB, Xia Y, Huebener P, Lee JM, Carlson S, et al. 2006. Bone marrow-derived fibroblast precursors mediate ischemic cardiomyopathy in mice. *Proc Natl Acad Sci U S A* 103:18284-9
105. Hayakawa J, Tsuchiya T. 1968. THE EFFECTS OF SPLEEN SHIELDED IRRADIATION ON $ sup 59$ Fe INCORPORATION INTO RED BLOOD CELLS IN THREE DIFFERENT STRAINS OF MICE, National Inst. of Radiological Sciences, Chiba, Japan
106. Health UDo, Services H. 2005. NIH strategic plan and research agenda for medical countermeasures against radiological and nuclear threats. *NIH Publication*
107. Heazlewood SY, Neaves RJ, Williams B, Haylock DN, Adams TE, Nilsson SK. 2013. Megakaryocytes co-localise with hemopoietic stem cells and release cytokines that up-regulate stem cell proliferation. *Stem Cell Res* 11:782-92
108. Hei TK, Zhou H, Ivanov VN, Hong M, Lieberman HB, et al. 2008. Mechanism of radiation-induced bystander effects: a unifying model. *J Pharm Pharmacol* 60:943-50
109. Herodin F, Drouet M. 2005. Cytokine-based treatment of accidentally irradiated victims and new approaches. *Exp Hematol* 33:1071-80
110. Herzog EL, Bucala R. 2010. Fibrocytes in health and disease. *Experimental hematology* 38:548-56
111. Heslet L, Bay C, Nepper-Christensen S. 2012. Acute radiation syndrome (ARS) - treatment of the reduced host defense. *Int J Gen Med* 5:105-15
112. Hong KM, Belperio JA, Keane MP, Burdick MD, Strieter RM. 2007. Differentiation of human circulating fibrocytes as mediated by transforming

growth factor-beta and peroxisome proliferator-activated receptor gamma. *J Biol Chem* 282:22910-20
113. Horowitz JC, Lee DY, Waghray M, Keshamouni VG, Thomas PE, et al. 2004. Activation of the pro-survival phosphatidylinositol 3-kinase/AKT pathway by transforming growth factor-beta1 in mesenchymal cells is mediated by p38 MAPK-dependent induction of an autocrine growth factor. *J Biol Chem* 279:1359-67
114. Hou J, Han ZP, Jing YY, Yang X, Zhang SS, et al. 2013. Autophagy prevents irradiation injury and maintains stemness through decreasing ROS generation in mesenchymal stem cells. *Cell Death Dis* 4:e844
115. Hubenak JR, Zhang Q, Branch CD, Kronowitz SJ. 2014. Mechanisms of injury to normal tissue after radiotherapy: a review. *Plast Reconstr Surg* 133:49e-56e
116. Iqbal S, Sidgwick G, Bayat A. 2012. Identification of fibrocytes from mesenchymal stem cells in keloid tissue: a potential source of abnormal fibroblasts in keloid scarring. *Archives of dermatological research* 304:665-71
117. Ironmonger L, Ohuma E, Ormiston-Smith N, Gildea C, Thomson CS, Peake MD. 2015. An evaluation of the impact of large-scale interventions to raise public awareness of a lung cancer symptom. *Br J Cancer* 112:207-16
118. Isgro M, Bianchetti L, Marini MA, Bellini A, Schmidt M, Mattoli S. 2013. The C-C motif chemokine ligands CCL5, CCL11, and CCL24 induce the migration of circulating fibrocytes from patients with severe asthma. *Mucosal Immunol* 6:718-27
119. Ishii T, Futami S, Nishida M, Suzuki T, Sakamoto T, et al. 2001. Brief Note and Evaluation of Acute-radiation Syndrome and Treatment of a Tokai-mura Criticality Accident Patient. *Journal of Radiation Research* 42:S167-S82
120. Ito K, Hirao A, Arai F, Takubo K, Matsuoka S, et al. 2006. Reactive oxygen species act through p38 MAPK to limit the lifespan of hematopoietic stem cells. *Nat Med* 12:446-51
121. Jackson IL, Vujaskovic Z, Down JD. 2010. Revisiting strain-related differences in radiation sensitivity of the mouse lung: recognizing and avoiding the confounding effects of pleural effusions. *Radiat Res* 173:10-20
122. Jang YY, Sharkis SJ. 2007. A low level of reactive oxygen species selects for primitive hematopoietic stem cells that may reside in the low-oxygenic niche. *Blood* 110:3056-63
123. Jelaska A, Korn JH. 2000. Role of apoptosis and transforming growth factor beta1 in fibroblast selection and activation in systemic sclerosis. *Arthritis Rheum* 43:2230-9
124. Jha V, Garcia-Garcia G, Iseki K, Li Z, Naicker S, et al. 2013. Chronic kidney disease: global dimension and perspectives. *Lancet* 382:260-72
125. Jing D, Fonseca AV, Alakel N, Fierro FA, Muller K, et al. 2010. Hematopoietic stem cells in co-culture with mesenchymal stromal cells--modeling the niche compartments in vitro. *Haematologica* 95:542-50
126. Johansson S, Svensson H, Denekamp J. 2002. Dose response and latency for radiation-induced fibrosis, edema, and neuropathy in breast cancer patients. *Int J Radiat Oncol Biol Phys* 52:1207-19

127. Kastan MB, Onyekwere O, Sidransky D, Vogelstein B, Craig RW. 1991. Participation of p53 protein in the cellular response to DNA damage. *Cancer research* 51:6304-11
128. Kawano H, Do YS, Kawano Y, Starnes V, Barr M, et al. 2000. Angiotensin II has multiple profibrotic effects in human cardiac fibroblasts. *Circulation* 101:1130-7
129. Keeley EC, Mehrad B, Janardhanan R, Salerno M, Hunter JR, et al. 2012. Elevated circulating fibrocyte levels in patients with hypertensive heart disease. *J Hypertens* 30:1856-61
130. Kerns SL, L West CM, Andreassen CN, Barnett GC, Bentzen SM, et al. 2014. Radiogenomics: the search for genetic predictors of radiotherapy response. *Future oncology* 10:2391-406
131. Kerns SL, Ruysscher Dd, Andreassen CN, Azria D, Barnett GC, et al. 2014. STROGAR – STrengthening the Reporting Of Genetic Association studies in Radiogenomics. *Radiotherapy and Oncology* 110:182-8
132. Kiel MJ, Morrison SJ. 2008. Uncertainty in the niches that maintain haematopoietic stem cells. *Nat Rev Immunol* 8:290-301
133. Kisseleva T, Uchinami H, Feirt N, Quintana-Bustamante O, Segovia JC, et al. 2006. Bone marrow-derived fibrocytes participate in pathogenesis of liver fibrosis. *Journal of Hepatology* 45:429-38
134. Kisseleva T, von Köckritz-Blickwede M, Reichart D, McGillvray SM, Wingender G, et al. 2011. Fibrocyte-like cells recruited to the spleen support innate and adaptive immune responses to acute injury or infection. *Journal of molecular medicine* 89:997-1013
135. Kleaveland KR, Moore BB, Kim KK. 2014. Paracrine functions of fibrocytes to promote lung fibrosis. *Expert Rev Respir Med* 8:163-72
136. Klocke R, Tian W, Kuhlmann MT, Nikol S. 2007. Surgical animal models of heart failure related to coronary heart disease. *Cardiovasc Res* 74:29-38
137. KNOSPE WH, BLOM J, CROSBY WH, Davis M. 1966. Regeneration of locally irradiated bone marrow. *Blood* 28:398-415
138. Kobayashi H, Naito M, Masuya M, Maruyama M, Urata K, et al. 2016. Circulating fibrocytes correlate with the asthma control test score. *Allergol Immunopathol (Madr)* 44:191-6
139. Koturbash I, Loree J, Kutanzi K, Koganow C, Pogribny I, Kovalchuk O. 2008. In vivo bystander effect: cranial X-irradiation leads to elevated DNA damage, altered cellular proliferation and apoptosis, and increased p53 levels in shielded spleen. *International Journal of Radiation Oncology* Biology* Physics* 70:554-62
140. Kramann R, DiRocco DP, Maarouf OH, Humphreys BD. 2013. Matrix-producing cells in chronic kidney disease: origin, regulation, and activation. *Current pathobiology reports* 1:301-11
141. Kunisaki Y, Bruns I, Scheiermann C, Ahmed J, Pinho S, et al. 2013. Arteriolar niches maintain haematopoietic stem cell quiescence. *Nature* 502:637-43
142. Kurnick N, Nokay N. 1964. ABSCOPAL EFFECTS AND BONE‐MARROW REPOPULATION IN MAN AND MOUSE. *Annals of the New York Academy of Sciences* 114:528-37

143. Larson RA, Le Beau MM. 2005. Therapy-related myeloid leukaemia: a model for leukemogenesis in humans. *Chem Biol Interact* 153-154:187-95
144. Le Caër S. 2011. Water radiolysis: influence of oxide surfaces on H2 production under ionizing radiation. *Water* 3:235-53
145. Le MH. 2007. Polonium 210, exposed. *Journal of Medical Toxicology* 3:82-4
146. Leone G, Pagano L, Ben-Yehuda D, Voso MT. 2007. Therapy-related leukemia and myelodysplasia: susceptibility and incidence. *Haematologica* 92:1389-98
147. Levine RL, Gilliland DG. 2008. Myeloproliferative disorders. *Blood* 112:2190-8
148. Li C, Wilson PB, Levine E, Barber J, Stewart AL, Kumar S. 1999. TGF‐β1 levels in pre‐treatment plasma identify breast cancer patients at risk of developing post‐radiotherapy fibrosis. *International journal of cancer* 84:155-9
149. Li L, Bhatia R. 2011. Stem cell quiescence. *Clin Cancer Res* 17:4936-41
150. Liang H, Ma Z, Peng H, He L, Hu Z, Wang Y. 2016. CXCL16 deficiency attenuates renal injury and fibrosis in salt-sensitive hypertension. *Scientific reports* 6:28715
151. Lieber MR, Ma Y, Pannicke U, Schwarz K. 2003. Mechanism and regulation of human non-homologous DNA end-joining. *Nat Rev Mol Cell Biol* 4:712-20
152. Lin RJ, Su ZZ, Liang SM, Chen YY, Shu XR, et al. 2016. Role of Circulating Fibrocytes in Cardiac Fibrosis. *Chin Med J (Engl)* 129:326-31
153. Little WC, Applegate RJ. 1993. Congestive heart failure: systolic and diastolic function. *Journal of cardiothoracic and vascular anesthesia* 7:2-5
154. Lomax ME, Folkes LK, O'Neill P. 2013. Biological consequences of radiation-induced DNA damage: relevance to radiotherapy. *Clin Oncol (R Coll Radiol)* 25:578-85
155. Ludin A, Itkin T, Gur-Cohen S, Mildner A, Shezen E, et al. 2012. Monocytes-macrophages that express α-smooth muscle actin preserve primitive hematopoietic cells in the bone marrow. *Nature immunology* 13:1072-82
156. Ma J, Ward EM, Siegel RL, Jemal A. 2015. Temporal trends in mortality in the united states, 1969-2013. *JAMA* 314:1731-9
157. Ma Z, Jin X, He L, Wang Y. 2016. CXCL16 regulates renal injury and fibrosis in experimental renal artery stenosis. *American Journal of Physiology-Heart and Circulatory Physiology* 311:H815-H21
158. Macri M, di Luzio S, Di Luzio S. 2002. Biological effects of electromagnetic fields. *International journal of immunopathology and pharmacology* 15:95-105
159. Makino H, Aono Y, Azuma M, Kishi M, Yokota Y, et al. 2013. Antifibrotic effects of CXCR4 antagonist in bleomycin-induced pulmonary fibrosis in mice. *J Med Invest* 60:127-37
160. Mannino DM, Buist AS. 2007. Global burden of COPD: risk factors, prevalence, and future trends. *The Lancet* 370:765-73
161. Marks LB, Bentzen SM, Deasy JO, Kong FM, Bradley JD, et al. 2010. Radiation dose-volume effects in the lung. *Int J Radiat Oncol Biol Phys* 76:S70-6
162. Martin KR, Barrett JC. 2002. Reactive oxygen species as double-edged swords in cellular processes: low-dose cell signaling versus high-dose toxicity. *Human & Experimental Toxicology* 21:71-5

163. Martin M, Lefaix J-L, Delanian S. 2000. TGF-β1 and radiation fibrosis: a master switch and a specific therapeutic target? *International Journal of Radiation Oncology* Biology* Physics* 47:277-90
164. Marusyk A, Casas-Selves M, Henry CJ, Zaberezhnyy V, Klawitter J, et al. 2009. Irradiation alters selection for oncogenic mutations in hematopoietic progenitors. *Cancer Res* 69:7262-9
165. Mauch P, Constine L, Greenberger J, Knospe W, Sullivan J, et al. 1995. Hematopoietic stem cell compartment: acute and late effects of radiation therapy and chemotherapy. *International Journal of Radiation Oncology* Biology* Physics* 31:1319-39
166. Mauch P, Rosenblatt M, Hellman S. 1988. Permanent loss in stem cell self renewal capacity following stress to the marrow. *Blood* 72:1193-6
167. McFee RB, McFee RB, Leikin JB. 2009. Death by Polonium-210: lessons learned from the murder of former Soviet spy Alexander Litvinenko. *Seminars in diagnostic pathology* 26:61-7
168. Mehrad B, Burdick MD, Strieter RM. 2009. Fibrocyte CXCR4 regulation as a therapeutic target in pulmonary fibrosis. *Int J Biochem Cell Biol* 41:1708-18
169. Mehrad B, Burdick MD, Zisman DA, Keane MP, Belperio JA, Strieter RM. 2007. Circulating peripheral blood fibrocytes in human fibrotic interstitial lung disease. *Biochemical and biophysical research communications* 353:104-8
170. Mehta PK, Griendling KK. 2007. Angiotensin II cell signaling: physiological and pathological effects in the cardiovascular system. *Am J Physiol Cell Physiol* 292:C82-97
171. Mendez-Ferrer S, Michurina TV, Ferraro F, Mazloom AR, Macarthur BD, et al. 2010. Mesenchymal and haematopoietic stem cells form a unique bone marrow niche. *Nature* 466:829-34
172. Meng A, Wang Y, Van Zant G, Zhou D. 2003. Ionizing radiation and busulfan induce premature senescence in murine bone marrow hematopoietic cells. *Cancer Res* 63:5414-9
173. Mettler FA, Jr., Gus'kova AK, Gusev I. 2007. Health effects in those with acute radiation sickness from the Chernobyl accident. *Health Phys* 93:462-9
174. Metz CN. 2003. Fibrocytes: a unique cell population implicated in wound healing. *Cell Mol Life Sci* 60:1342-50
175. Mignani S, Bryszewska M, Klajnert-Maculewicz B, Zablocka M, Majoral JP. 2015. Advances in combination therapies based on nanoparticles for efficacious cancer treatment: an analytical report. *Biomacromolecules* 16:1-27
176. Mills KT, Xu Y, Zhang W, Bundy JD, Chen CS, et al. 2015. A systematic analysis of worldwide population-based data on the global burden of chronic kidney disease in 2010. *Kidney Int* 88:950-7
177. Miousse IR, Shao L, Chang J, Feng W, Wang Y, et al. 2014. Exposure to low-dose (56)Fe-ion radiation induces long-term epigenetic alterations in mouse bone marrow hematopoietic progenitor and stem cells. *Radiat Res* 182:92-101
178. Mittal M, Siddiqui MR, Tran K, Reddy SP, Malik AB. 2014. Reactive oxygen species in inflammation and tissue injury. *Antioxid Redox Signal* 20:1126-67

179. Moeller A, Gilpin SE, Ask K, Cox G, Cook D, et al. 2009. Circulating fibrocytes are an indicator of poor prognosis in idiopathic pulmonary fibrosis. *Am J Respir Crit Care Med* 179:588-94
180. Möllmann H, Nef HM, Kostin S, von Kalle C, Pilz I, et al. 2006. Bone marrow-derived cells contribute to infarct remodelling. *Cardiovascular research* 71:661-71
181. Moonim MT, Porwit A. 2011. CHAPTER 3 - Normal bone marrow histology. In *Blood and Bone Marrow Pathology (Second Edition)*:45-62. Edinburgh: Churchill Livingstone. Number of 45-62 pp.
182. Moore BB. 2009. Fibrocytes as potential biomarkers in idiopathic pulmonary fibrosis. Am Thoracic Soc
183. Moore BB, Hogaboam CM. 2008. Murine models of pulmonary fibrosis. *American Journal of Physiology-Lung Cellular and Molecular Physiology* 294:L152-L60
184. Moore BB, Murray L, Das A, Wilke CA, Herrygers AB, Toews GB. 2006. The role of CCL12 in the recruitment of fibrocytes and lung fibrosis. *Am J Respir Cell Mol Biol* 35:175-81
185. Mori L, Bellini A, Stacey MA, Schmidt M, Mattoli S. 2005. Fibrocytes contribute to the myofibroblast population in wounded skin and originate from the bone marrow. *Experimental cell research* 304:81-90
186. Mozaffarian D, Benjamin EJ, Go AS, Arnett DK, Blaha MJ, et al. 2016. Executive Summary: Heart Disease and Stroke Statistics--2016 Update: A Report From the American Heart Association. *Circulation* 133:447-54
187. Mueller SN, Hosiawa-Meagher KA, Konieczny BT, Sullivan BM, Bachmann MF, et al. 2007. Regulation of homeostatic chemokine expression and cell trafficking during immune responses. *Science* 317:670-4
188. Naka K, Muraguchi T, Hoshii T, Hirao A. 2008. Regulation of reactive oxygen species and genomic stability in hematopoietic stem cells. *Antioxid Redox Signal* 10:1883-94
189. Nakajima M, Hutchinson HG, Fujinaga M, Hayashida W, Morishita R, et al. 1995. The angiotensin II type 2 (AT2) receptor antagonizes the growth effects of the AT1 receptor: gain-of-function study using gene transfer. *Proceedings of the National Academy of Sciences* 92:10663-7
190. Nakamura-Ishizu A, Takubo K, Fujioka M, Suda T. 2014. Megakaryocytes are essential for HSC quiescence through the production of thrombopoietin. *Biochemical and biophysical research communications* 454:353-7
191. Nelson PJ. 2013. The contentious ontogeny of fibrosis in the kidney. *Kidney Int* 84:14-5
192. Nemzek JA, Fry C, Moore BB. 2013. Adoptive transfer of fibrocytes enhances splenic T-cell numbers and survival in septic peritonitis. *Shock* 40:106-14
193. Neote K, DiGregorio D, Mak JY, Horuk R, Schall TJ. 1993. Molecular cloning, functional expression, and signaling characteristics of a CC chemokine receptor. *Cell* 72:415-25
194. Niedermeier M, Reich B, Rodriguez Gomez M, Denzel A, Schmidbauer K, et al. 2009. CD4+ T cells control the differentiation of Gr1+ monocytes into fibrocytes. *Proc Natl Acad Sci U S A* 106:17892-7

195. Nikam VS, Wecker G, Schermuly R, Rapp U, Szelepusa K, et al. 2011. Treprostinil Inhibits the Adhesion and Differentiation of Fibrocytes via the Cyclic Adenosine Monophosphate–Dependent and Ras-Proximate Protein–Dependent Inactivation of Extracellular Regulated Kinase. *American journal of respiratory cell and molecular biology* 45:692-703
196. Nombela-Arrieta C, Pivarnik G, Winkel B, Canty KJ, Harley B, et al. 2013. Quantitative imaging of haematopoietic stem and progenitor cell localization and hypoxic status in the bone marrow microenvironment. *Nat Cell Biol* 15:533-43
197. Ohkubo N, Matsubara H, Nozawa Y, Mori Y, Murasawa S, et al. 1997. Angiotensin type 2 receptors are reexpressed by cardiac fibroblasts from failing myopathic hamster hearts and inhibit cell growth and fibrillar collagen metabolism. *Circulation* 96:3954-62
198. Olive PL. 1998. The role of DNA single- and double-strand breaks in cell killing by ionizing radiation. *Radiat Res* 150:S42-51
199. Orford KW, Scadden DT. 2008. Deconstructing stem cell self-renewal: genetic insights into cell-cycle regulation. *Nat Rev Genet* 9:115-28
200. Otake M, Yoshimaru H, Schull WJ. 1988. Severe mental retardation among the prenatally exposed survivors of the Atomic bombing of Hiroshima and Nagasaki, Radiation Effects Research Foundation
201. Ottone C, Krusche B, Whitby A, Clements M, Quadrato G, et al. 2014. Direct cell-cell contact with the vascular niche maintains quiescent neural stem cells. *Nat Cell Biol* 16:1045-56
202. Parmar K, Mauch P, Vergilio JA, Sackstein R, Down JD. 2007. Distribution of hematopoietic stem cells in the bone marrow according to regional hypoxia. *Proc Natl Acad Sci U S A* 104:5431-6
203. Pazhanisamy SK, Li H, Wang Y, Batinic-Haberle I, Zhou D. 2011. NADPH oxidase inhibition attenuates total body irradiation-induced haematopoietic genomic instability. *Mutagenesis* 26:431-5
204. Petrov VV, Fagard RH, Lijnen PJ. 2002. Stimulation of collagen production by transforming growth factor-β1 during differentiation of cardiac fibroblasts to myofibroblasts. *Hypertension* 39:258-63
205. Pham TM, Sakata R, Grant EJ, Shimizu Y, Furukawa K, et al. 2013. Radiation exposure and the risk of mortality from noncancer respiratory diseases in the life span study, 1950-2005. *Radiat Res* 180:539-45
206. Phillips RJ, Burdick MD, Hong K, Lutz MA, Murray LA, et al. 2004. Circulating fibrocytes traffic to the lungs in response to CXCL12 and mediate fibrosis. *J Clin Invest* 114:438-46
207. Pilling D, Fan T, Huang D, Kaul B, Gomer RH. 2009. Identification of markers that distinguish monocyte-derived fibrocytes from monocytes, macrophages, and fibroblasts. *PLoS One* 4:e7475
208. Poulsom R, Forbes SJ, Hodivala-Dilke K, Ryan E, Wyles S, et al. 2001. Bone marrow contributes to renal parenchymal turnover and regeneration. *J Pathol* 195:229-35
209. Prockop DJ. 1997. Marrow stromal cells as stem cells for nonhematopoietic tissues. *Science* 276:71-4

210. Qin S, Rottman JB, Myers P, Kassam N, Weinblatt M, et al. 1998. The chemokine receptors CXCR3 and CCR5 mark subsets of T cells associated with certain inflammatory reactions. *Journal of Clinical Investigation* 101:746-54
211. Ramaswamy A, Moll R, Barth PJ. 2003. CD34+ fibrocytes in tubular carcinomas and radial scars of the breast. *Virchows Arch* 443:536-40
212. Ravanat J-L, Douki T, Cadet J. 2001. Direct and indirect effects of UV radiation on DNA and its components. *Journal of Photochemistry and Photobiology B: Biology* 63:88-102
213. Raventos A. 1954. An abscopal effect of X-ray upon mouse spleen weight. *Radiation research* 1:381-7
214. Ravitz MJ, Yan S, Dolce C, Kinniburgh AJ, Wenner CE. 1996. Differential regulation of p27 and cyclin D1 by TGF-beta and EGF in C3H 10T1/2 mouse fibroblasts. *J Cell Physiol* 168:510-20
215. Reich B, Schmidbauer K, Rodriguez Gomez M, Johannes Hermann F, Gobel N, et al. 2013. Fibrocytes develop outside the kidney but contribute to renal fibrosis in a mouse model. *Kidney Int* 84:78-89
216. Riddell M, Winkler-Lowen B, Chakrabarti S, Dunk C, Davidge S, Guilbert L. 2012. The characterization of fibrocyte-like cells: a novel fibroblastic cell of the placenta. *Placenta* 33:143-50
217. Riley PA. 1994. Free radicals in biology: oxidative stress and the effects of ionizing radiation. *Int J Radiat Biol* 65:27-33
218. Roberts AB, Sporn MB, Assoian RK, Smith JM, Roche NS, et al. 1986. Transforming growth factor type beta: rapid induction of fibrosis and angiogenesis in vivo and stimulation of collagen formation in vitro. *Proceedings of the National Academy of Sciences* 83:4167-71
219. Rogakou EP, Pilch DR, Orr AH, Ivanova VS, Bonner WM. 1998. DNA double-stranded breaks induce histone H2AX phosphorylation on serine 139. *J Biol Chem* 273:5858-68
220. Roos WP, Kaina B. 2006. DNA damage-induced cell death by apoptosis. *Trends in Molecular Medicine* 12:440-50
221. Roos WP, Kaina B. 2013. DNA damage-induced cell death: From specific DNA lesions to the DNA damage response and apoptosis. *Cancer Letters* 332:237-48
222. Roos WP, Thomas AD, Kaina B. 2016. DNA damage and the balance between survival and death in cancer biology. *Nat Rev Cancer* 16:20-33
223. Rosenbloom B, Schreck R, Koeffler H. 1992. Therapy-related myelodysplastic syndromes. *Hematology/oncology clinics of North America* 6:707-22
224. ROSS P, LOGAN W. 1969. Roentgen findings in extramedullary hematopoiesis. *American Journal of Roentgenology* 106:604-13
225. Rübe CE, Uthe D, Schmid KW, Richter KD, Wessel J, et al. 2000. Dose-dependent induction of transforming growth factor β (TGF-β) in the lung tissue of fibrosis-prone mice after thoracic irradiation. *International Journal of Radiation Oncology* Biology* Physics* 47:1033-42
226. Rubin P, Johnston CJ, Williams JP, McDonald S, Finkelstein JN. 1995. A perpetual cascade of cytokines postirradiation leads to pulmonary fibrosis. *Int J Radiat Oncol Biol Phys* 33:99-109

227. Sakai N, Furuichi K, Shinozaki Y, Yamauchi H, Toyama T, et al. 2010. Fibrocytes are involved in the pathogenesis of human chronic kidney disease. *Hum Pathol* 41:672-8
228. Sakai N, Wada T, Matsushima K, Bucala R, Iwai M, et al. 2008. The renin–angiotensin system contributes to renal fibrosis through regulation of fibrocytes. *Journal of hypertension* 26:780-90
229. Sakai N, Wada T, Yokoyama H, Lipp M, Ueha S, et al. 2006. Secondary lymphoid tissue chemokine (SLC/CCL21)/CCR7 signaling regulates fibrocytes in renal fibrosis. *Proc Natl Acad Sci U S A* 103:14098-103
230. Sanjabi S, Zenewicz LA, Kamanaka M, Flavell RA. 2009. Anti-inflammatory and pro-inflammatory roles of TGF-β, IL-10, and IL-22 in immunity and autoimmunity. *Current opinion in pharmacology* 9:447-53
231. Sanquist TF, Doctor P, Parasuraman R. 2008. Designing effective alarms for radiation detection in homeland security screening. *IEEE Transactions on Systems, Man, and Cybernetics, Part C (Applications and Reviews)* 38:856-60
232. Scarantino CW, Rubin P, Constine LS. 1984. The paradoxes in patterns and mechanism of bone marrow regeneration after irradiation: 1. Different volumes and doses. *Radiotherapy and Oncology* 2:215-25
233. Schmidt M, Sun G, Stacey MA, Mori L, Mattoli S. 2003. Identification of circulating fibrocytes as precursors of bronchial myofibroblasts in asthma. *The Journal of Immunology* 171:380-9
234. Schneider U, Kaser-Hotz B. 2005. A simple dose-response relationship for modeling secondary cancer incidence after radiotherapy** Parts of this work were presented at the 15th annual NASA space radiation health investigators' workshop; May 2004, Port Jefferson, USA. *Zeitschrift für Medizinische Physik* 15:31-7
235. Scholten D, Reichart D, Paik YH, Lindert J, Bhattacharya J, et al. 2011. Migration of fibrocytes in fibrogenic liver injury. *Am J Pathol* 179:189-98
236. Schonmeyr BH, Wong AK, Soares M, Fernandez J, Clavin N, Mehrara BJ. 2008. Ionizing radiation of mesenchymal stem cells results in diminution of the precursor pool and limits potential for multilineage differentiation. *Plast Reconstr Surg* 122:64-76
237. Schulz O, Hammerschmidt SI, Moschovakis GL, Förster R. 2016. Chemokines and chemokine receptors in lymphoid tissue dynamics. *Annual review of immunology* 34:203-42
238. Selman M, King TE, Pardo A. 2001. Idiopathic pulmonary fibrosis: prevailing and evolving hypotheses about its pathogenesis and implications for therapy. *Annals of internal medicine* 134:136-51
239. Serafini P, Borrello I, Bronte V. Myeloid suppressor cells in cancer: recruitment, phenotype, properties, and mechanisms of immune suppression. *Proc. Seminars in cancer biology*, *2006*, 16:53-65: Elsevier
240. Shankar G, Cohen DA. 2001. Idiopathic pneumonia syndrome after bone marrow transplantation: the role of pre-transplant radiation conditioning and local cytokine dysregulation in promoting lung inflammation and fibrosis. *Int J Exp Pathol* 82:101-13

241. Shao DD, Suresh R, Vakil V, Gomer RH, Pilling D. 2008. Pivotal Advance: Th-1 cytokines inhibit, and Th-2 cytokines promote fibrocyte differentiation. *J Leukoc Biol* 83:1323-33
242. Shao L, Feng W, Li H, Gardner D, Luo Y, et al. 2014. Total body irradiation causes long-term mouse BM injury via induction of HSC premature senescence in an Ink4a- and Arf-independent manner. *Blood* 123:3105-15
243. Shao L, Wang Y, Chang J, Luo Y, Meng A, Zhou D. 2013. Hematopoietic stem cell senescence and cancer therapy-induced long-term bone marrow injury. *Transl Cancer Res* 2:397-411
244. Shi Y, Ou L, Han S, Li M, Pena M, et al. 2014. Deficiency of Kruppel-like factor KLF4 in myeloid-derived suppressor cells inhibits tumor pulmonary metastasis in mice accompanied by decreased fibrocytes. *Oncogenesis* 3:e129
245. Shrivastav M, De Haro LP, Nickoloff JA. 2008. Regulation of DNA double-strand break repair pathway choice. *Cell Res* 18:134-47
246. Song JS, Kang CM, Kang HH, Yoon HK, Kim YK, et al. 2010. Inhibitory effect of CXC chemokine receptor 4 antagonist AMD3100 on bleomycin induced murine pulmonary fibrosis. *Exp Mol Med* 42:465-72
247. Sonis ST, Elting LS, Keefe D, Peterson DE, Schubert M, et al. 2004. Perspectives on cancer therapy-induced mucosal injury. *Cancer* 100:1995-2025
248. Sonnemann KJ, Bement WM. 2011. Wound repair: toward understanding and integration of single-cell and multicellular wound responses. *Annu Rev Cell Dev Biol* 27:237-63
249. Spinale FG. 2007. Myocardial matrix remodeling and the matrix metalloproteinases: influence on cardiac form and function. *Physiological reviews* 87:1285-342
250. Steinert M, Weiss M, Gottlober P, Belyi D, Gergel O, et al. 2003. Delayed effects of accidental cutaneous radiation exposure: fifteen years of follow-up after the Chernobyl accident. *J Am Acad Dermatol* 49:417-23
251. Strutz F, Zeisberg M. 2006. Renal fibroblasts and myofibroblasts in chronic kidney disease. *Journal of the American Society of Nephrology* 17:2992-8
252. Sugiyama T, Kohara H, Noda M, Nagasawa T. 2006. Maintenance of the hematopoietic stem cell pool by CXCL12-CXCR4 chemokine signaling in bone marrow stromal cell niches. *Immunity* 25:977-88
253. Sugrue T, Lowndes NF, Ceredig R. 2013. Mesenchymal stromal cells: radio-resistant members of the bone marrow. *Immunol Cell Biol* 91:5-11
254. Supramaniam R. 2008. New malignancies among cancer survivors: SEER cancer registries, 1973–2000. BMJ Publishing Group Ltd
255. Suzuki A, Kondoh Y. 2017. The clinical impact of major comorbidities on idiopathic pulmonary fibrosis. *Respiratory Investigation* 55:94-103
256. Suzuki K, Kodama S, Watanabe M. 1999. Recruitment of ATM protein to double strand DNA irradiated with ionizing radiation. *J Biol Chem* 274:25571-5
257. Swirski FK, Nahrendorf M, Etzrodt M, Wildgruber M, Cortez-Retamozo V, et al. 2009. Identification of splenic reservoir monocytes and their deployment to inflammatory sites. *Science* 325:612-6
258. Takata M, Sasaki MS, Sonoda E, Morrison C, Hashimoto M, et al. 1998. Homologous recombination and non-homologous end-joining pathways of DNA

double-strand break repair have overlapping roles in the maintenance of chromosomal integrity in vertebrate cells. *EMBO J* 17:5497-508
259. Tashiro J, Rubio GA, Limper AH, Williams K, Elliot SJ, et al. 2017. Exploring Animal Models That Resemble Idiopathic Pulmonary Fibrosis. *Front Med (Lausanne)* 4:118
260. Taunk NK, Haffty BG, Kostis JB, Goyal S. 2015. Radiation-induced heart disease: pathologic abnormalities and putative mechanisms. *Frontiers in oncology* 5:39
261. Téoule R. 1987. Radiation-induced DNA Damage and Its Repair. *International Journal of Radiation Biology and Related Studies in Physics, Chemistry and Medicine* 51:573-89
262. Terai S, Fushida S, Tsukada T, Kinoshita J, Oyama K, et al. 2015. Bone marrow derived "fibrocytes" contribute to tumor proliferation and fibrosis in gastric cancer. *Gastric Cancer* 18:306-13
263. Tesch GH. 2010. Review: Serum and urine biomarkers of kidney disease: A pathophysiological perspective. *Nephrology (Carlton)* 15:609-16
264. Testa NG, Hendry JH, Molineux G. 1985. Long-term bone marrow damage in experimental systems and in patients after radiation or chemotherapy. *Anticancer Res* 5:101-10
265. Thelen M, Stein JV. 2008. How chemokines invite leukocytes to dance. *Nat Immunol* 9:953-9
266. Thiele J, Kvasnicka HM, Schmitt-Graff A, Hulsemann R, Diehl V. 2004. Therapy-related changes of the bone marrow in chronic idiopathic myelofibrosis. *Histol Histopathol* 19:239-50
267. Thomas BJ, Kan OK, Loveland KL, Elias JA, Bardin PG. 2016. In the Shadow of Fibrosis: Innate Immune Suppression Mediated by Transforming Growth Factor-beta. *Am J Respir Cell Mol Biol* 55:759-66
268. Travlos GS. 2006. Normal structure, function, and histology of the bone marrow. *Toxicol Pathol* 34:548-65
269. Tsai Y-M, Hsu S-C, Zhang J, Zhou Y-F, Plunkett B, et al. 2013. Functional interaction of cockroach allergens and mannose receptor (CD206) in human circulating fibrocytes. *PloS one* 8:e64105
270. Tzeng Y-S, Li H, Kang Y-L, Chen W-C, Cheng W-C, Lai D-M. 2011. Loss of Cxcl12/Sdf-1 in adult mice decreases the quiescent state of hematopoietic stem/progenitor cells and alters the pattern of hematopoietic regeneration after myelosuppression. *Blood* 117:429-39
271. Vacchini A, Locati M, Borroni EM. 2016. Overview and potential unifying themes of the atypical chemokine receptor family. *J Leukoc Biol* 99:883-92
272. van Amerongen MJ, Bou-Gharios G, Popa E, van Ark J, Petersen AH, et al. 2008. Bone marrow-derived myofibroblasts contribute functionally to scar formation after myocardial infarction. *J Pathol* 214:377-86
273. Vignard J, Mirey G, Salles B. 2013. Ionizing-radiation induced DNA double-strand breaks: a direct and indirect lighting up. *Radiother Oncol* 108:362-9
274. Vionnie W, Scadden DT. 2016. Heterogeneity of the bone marrow niche. *Current opinion in hematology* 23:331-8

275. Vujaskovic Z, Groen HJ. 2000. TGF-beta, radiation-induced pulmonary injury and lung cancer. *Int J Radiat Biol* 76:511-6
276. Wanebo C, Johnson K, Sato K, Thorslund T. 1968. Breast cancer after exposure to the atomic bombings of Hiroshima and Nagasaki. *New England Journal of Medicine* 279:667-71
277. Wang C-H, Huang C-D, Lin H-C, Lee K-Y, Lin S-M, et al. 2008. Increased circulating fibrocytes in asthma with chronic airflow obstruction. *American journal of respiratory and critical care medicine* 178:583-91
278. Wang D, Jang DJ. 2009. Protein kinase CK2 regulates cytoskeletal reorganization during ionizing radiation-induced senescence of human mesenchymal stem cells. *Cancer Res* 69:8200-7
279. Wang J, Qiao X, Lu F, Zhou Z, Song Y, et al. 2010. TGF-beta1 in serum and induced sputum for predicting radiation pneumonitis in patients with non-small cell lung cancer after radiotherapy. *Chinese journal of cancer* 29:325-9
280. Wang Y, Liu L, Pazhanisamy SK, Li H, Meng A, Zhou D. 2010. Total body irradiation causes residual bone marrow injury by induction of persistent oxidative stress in murine hematopoietic stem cells. *Free Radic Biol Med* 48:348-56
281. Wang Y, Schulte BA, LaRue AC, Ogawa M, Zhou D. 2006. Total body irradiation selectively induces murine hematopoietic stem cell senescence. *Blood* 107:358-66
282. Wara WM, Phillips TL, Margolis LW, Smith V. 1973. Radiation pneumonitis: A new approach to the derivation of time‐dose factors. *Cancer* 32:547-52
283. Waselenko JK, MacVittie TJ, Blakely WF, Pesik N, Wiley AL, et al. 2004. Medical management of the acute radiation syndrome: recommendations of the Strategic National Stockpile Radiation Working Group. *Annals of internal medicine* 140:1037-51
284. West C, Rosenstein BS. Establishment of a Radiogenomics Consortium. *International Journal of Radiation Oncology • Biology • Physics* 76:1295-6
285. White MJ, Galvis-Carvajal E, Gomer RH. 2015. A brief exposure to tryptase or thrombin potentiates fibrocyte differentiation in the presence of serum or serum amyloid p. *J Immunol* 194:142-50
286. White MJ, Gomer RH. 2015. Trypsin, Tryptase, and Thrombin Polarize Macrophages towards a Pro-Fibrotic M2a Phenotype. *PLoS One* 10:e0138748
287. Williams JP, Brown SL, Georges GE, Hauer-Jensen M, Hill RP, et al. 2010. Animal models for medical countermeasures to radiation exposure. *Radiat Res* 173:557-78
288. Williams SM, Golden-Mason L, Ferguson BS, Schuetze KB, Cavasin MA, et al. 2014. Class I HDACs regulate angiotensin II-dependent cardiac fibrosis via fibroblasts and circulating fibrocytes. *Journal of molecular and cellular cardiology* 67:112-25
289. Wilson A, Laurenti E, Oser G, van der Wath RC, Blanco-Bose W, et al. 2008. Hematopoietic stem cells reversibly switch from dormancy to self-renewal during homeostasis and repair. *Cell* 135:1118-29
290. Wilson A, Trumpp A. 2006. Bone-marrow haematopoietic-stem-cell niches. *Nat Rev Immunol* 6:93-106

291. Wilson MS, Madala SK, Ramalingam TR, Gochuico BR, Rosas IO, et al. 2010. Bleomycin and IL-1beta-mediated pulmonary fibrosis is IL-17A dependent. *J Exp Med* 207:535-52
292. Winkler IG, Barbier V, Nowlan B, Jacobsen RN, Forristal CE, et al. 2012. Vascular niche E-selectin regulates hematopoietic stem cell dormancy, self renewal and chemoresistance. *Nat Med* 18:1651-7
293. Wong L, Rehm J. 2004. Images in clinical medicine. Radiation injury from a fluoroscopic procedure. *N Engl J Med* 350:e23
294. Wright A, Newby C, Hartley R, Mistry V, Gupta S, et al. 2017. Myeloid‐derived suppressor cell‐like fibrocytes are increased and associated with preserved lung function in chronic obstructive pulmonary disease. *Allergy* 72:645-55
295. Wu J, Montaniel KRC, Saleh MA, Xiao L, Chen W, et al. 2016. Origin of Matrix-Producing Cells That Contribute to Aortic Fibrosis in HypertensionNovelty and Significance. *Hypertension* 67:461-8
296. Wynn TA, Ramalingam TR. 2012. Mechanisms of fibrosis: therapeutic translation for fibrotic disease. *Nat Med* 18:1028-40
297. Xia Y, Entman ML, Wang Y. 2013. CCR2 regulates the uptake of bone marrow-derived fibroblasts in renal fibrosis. *PLoS One* 8:e77493
298. Xiong S, Guo R, Yang Z, Xu L, Du L, et al. 2015. Treg depletion attenuates irradiation-induced pulmonary fibrosis by reducing fibrocyte accumulation, inducing Th17 response, and shifting IFN-γ, IL-12/IL-4, IL-5 balance. *Immunobiology* 220:1284-91
299. Xu G, Wu H, Zhang J, Li D, Wang Y, et al. 2015. Metformin ameliorates ionizing irradiation-induced long-term hematopoietic stem cell injury in mice. *Free Radic Biol Med* 87:15-25
300. Xu J, Cong M, Park TJ, Scholten D, Brenner DA, Kisseleva T. 2015. Contribution of bone marrow-derived fibrocytes to liver fibrosis. *Hepatobiliary Surg Nutr* 4:34-47
301. Xu J, Lin SC, Chen J, Miao Y, Taffet GE, et al. 2011. CCR2 mediates the uptake of bone marrow-derived fibroblast precursors in angiotensin II-induced cardiac fibrosis. *Am J Physiol Heart Circ Physiol* 301:H538-47
302. Xu J, Mora A, Shim H, Stecenko A, Brigham KL, Rojas M. 2007. Role of the SDF-1/CXCR4 axis in the pathogenesis of lung injury and fibrosis. *Am J Respir Cell Mol Biol* 37:291-9
303. Xu L, Xiong S, Guo R, Yang Z, Wang Q, et al. 2014. Transforming growth factor β3 attenuates the development of radiation-induced pulmonary fibrosis in mice by decreasing fibrocyte recruitment and regulating IFN-γ/IL-4 balance. *Immunology letters* 162:27-33
304. Xu XG, Bednarz B, Paganetti H. 2008. A review of dosimetry studies on external-beam radiation treatment with respect to second cancer induction. *Phys Med Biol* 53:R193-241
305. Yamazaki S, Ema H, Karlsson G, Yamaguchi T, Miyoshi H, et al. 2011. Nonmyelinating Schwann cells maintain hematopoietic stem cell hibernation in the bone marrow niche. *Cell* 147:1146-58
306. Yan J, Zhang Z, Jia L, Wang Y. 2016. Role of Bone Marrow-Derived Fibroblasts in Renal Fibrosis. *Frontiers in Physiology* 7

307. Yang H-C, Zuo Y, Fogo AB. 2010. Models of chronic kidney disease. *Drug Discovery Today: Disease Models* 7:13-9
308. Yang L, Scott PG, Giuffre J, Shankowsky HA, Ghahary A, Tredget EE. 2002. Peripheral blood fibrocytes from burn patients: identification and quantification of fibrocytes in adherent cells cultured from peripheral blood mononuclear cells. *Laboratory investigation* 82:1183
309. Yarnold J, Brotons M-CV. 2010. Pathogenetic mechanisms in radiation fibrosis. *Radiotherapy and oncology* 97:149-61
310. Yi ES, Bedoya A, Lee H, Chin E, Saunders W, et al. 1996. Radiation-induced lung injury in vivo: Expression of transforming growth factor—Beta precedes fibrosis. *Inflammation* 20:339-52
311. Yona S, Kim K-W, Wolf Y, Mildner A, Varol D, et al. 2013. Fate mapping reveals origins and dynamics of monocytes and tissue macrophages under homeostasis. *Immunity* 38:79-91
312. Yoshihara H, Arai F, Hosokawa K, Hagiwara T, Takubo K, et al. 2007. Thrombopoietin/MPL signaling regulates hematopoietic stem cell quiescence and interaction with the osteoblastic niche. *Cell stem cell* 1:685-97
313. Yu V, Burdick M, Zhang Z, Belperio JA, Horton M, Mehrad B. 2017. Longitudinal Measurements Of Circulating Fibrocytes As A Biomarkers Of Prognosis In Idiopathic Pulmonary Fibrosis. In *C78. FIBROSIS: MEDIATORS AND MODULATORS*:A6424-A: Am Thoracic Soc. Number of A6424-A pp.
314. Zeisberg EM, Tarnavski O, Zeisberg M, Dorfman AL, McMullen JR, et al. 2007. Endothelial-to-mesenchymal transition contributes to cardiac fibrosis. *Nat Med* 13:952-61
315. Zhang H, Maric I, DiPrima MJ, Khan J, Orentas RJ, et al. 2013. Fibrocytes represent a novel MDSC subset circulating in patients with metastatic cancer. *Blood* 122:1105-13
316. Zhang H, Zhai Z, Wang Y, Zhang J, Wu H, et al. 2013. Resveratrol ameliorates ionizing irradiation-induced long-term hematopoietic stem cell injury in mice. *Free Radic Biol Med* 54:40-50
317. Zhang HY, Phan SH. 1999. Inhibition of myofibroblast apoptosis by transforming growth factor beta(1). *Am J Respir Cell Mol Biol* 21:658-65
318. Zhao M, Perry JM, Marshall H, Venkatraman A, Qian P, et al. 2014. Megakaryocytes maintain homeostatic quiescence and promote post-injury regeneration of hematopoietic stem cells. *Nat Med* 20:1321-6
319. Zoso A, Mazza EMC, Bicciato S, Mandruzzato S, Bronte V, et al. 2014. Human fibrocytic myeloid-derived suppressor cells express IDO and promote tolerance via Treg-cell expansion. *European Journal of Immunology* 44:3307-19